

**DESIGN AND SYNTHESIS OF NOVEL COUMARIN
COMPOUNDS FOR PLANT HORMONE CONTROLLED
RELEASE ACTIVATED BY LIGHT**



WITSANU SOMBAT

**A THESIS SUBMITTED IN PARTIAL FULFILLMENT OF THE
REQUIREMENTS FOR THE DEGREE OF MASTER OF SCIENCE**

MAJOR IN CHEMISTRY

FACULTY OF SCIENCE

UBON RATCHATHANI UNIVERSITY

ACADEMIC YEAR 2017

COPYRIGHT OF UBON RATCHATHANI UNIVERSITY



UBON RATCHATHANI UNIVERSITY
THESIS APPROVAL
MASTER OF SCIENCE
MAJOR IN CHEMISTRY FACULTY OF SCIENCE

TITLE DESIGN AND SYNTHESIS OF NOVEL COUMARIN COMPOUNDS FOR
PLANT HORMONE CONTROLLED RELEASE ACTIVATED BY LIGHT

AUTHOR MR. WITSANU SOMBAT

EXAMINATION COMMITTEE

DR. SUWATCHAI JARUSSOPON

CHAIRPERSON

ASST. PROF. DR. RUKKIAT JITCHATI

MEMBER

ASST. PROF. DR. KITTIYA WONGKHAN

MEMBER

ADVISOR

.....
(ASST. PROF. DR. KITTIYA WONGKHAN)

.....
(ASST. PROF. DR. CHARIDA PUKAHUTA)

DEAN, FACULTY OF SCIENCE

.....
(ASSOC. PROF. DR. ARIYAPORN PONGRAT)
VICE PRESIDENT FOR ACADEMIC AFFAIRS

COPYRIGHT OF UBON RATCHATHANI UNIVERSITY
ACADEMIC YEAR 2017

ACKNOWLEDGEMENTS

Firstly, I would like to acknowledge my advisor, Asst. Prof. Dr. Rukkiat Jitchati, and Asst. Prof. Dr. Kittiya Wongkhan for allowing me to undertake this project, all the brilliant ideas, their enthusiasm, advice and guiding me throughout the years. Thank for their support, patience, and encouragement throughout my graduate studies. It is not often that one finds an advisor and colleague that always finds the time for listening to the little problems and roadblocks that unavoidably crop up in the course of performing research. His technical and editorial advice was essential to the completion of this dissertation and has taught me innumerable lessons and insights on the workings of academic research in general. His advice was most valuable to understand the obtained results and to determine the next steps for the research presented in this thesis. I would like to thank Dr. Suwatchai Jarussophon and Miss Pawinee Pongwan for their kind consideration and suggestion on this thesis as well as content formulation and sharing their extensive knowledge of nanoformulation and measurement. Furthermore, I would like to acknowledge National Nanotechnology Center (NANOTEC), National Science and Technology Development Agency for particle size and contact angle measurements in my work.

In addition, scholarship from Science Achievement Scholarship of Thailand, SAST.

Unforgettably, I would like to thank to the Organometallic and Catalytic Center (OCC), Department of Chemistry, Faculty of Science, Ubon Ratchathani University for the synthesis facilities. Thanks everyone in the OCC group for contributing and helping me to make this research work possible at Ubon Ratchathani University.

Finally, I must thank my family especially Miss Napaporn Chanachai for their love and personal support during my study.

W. Sombat.

Witsanu Sombat
Researcher

บทคัดย่อ

เรื่อง : การออกแบบและสังเคราะห์สารคูมารินชนิดใหม่เพื่อใช้เป็นสารควบคุมการปลดปล่อย
ฮอโมนพืชกระตุ้นด้วยแสง

ผู้วิจัย : วิษณุ สมบัติ

ชื่อปริญญา : วิทยาศาสตร์มหาบัณฑิต

สาขาวิชา : เคมี

อาจารย์ที่ปรึกษา : ผู้ช่วยศาสตราจารย์ ดร.กิตติยา วงษ์ขันธุ์

คำสำคัญ : คูมาริน, ฮอโมนพืช, สารควบคุมการปลดปล่อยด้วยแสง

งานวิจัยนี้รายงานการสังเคราะห์อนุกรมของสารคูมารินที่ตอบสนองต่อแสง สำหรับควบคุมการปลดปล่อยฮอโมนพืชและสารกำจัดวัชพืช ซึ่งสารเหล่านี้ถูกออกแบบโดยการปรับเปลี่ยนตำแหน่งหมู่แทนที่ของแอลคอกซีสายโซ่ยาว ($-OC_{16}H_{33}$) บนโครงสร้างของคูมาริน ทำให้ได้สมบัติในการเกาะติดบนใบของพืช สารโมเลกุลเป้าหมายสังเคราะห์ด้วยปฏิกิริยาวิลเลียมสัน ปฏิกิริยาเพคแมนน์ และปฏิกิริยาเอสเทอร์ฟิเคชัน ตามลำดับ โครงสร้างของสารที่สังเคราะห์ได้ทั้งหมดพิสูจน์เอกลักษณ์โดยใช้เทคนิค 1H NMR ^{13}C NMR FTIR และ แมสสเปคโตรสโคปี นอกจากนี้มีอัลชันในระดับนาโนเมตรของสารที่ได้จากการสังเคราะห์ยังถูกเตรียมโดยใช้โพลิไวนิลแอลกอฮอล์ (PVA) เป็นสารให้ความคงตัว และใช้โซเดียมโดเดซิลซัลเฟต (SDS) เป็นสารลดแรงตึงผิว จากการศึกษาพบว่าสภาวะที่เหมาะสมในการเตรียมนาโนอิมัลชันคือ ใช้สารให้ความคงตัว 3 wt% สารลดแรงตึงผิว 1 wt% และสารสังเคราะห์ 0.2 wt% ในอัตราส่วนต่อปริมาตรของวัฏภาคน้ำมันต่อวัฏภาคน้ำเท่ากับ 75:25 ศึกษาขนาดของอนุภาค คุณสมบัติการเกาะติด และการปลดปล่อยโดยกระตุ้นด้วยแสงของนาโนอิมัลชันที่เตรียมได้ พบว่าสูตรนาโนอิมัลชันที่ได้มีความเสถียร โดยมีขนาดของอนุภาคอยู่ระหว่าง 292-403 นาโนเมตร และยังสามารถในการเกาะติดผิวสัมผัสที่ดี โดยมีค่ามุมสัมผัสระหว่างใบกับหยดของนาโนอิมัลชันอยู่ระหว่าง 48-57 องศา นอกจากนี้การควบคุมการปลดปล่อยฮอโมนพืช และสารกำจัดวัชพืชจากสารคูมารินที่ตอบสนองต่อแสง เมื่อฉายแสงที่ความยาวคลื่น 365 นาโนเมตร และแสงแดด โดยใช้เทคนิคการดูดกลืนแสงและการคายแสงติดตามการปลดปล่อย พบว่าตำแหน่งการแทนที่ของหมู่แอลคอกซีบนโครงสร้างของคูมารินและตำแหน่งการแทนที่ของพันธะคาร์บอนกับคาร์บอนโครงสร้างของอินโดลมีผลต่ออัตราเร็วของการเกิดปฏิกิริยาการปลดปล่อย

ABSTRACT

TITLE : DESIGN AND SYNTHESIS OF NOVEL COUMARIN
COMPOUNDS FOR PLANT HORMONE CONTROLLED
RELEASE ACTIVATED BY LIGHT
AUTHOR : WITSANU SOMBAT
DEGREE : MASTER OF SCIENCE
MAJOR : CHEMISTRY
ADVISOR : ASST. PROF. KITTIYA WONGKHAN, Ph.D
KEYWORDS : COUMARIN, PLANT HORMONE, PHOTORESPONSIVE

This study reported the synthesis of the photoresponsive coumarin series for controlled releases of plant hormones and herbicides. The materials were designed by varying substituted positions of long alkoxy side chains ($-\text{OC}_{16}\text{H}_{33}$), introduced to gain adhesive properties on plant leaves, in the coumarin core structure. The target compounds were synthesized *via* Williamson reaction, Pechmann reaction and esterification, respectively. All chemical structures were characterized by ^1H NMR, ^{13}C NMR, FTIR, and mass spectroscopy. In addition, nanocmulsion of these compounds were prepared by using PVA as a stabilizer and SDS as a surfactant. The optimized condition was obtained by using 3 wt% PVA, 1 wt% SDS, and 0.2 wt% of coumarin with a volume ratio of oil-in-water at 75:25. The particle size, wettability and photolysis of nanoformulations were studied. It was found that the obtained nanoemulsion gave high physical stability with average particle diameter about 292-403 nm and expressed good wettability (contact angle $48-57^\circ$) on *Cassia fistula* leaf surface. Moreover, the controlled releases of plant hormones and herbicides from photoresponsive compounds were studied by irradiating under the specific wavelength (365 nm) and normal sunlight. Photolysis was monitored by UV-vis absorption and emission. We found that the substituted position of the alkoxy group on coumarin rings and substituted position of the carboxylate linkage on indoles also effected a photolysis rate.

CONTENTS

	PAGE
ACKNOWLEDGEMENTS	I
THAI ABSTRACT	II
ENGLISH ABSTRACT	III
CONTENTS	IV
LIST OF TABLES	VI
LIST OF FIGURES	VII
LIST OF APPREVIATIONS	XII
CHAPTER 1 INTRODUCTION	
1.1 Importance in research and development	1
1.2 Aim of the synthesis	3
CHAPTER 2 LITERATURE REVIEWS	
2.1 Literature reviews	5
CHAPTER 3 EXPERIMENTAL	
3.1 Chemical	11
3.2 Instruments and general chemical characterization techniques	12
3.3 Experimental section	13
3.4 Preparation of photoresponsive coumarin CM1-CM12 nanoemulsion	36
CHAPTER 4 RESULTS AND DISSCUSSIONS	
4.1 Synthesis and characterization of novel photoresponsive coumarin	37
4.2 Nanoformulation and characterization of photoresponsive coumarin CM1-CM12	48
CHAPTER 5 CONCLUSIONS	58

CONTENTS (CONTINUED)

	PAGE
REFERENCES	59
APPENDICES	
A Characterized data	64
B Photophysical properties and photolysis data	97
C Publication	106
CURRICULUM VITAE	117

LIST OF TABLES

TABLE		PAGES
1.1	Agricultural chemicals imported to Thailand in 2015	1
3.1	Chemicals for the synthesis	11
4.1	The result for optimization condition	48
4.2	Characteristics of the CM1-CM12 nanoemulsion	49

LIST OF FIGURES

FIGURE	PAGES
1.1 The common pesticides, herbicides fungicide and plant hormones	1
1.2 Traditional direct fertilizer process by The Chaipattana Foundation	2
1.3 Plant leaves feeding process by Melotto and coworker	2
1.4 The chemical structures of target compounds CM1-CM12	4
2.1 Chemical structure and atomic numbering of coumarin	5
2.2 Proposed bio-adhesive photo-responsive coumarin compound for light controlled release system	6
2.3 Structure of photoresponsive coumarin by Hagen and coworker	6
2.4 Proposed mechanism of photo releasing coumarin linkage by Hagen and coworker	7
2.5 Structure of photoresponsive coumarin with herbicide by Atta and coworker	7
2.6 Emission spectra of photoresponsive coumarin after irradiated by light	8
2.7 Proposed the photolysis mechanism of photoresponsive compounds to release 2,4-D by Atta and coworker	8
2.8 Structure of photoresponsive with plant hormones by Atta and coworker	9
2.9 Organic nanodispersion after addition of water by Haifei Zhang and coworker	9
3.1 Experimental chart model of this work	13
4.1 Synthetic route of the photoresponsive coumarin	37
4.2 Synthetic method of 1A and 1B	38
4.3 The mechanism of Williamson ether synthesis reaction	38
4.4 ¹ H NMR spectrum in CDCl ₃ of 1A	39
4.5 Synthetic method of C1 and C2	39

LIST OF FIGURES (CONTINUED)

FIGURE	PAGES
4.6 The mechanism of Pechmann coumarin synthesis	40
4.7 ^1H NMR spectrum of C1 in CDCl_3	41
4.8 ^1H NMR spectrum of C2 in CDCl_3	41
4.9 Synthetic route of photoresponsive coumarins (CM1-CM2)	42
4.9 Synthetic route of photoresponsive coumarins (CM1-CM2) (continued)	43
4.10 The mechanism of esterification synthesis	44
4.11 ^1H NMR spectrum of CM1 in CDCl_3	44
4.12 ^1H NMR spectrum of CM1 and CM2 in CDCl_3	45
4.13 ^1H NMR spectrum of CM1 , CM7 and CM9 in CDCl_3	46
4.14 ^1H NMR spectrum of CM3 , CM5 and CM11 in CDCl_3	47
4.15 Image of droplets and contact angle (θ) of pure DI-water, mixed additive (PVA/SDS) and nanoformulation photoresponsive coumarin on <i>Cassia fistula</i> leaf	51
4.16 (a) Absorption and (b) emission spectra of nanoformulation photoresponsive CM1 and CM2	52
4.17 HOMO and LUMO distributions calculated for coumarin- chalcone hybrids by Xue and coworker	53
4.18 (a) Absorption and (b) emission spectra of nanoformulation photoresponsive CM1 , CM7 and CM9	53
4.19 Absorption spectra of CM1 under (a) 365 nm and (b) sunlight	54
4.20 Emission spectra of CM1 under (a) 365 nm and (b) sunlight	54
4.21 Mechanism of the photolysis of photoresponsive coumarin (CM1-CM12) to release plant hormone and herbicide	55
4.22 Photolysis emission spectra rate of CM1 at 365 nm and under sunlight	55

LIST OF FIGURES (CONTINUED)

FIGURE		PAGES
4.23	Photolysis emission spectra rate of CM1 and CM2 at 365 nm	56
4.24	The intermediates of the CM1 and CM2	56
4.25	Photolysis emission spectra rate of CM1 , CM7 and CM9	57
4.26	The electronic effect of the CM1 and CM7 intermediates	57
A.1	^1H , ^{13}C NMR in CDCl_3 and ATR-FTIR of 1A	65
A.2	Mass spectroscopy of 1A	66
A.3	^1H , ^{13}C NMR in CDCl_3 and ATR-FTIR of 1B	67
A.4	Mass spectroscopy of 1B	68
A.5	^1H , ^{13}C NMR in CDCl_3 and ATR-FTIR of C1	69
A.6	Mass spectroscopy of C1	70
A.7	^1H , ^{13}C NMR in CDCl_3 and ATR-FTIR of C2	71
A.8	Mass spectroscopy of C2	72
A.9	^1H , ^{13}C NMR in CDCl_3 and ATR-FTIR CM1	73
A.10	Mass spectroscopy of CM1	74
A.11	^1H , ^{13}C NMR in CDCl_3 and ATR-FTIR CM2	75
A.12	Mass spectroscopy of CM2	76
A.13	^1H , ^{13}C NMR in CDCl_3 and ATR-FTIR CM3	77
A.14	Mass spectroscopy of CM3	78
A.15	^1H , ^{13}C NMR in CDCl_3 and ATR-FTIR CM4	79
A.16	Mass spectroscopy of CM4	80
A.17	^1H , ^{13}C NMR in CDCl_3 and ATR-FTIR CM5	81
A.18	Mass spectroscopy of CM5	82
A.19	^1H , ^{13}C NMR in CDCl_3 and ATR-FTIR CM6	83
A.20	Mass spectroscopy of CM6	84
A.21	^1H , ^{13}C NMR in CDCl_3 and ATR-FTIR CM7	85
A.22	Mass spectroscopy of CM7	86
A.23	^1H , ^{13}C NMR in CDCl_3 and ATR-FTIR CM8	87

LIST OF FIGURES (CONTINUED)

FIGURE	PAGES
A.24 Mass spectroscopy of CM8	88
A.25 ^1H , ^{13}C NMR in CDCl_3 and ATR-FTIR CM9	89
A.26 Mass spectroscopy of CM9	90
A.27 ^1H , ^{13}C NMR in CDCl_3 and ATR-FTIR CM10	91
A.28 Mass spectroscopy of CM10	92
A.29 ^1H , ^{13}C NMR in CDCl_3 and ATR-FTIR CM11	93
A.30 Mass spectroscopy of CM11	94
A.31 ^1H , ^{13}C NMR in CDCl_3 and ATR-FTIR CM12	95
A.32 Mass spectroscopy of CM12	96
B.1 Absorption spectra after 5 day irradiation by UV light (left) and sunlight (right)	98
B.2 Fluorescence spectra after 5 day irradiation by UV light (left) and sunlight (right)	102

LIST OF ABBREVIATIONS

ABBREVIATION	FULL WORD
AR.	Analysis reagent
anh.	Anhydrous
^{13}C NMR	Carbon nuclear magnetic resonance
CRFs	Control release formulations
cm^{-1}	Reciprocal centimeter (unit of wavenumber)
δ	Chemical shift in ppm relative to tetramethylsilane
conc.	Concentrated
J	Coupling constant (for NMR spectral data)
$^{\circ}\text{C}$	Degree Celsius
DI	Deionized Water
DFT	Density functional theory
DCM	Dichloromethane
DDT	Dichlorodiphenyltrichloroethane
2,4-D	2,4-Dichlorophenoxyacetic acid
d	Doublet (for NMR spectral data)
dd	Double of doublet (for NMR spectral data)
DLS	Dynamic light scattering
ESI-MS	Electrospray ionization mass spectrometry
EtOAc	Ethyl acetate
FTIR	Fourier transform infrared spectroscopy
g	Grams
Hz	Hertz
HOMO	Highest occupied molecular orbital
HRMS	High Resolution Mass Spectrometry
h	Hour
2-In	2-Indole

LIST OF ABBREVIATIONS (CONTINUED)

ABBREVIATION	FULL WORD
3-In	3-Indole
5-In	5-Indole
6-In	6-Indole
LUMO	Lowest unoccupied molecular orbital
IR	Infrared
IMC	Indomethacin
MS	Mass spectroscopy
MHz	Mega hertz
μ l	Microliter
mmol	Milimole
ml	Milliliter
mmol	Milimole
mV	Millivolt
M	Molarity
Mw	Molecular weight
m	Multiplet (for NMR spectral data)
nm	Nanometers
1-Naph	1-Naphthalene
NMR	Nuclear magnetic resonance
O/W	Oil-in-water
ppm	Parts per million
PGRs	Plant growth regulators
PVA	Poly(vinyl alcohol)
s	Singlet (for NMR spectral data)
SDS	Sodium dodecyl sulfate
TMS	Tetra methylsilane

LIST OF ABBREVIATIONS (CONTINUED)

ABBREVIATION	FULL WORD
t	Triplet (for NMR spectral data)
UV-Vis	Ultra violet-visible
v/v	Volume/volume
wt. %	Weight percent

CHAPTER 1

INTRODUCTION

1.1 Importance of research and development

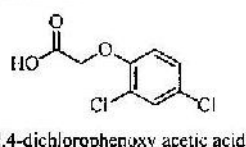
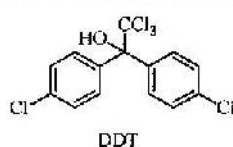
A statistics in 2015 showed that the agricultural chemicals imported to Thailand is more than 150,000 million tons, valued at 19,000 million baht in Table 1.1 [1].

Table 1.1 Agricultural chemicals imported to Thailand in 2015

order	types	Amount (million tons)	Value (million Baht)
1	Pesticide	12.9	3,684.8
2	Fungicide	11.0	3,839.1
3	Herbicide	119.9	11,016.7
4	Acaricide	1.4	248.5
5	Rodenticide	0.2	54.4
6	Plant hormone	2.2	217.8
7	Mollussicide	0.2	11.41
8	Fumigants	1.4	228.9
total		149.5	19,301.9

The most common chemicals were used in agriculture such as pesticides, herbicides and plant hormones are shown in Figure 1.1.

Pesticides and Herbicides



Fungicides



Plant hormones

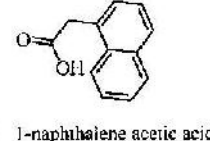
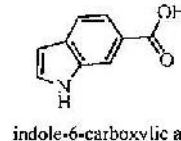
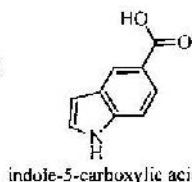
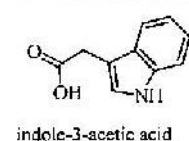


Figure 1.1 The common pesticides, herbicides fungicide and plant hormones

Traditional direct fertilizer process (Figure 1.2) of agricultural chemicals is the solution feeding by root which retains between 30-70 percent of chemicals applied. This significance impacts on the environmental system by leaching to the soil, groundwater and runoff entering waterway. Moreover, enormous losses of agricultural chemicals not only affect productivity, but also increases the need to apply larger quantities of chemical inputs, thus further increasing the costs.



Figure 1.2 Traditional direct fertilizer process by The Chaipattana Foundation

Thus, through plant leaf feeding process in Figure 1.3 has been interested because agricultural chemicals could be taken up through the stomata opening. This method not only directs to plant system but also used a small amount of chemicals.

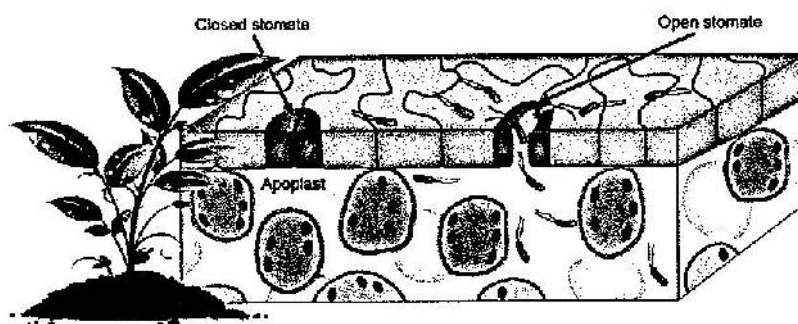


Figure 1.3 Plant leaves feeding process by Melotto and coworker [2]

Recently, photoresponsive materials have been studied together with plant hormone and herbicide that are chemically modified into the control release formulations (CRFs). This feature is not only to increase the effectiveness of the active agents, but it also facilitates minimizing the number of chemicals [3] [4, 5].

Photoresponsive materials have been utilized for controlled release of active molecules such as peptides, herbicides, and PGRs [6-10]. Derivatives of 2-(dimethylamino)-5-nitrophenol [11], α -carboxy nitrobenzyl [12], 3-nitro-2-naphthalenemethanol [13], *p*-hydroxyphenacyl [14], anthracene-9-methanol [15], quinoline [16] and coumarin [17] were reported. Among them, coumarin derivatives were preferred for caging bioactive molecules due to their high extinction coefficient in the visible region, photochemical quantum yields, hydrolytic stability and strong fluorescence properties.

1.2 Aim of the thesis

We envisaged a long chain hydrophobic tail of photoresponsive coumarins in which hormone and herbicide were linked by conjugated ester linkage with light sensitive property. The ideal target of this study is to understand our photoresponsive coumarin system created that could affect the release rate of active substrates and to formulate the compound into the emulsion that could be utilized for agricultural application. Our research work comprises three parts: (i) varied the position of a long chain hydrophobic tail, (ii) varied the position of indole hormone and (iii) varied the aromatic linkage moiety. The target molecules are **CM1-CM12** (their structure shown in Figure 1.4).

1.2.1 To synthesize and characterize the molecular structure of the target compounds by ^1H and ^{13}C NMR, Fourier transforms infrared spectroscopy (FT-IR) and mass spectroscopy (MS).

1.2.2 To study the nanoformulation of **CM1-CM12** by dynamic light scattering (DLS).

1.2.3 To study the wettability property of nanoformulation on plant leave surface.

1.2.4 To study the photolysis of nanoformulation under UV light and sunlight.

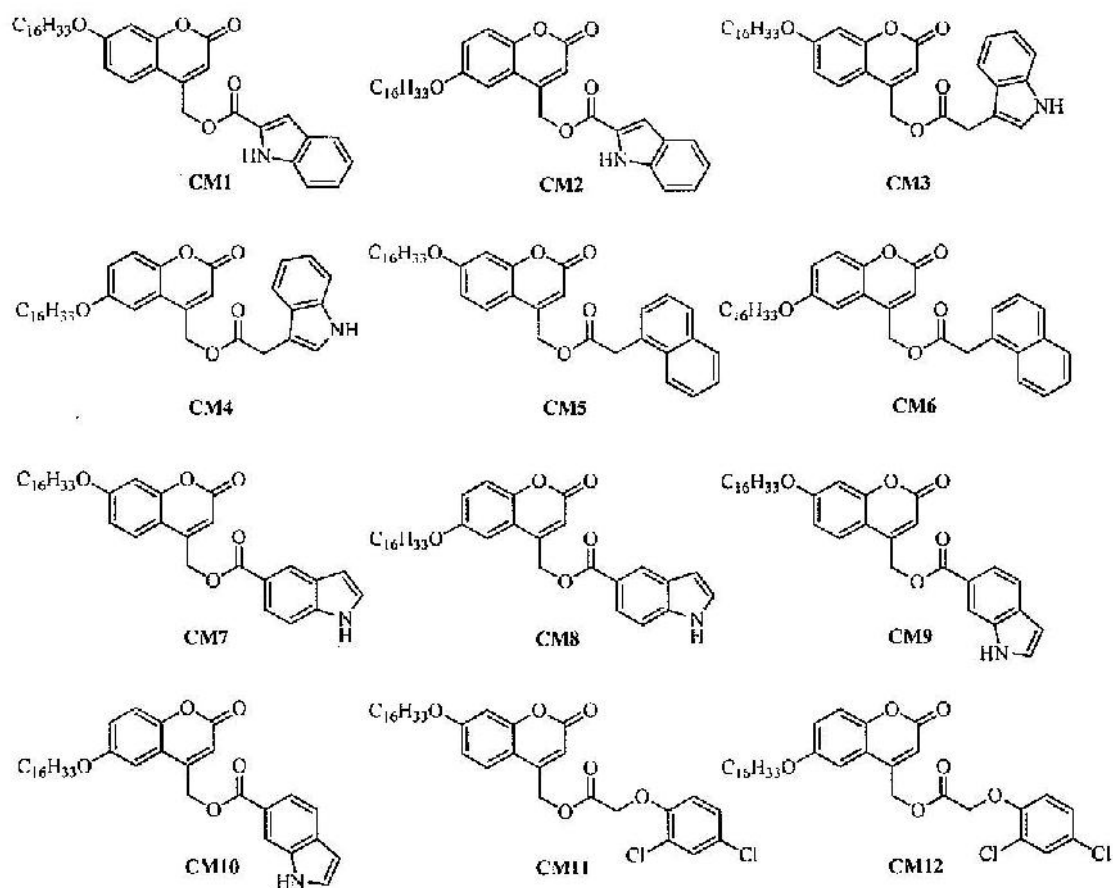


Figure 1.4 The chemical structures of target compounds CM1-CM12

CHAPTER 2

LITERATURE REVIEWS

2.1 Literature reviews

2*H*-chromen-2-one (coumarin) in Figure 2.1 is a phenolic derivative found naturally in many plants such as sweet-clover, cinnamon, tonka bean, vanilla grass, and etc. The compound is presumed to be produced chemical in order to protect themselves from plant predators. Coumarin is also used in the pharmaceutical industry as a precursor molecule for the synthesis of numerous synthetic anticoagulant pharmaceuticals.

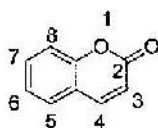


Figure 2.1 Chemical structure and atomic numbering of coumarin

Photoresponsive based on coumarin derivative in agriculture has arisen. The advantages of the material include [18]:

- (1) Reduction in the quantity of active agent required to control pests and diseases
- (2) Reduced risk of environmental contamination
- (3) Reduced energy costs, since the number of applications required is less than for conventional formulations
- (4) Improved safety of the individuals responsible for product application in the field
- (5) Removable from active carboxylates, alcohols, carbonyl groups, diols, amines, etc. [19] by photo-controlled release (Figure.2.2) [20, 21].

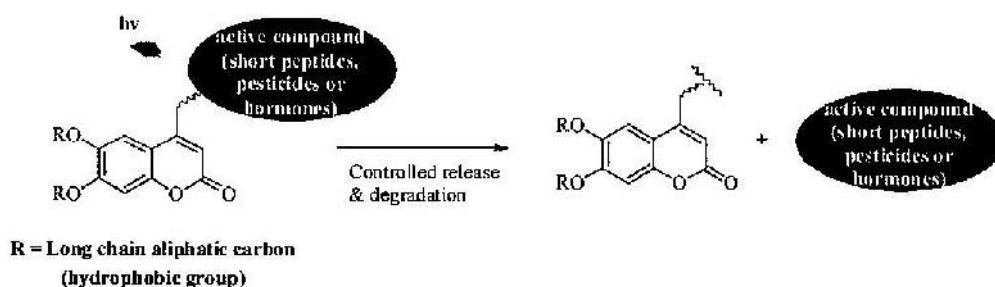


Figure 2.2 Proposed bio-adhesive photo-responsive coumarin compound for light controlled release system

In 2010, Hagen and coworker [22] introduced a variant of photoresponsive coumarin for protecting of a carboxylic acid, an amine, a carbonyl and a phenol, as it is shown in Figure 2.3.

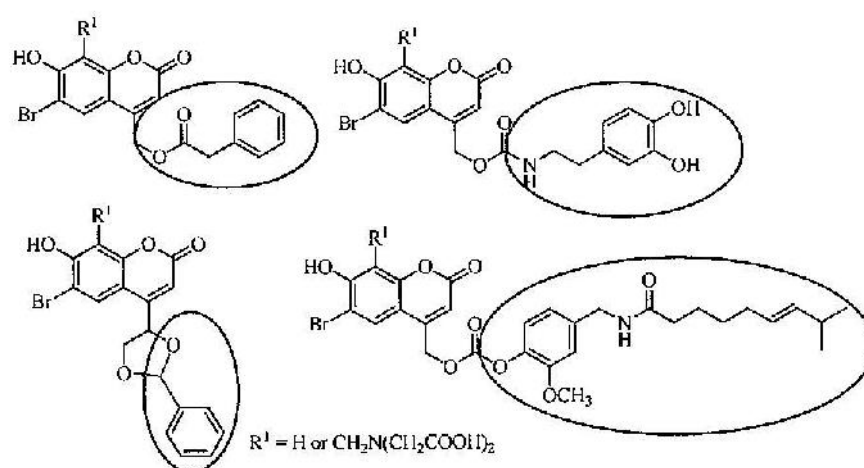


Figure 2.3 Structure of photoresponsive coumarin by Hagen and coworker

They found that the coumarin compound showed dramatically increased solubility in aqueous solution and higher photolysis quantum yield in the case of photoprotected with ester compound. The coumarin caged compounds could be uncaged by irradiation under UV light in aqueous solution. Proposed photo-responsive coumarin compound for light controlled release system shown in Figure 2.4.

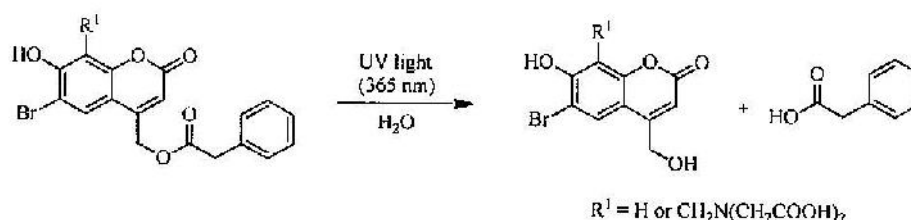


Figure 2.4 Proposed mechanism of photo releasing coumarin linkage by Hagen and coworker

In addition, Atta and coworker [21] developed a photoresponsive coumarin with the herbicide (2,4-D) in Figure 2.5. They found that photo release of these compounds achieved by irradiating UV-vis light and also demonstrated the potential of the photoreponsive not only to act as a delivery device but also to possess herbicidal activity after photorelease.

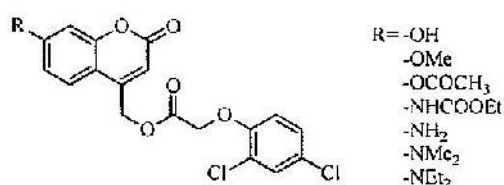


Figure 2.5 Structure of photoresponsive coumarin with herbicide by Atta and coworker

Furthermore, they monitored the course of photorelease of photoresponsive using fluorescence (Figure 2.6). The result showed that the fluorescence intensity of the compound at regular intervals of irradiation in MeOH/HEPES (80:20) was decrease when irradiation time increase.

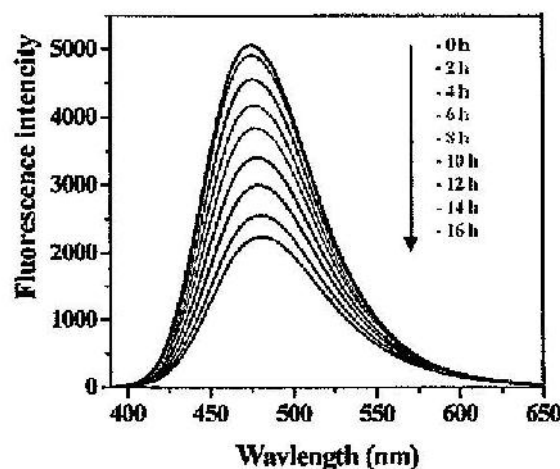


Figure 2.6 Emission spectra of photoresponsive coumarin after irradiated by light

Moreover, they also proposed the photolysis mechanism of photoresponsive compounds to release 2,4-D. This process occurs *via* formation of an ionic intermediate (coumarin-CH₂⁺) shown in Figure 2.7.

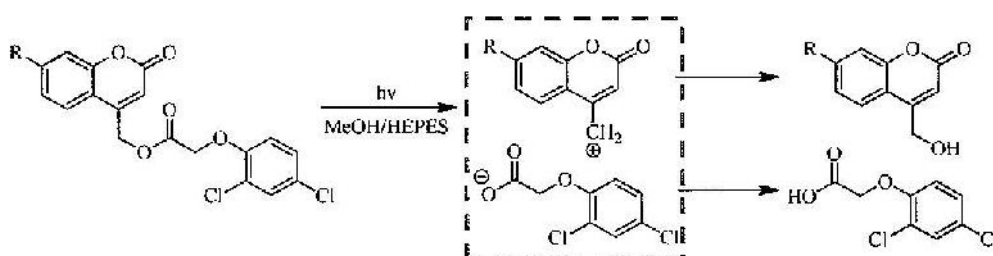


Figure 2.7 Proposed the photolysis mechanism of photoresponsive compounds to release 2,4-D by Atta and coworker

Furthermore, Atta and coworker [23] synthesized carboxyl-containing auxin hormones (indoleacetic acid and naphthoxyacetic acid) based on coumarin derivatives the structure shown in Figure 2.8. Photolysis of these compounds by sunlight in both aqueous ethanol and soil media resulted in the controlled release of plant hormones. They found that the bioactivity experiments indicated all compounds showed better enhancement in the root and shoot length growth of *Cicer arietinum* compared to free plant hormones after sunlight exposure.

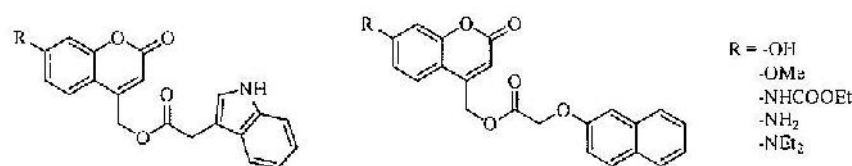


Figure 2.8 Structure of photoresponsive with plant hormones by Atta and coworker

To enhanced solubility properties of organic compounds, Haifei Zhang and coworker [24] reported a generic method of water-dispersible organic nanoparticles by freeze-drying emulsions containing water-insoluble compounds (red oil) dissolved in a volatile oil phase. They generated an oil-in-water (O/W) emulsion using poly(vinyl alcohol) (PVA) and sodium dodecyl sulphate (SDS) as stabilizer and surfactant, respectively. They found that water-soluble materials present in the aqueous phase form a porous solid support that dissolves rapidly on the addition of water to disperse the nanoparticles (Figure 2.9). This technique has wide applicability because nanodispersions are a valuable alternative to molecular solutions. Water-insoluble commercial biocides showed increased activity, suggesting the potential for decreased application doses and lower rates of acquired bacterial resistance.

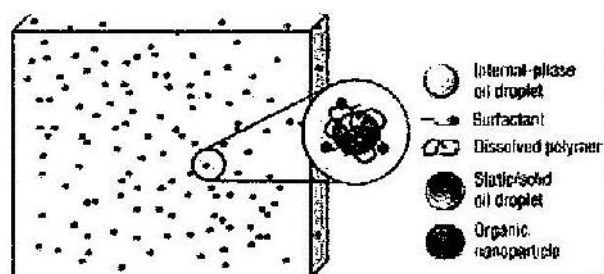


Figure 2.9 Organic nanodispersion after addition of water by Haifei Zhang and coworker

Moreover, In 2011, Zhang and coworkers [25] reported the preparation of nanoparticles *via* an emulsion-freeze-drying approach by in situ mixing within porous poly(vinyl alcohol). Sodium dodecyl sulphate (SDS) was used as a surfactant to enhanced solubility properties of a poorly water-soluble drug indomethacin (IMC). They found that

the IMC nanoparticles could be form stable nanodispersions in water by rapid dissolution of the porous polymeric scaffold. This method might be regard as a general route to prepare poorly water-soluble organic (drug) nanoparticles to enhance water solubility for potential applications.

CHAPTER 3

EXPERIMENTAL

3.1 Chemicals

All the chemicals used in this thesis are shown in Table 3.1.

Table 3.1 Chemicals for the synthesis

Chemicals	Formula	Grade	Manufacturer
1-Bromohexadecane	$C_{16}H_{33}Br$	97%	ACROS
Dichloromethane	CH_2Cl_2	AR	CARLO ERBA
2,4-Dichlorophenoxyacetic acid	$C_8H_6Cl_2O_3$	98%	Aldrich
Ethyl 4-chloroacetoacetate	$C_6H_9ClO_3$	98%	ACROS
Hydroquinone	$C_6H_6O_2$	99.5%	ACROS
Hexane	$CH_3(CH_2)_4CH_3$	AR	CARLO ERBA
Indole-2-carboxylic acid	$C_{10}H_9NO_2$	99%	ACROS
3-Indoleacetic acid	$C_{10}H_9NO_2$	98%	Aldrich
Indole-5-carboxylic acid	$C_9H_7NO_2$	98%	Aldrich
Indole-6-carboxylic acid	$C_9H_7NO_2$	98%	Aldrich
Methanol	CH_3OH	AR	CARLO ERBA
Methane sulfonic acid	CH_3SO_3H	99%	ACROS
N,N-Dimethylformamide	$HCON(CH_3)_2$	AR	CARLO ERBA
1-Naphthaleneacetic acid	$C_{12}H_{10}O_2$	95%	ACROS
Poly(vinyl)alcohol	$[-CH_2CH(OH)-]_n$	80%	Aldrich
Potassium carbonate	K_2CO_3	99%	CARLO ERBA
Potassium iodide	KI	99%	CARLO ERBA
Resorcinol	$C_6H_6O_2$	99% AR	SDFCL
Sodium dodecyl sulphate	$C_{12}H_{25}NaO_4S$	99%	ACROS
Sodium hydrogen carbonate	$NaHCO_3$	98%	CARLO ERBA
Sodium sulfate anhydrous	Na_2SO_4	99%	CARLO ERBA

3.2 Instruments and general chemical characterization techniques

The FT-IR spectra were recorded by attenuated total reflectance (ATR) technique using neat sample with a Perkin-Elmer Spectrum RX.I on Fourier transform infrared spectrophotometer over the 550 - 4000 cm^{-1} . The data of FTIR spectra are reported as frequency (cm^{-1}).

UV-Visible spectra were recorded in a 1 cm path length quartz cell using a UV-2600 spectrophotometer high resolution. The samples were dissolved in DI water and diluted to a concentration of $4 - 5 \times 10^{-5}$ M.

^1H and ^{13}C NMR spectra were performed in CDCl_3 recorded on Bruker AVANCE 300 MHz spectrometer, using TMS as the internal reference. Data for NMR spectra are reported as followed: chemical shift (δ , ppm), multiplicity, coupling constant (J), (Hz) and integration.

Molecular weight of target compounds were measured by the high resolution mass spectra which were recorded with the time of flight (TOF) mode on a Bruker MicroTOF model by electrospray ionization techniques (ESI).

Particle size and zeta potential were measured on dynamic light scattering (DLS) particle size analyzer (Zetasizer Nano ZS, Malvern Instruments Ltd., Worcestershire, UK). The measuring range of the Zetasizer Nano ZS was 0.6-6000 nm, and the measurement temperature was set at 25 $^{\circ}\text{C}$.

Contact angle were recorded with the "contact angle system OCA" (OCA40 Micro) 1 μl dosing volume and 1 $\mu\text{l/s}$ dosing rate from DataPhysics Instruments GmbH, Germany.

3.3 Experimental section

This experimental section part gives a summarized description of the photoresponsive coumarin CM1-CM12 study for controlled release of plant hormones and herbicide. It is divided into three main steps. The first step is the photoresponsive coumarin synthesis *via* Williamson reaction, Pechmann condensation, and esterification reaction, respectively. The second step is the compounds characterization by ^1H , ^{13}C NMR, FT-IR and mass techniques. The last step is to study the formulation, particle size, wettability properties and photolysis of the nanodispersion. The overall experimental flow chart is shown in Figure 3.1.

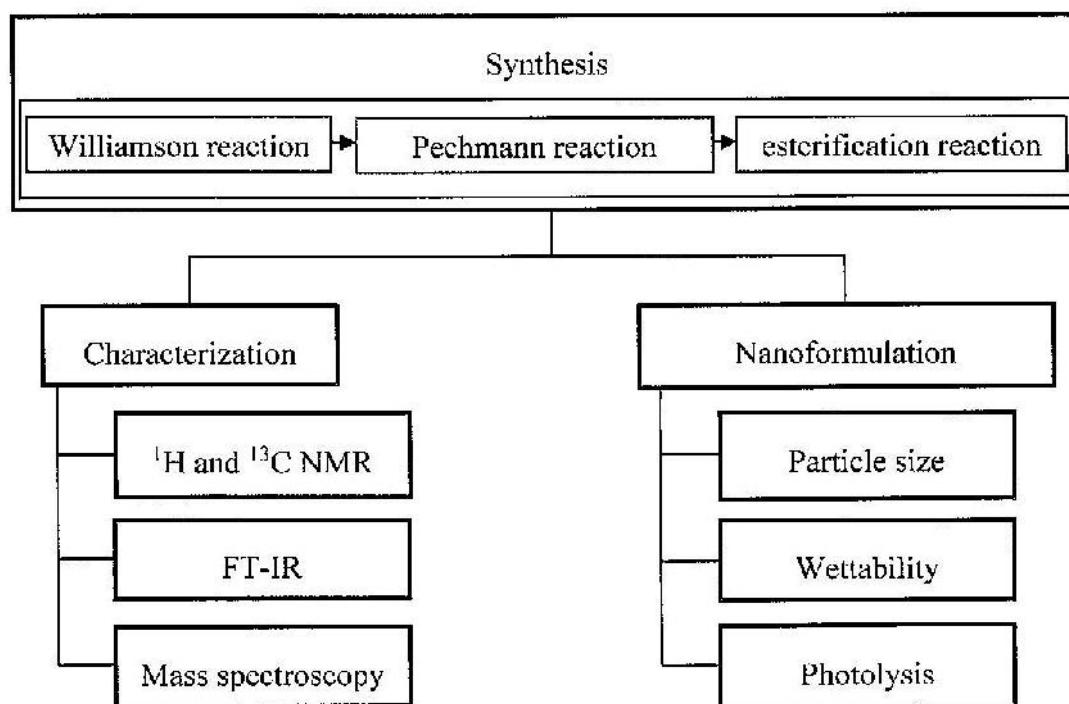
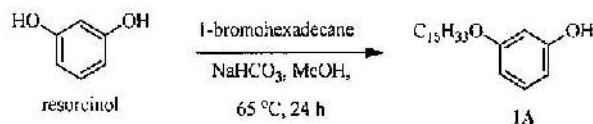


Figure 3.1 Experimental chart model of this work

3.3.1 Williamson reaction

3.3.1.1 Synthesis of 3-(hexadecyloxy)phenol (1A)



Compound **1A** was prepared by Williamson reaction. The mixture of resorcinol (0.5 g, 4.5 mmol), 1-bromohexadecane (1.4 ml, 4.5 mmol) and sodium hydrogen carbonate (NaHCO_3) (0.8 g, 9 mmol) was heated at 65 °C in methanol for 24 h. After cooling down to room temperature, the reaction was extracted with dichloromethane (DCM), dried over Na_2SO_4 and evaporated to dryness. The residue was purified by column chromatography using 40% DCM:hexane as eluent and solvent were removed by rotary evaporator to get the white solid product (0.471 g, 31%).

Compound **1A**: 3-(hexadecyloxy)phenol



^1H NMR (300 MHz, CDCl_3):

δ = 7.12 (t, $J = 10.4$, 1H, Ar-*H*)
 6.48 (d, $J = 8.1$ Hz, 1H, Ar-*H*)
 6.44 – 6.34 (m, 2H, Ar-*H*)
 4.94 – 4.75 (m, 1H, OH)
 3.92 (t, $J = 6.5$ Hz, 2H, OCH_2)
 1.87 – 1.67 (m, 2H, OCH_2CH_2)
 1.41 – 1.26 (m, 26H, $(\text{CH}_2)_{13}$)
 0.88 (t, $J = 6.4$ Hz, 3H, CH_3)

^{13}C NMR (75 MHz, CDCl_3):

δ = 160.5, 156.6, 130.0, 107.5, 107.1, 102.0, 68.0, 31.9, 29.7-
 29.2(11C), 26.0, 22.6, 14.1

FT-IR (ATR):

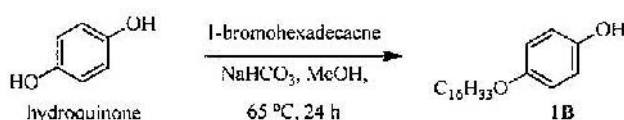
$$\nu_{\max} = 3447, 2915, 2848, 1595, 1180 \text{ cm}^{-1}$$

HRMS (ESI):

calculated for $\text{C}_{22}\text{H}_{39}\text{O}_2$ $[\text{M}+\text{H}^+] = 335.2950 \text{ m/z}$

found $[\text{M}+\text{H}^+] = 335.2952 \text{ m/z}$

3.3.1.2 Synthesis of 4-(hexadecyloxy)phenol (**1B**)



4-(hexadecyloxy)phenol (**1B**) was synthesized using a similar route as used for the synthesis of **1A**, except the hydroquinone was used instead of resorcinol to get the white solid product (0.379 g, 25%).

Compound **1B**: 4-(hexadecyloxy)phenol



^1H NMR (300 MHz, CDCl_3):

- $\delta = 6.76$ (m, 4H, Ar-H)
- 4.60 (s, 1H, OH)
- 3.88 (t, $J = 6.2$ Hz, 2H, OCH_2)
- 1.87-1.68 (m, 2H, OCH_2CH_2)
- 1.42-1.26 (m, 26H, $(\text{CH}_2)_{13}$)
- 0.87 (t, $J = 6.1$ Hz, 3H, CH_3)

^{13}C NMR (75 MHz, CDCl_3):

- $\delta = 153.3, 149.2, 115.9(2\text{C}), 115.6(2\text{C}), 68.7, 31.9, 29.6-29.3(11\text{C}), 26.0,$
- 22.6, 14.1

FT-IR (ATR):

$$\nu_{\max} = 3434, 2916, 2849, 1513, 1231 \text{ cm}^{-1}$$

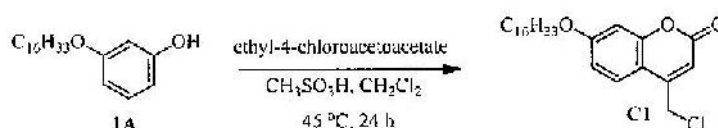
HRMS (ESI):

calculated for $C_{22}H_{39}O_2$ $[M+H]^+ = 335.2950$ m/z

found $[M+H]^+ = 335.2950$ m/z

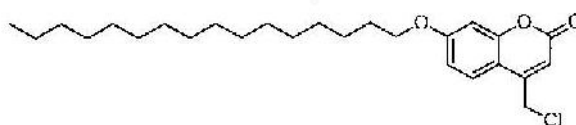
3.3.2 Pechmann reaction

3.3.2.1 Synthesis of 4-(chloromethyl)-7-(hexadecyloxy)-2H-chromen-2-one (C1)



A mixture of **1A** (0.2 g, 0.6 ml) in chloroform (3 ml) was slowly added by ethyl-4-chloroacetoacetate (0.13 ml, 0.9 mmol) and methanesulfonic acid (1 mL, dropwisely) at room temperature. The mixture was stirred at room temperature overnight. The reaction was monitored by TLC and completed reaction was extracted with dichloromethane. The combined organic extracts were concentrated on a rotary evaporator and the residue was purified by column chromatography using 50% DCM: hexane as eluent. The solvent was removed by rotary evaporator to give the coumarin product (0.132 g, 58%).

Compound **C1**: 4-(chloromethyl)-7-(hexadecyloxy)-2H-chromen-2-one



1H NMR (300 MHz, $CDCl_3$):

δ = 7.55 (d, $J = 8.8$ Hz, 1H, Ar-*H*)

6.88 (d, $J = 8.8$ Hz, 1H, Ar-*H*)

6.84 (s, 1H, Ar-*H*)

6.39 (s, 1H, =CH)

4.62 (s, 2H, -CH₂Cl)

4.02 (t, $J = 6.5$ Hz, 2H, OCH₂)

1.80 (m, 2H, OCH₂CH₂)
 1.46-1.26 (m, 26H, (CH₂)₁₃)
 0.88 (t, *J* = 6.4 Hz, 3H, CH₃)

¹³C NMR (75 MHz, CDCl₃):

δ = 162.6, 160.8, 155.7, 149.6, 125.0, 113.0, 112.4, 110.5, 101.7, 68.7,
 41.3, 31.9, 29.6-28.9(11C), 25.9, 22.6, 14.1

FT-IR (ATR):

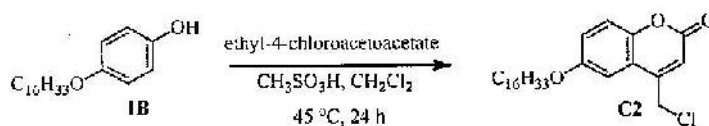
ν_{max} = 2918, 2850, 1702, 1282, 769 cm⁻¹

HRMS (ESI):

calculated for C₂₆H₄₀ClO₃ [M+H]⁺ = 435.2666 *m/z*

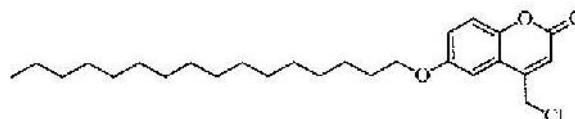
found [M+H]⁺ = 435.2666 *m/z*

3.3.1.5 Synthesis of 4-(chloromethyl)-6-(hexadecyloxy)-2*H*-chromen-2-one (C2)



Compound **C2** was synthesized using a similar route as used for the synthesis of **C1**, except compound **1B** was used instead of **1A** to give the coumarin product (0.155 g, 60%).

Compound **C2**: 4-(chloromethyl)-6-(hexadecyloxy)-2*H*-chromen-2-one



¹H NMR (300 MHz, CDCl₃):

δ = 7.30 (d, *J* = 9.0 Hz, 1H, Ar-*H*)
 7.14 (d, *J* = 9.0 Hz, 1H, Ar-*H*)
 7.08 (s, 1H, Ar-*H*)
 6.58 (s, 1H, =CH)

4.65 (s, 2H, $-\text{CH}_2\text{Cl}$)
 4.00 (t, $J = 6.2$ Hz, 2H, OCH_2)
 1.77 (m, 2H, OCH_2CH_2)
 1.66-1.10 (m, 26H, $(\text{CH}_2)_{13}$)
 0.87 (t, $J = 6.3$ Hz, 3H, CH_3)

^{13}C NMR (75 MHz, CDCl_3):

$\delta = 160.4, 155.6, 149.1, 148.1, 119.8, 118.3, 117.7, 116.2, 107.8, 68.8,$
 41.3, 31.9, 29.6-29.1(11C), 26.0, 22.6, 14.1

FT-IR (ATR):

$\nu_{\text{max}} = 2913, 2849, 1782, 1248, 734 \text{ cm}^{-1}$

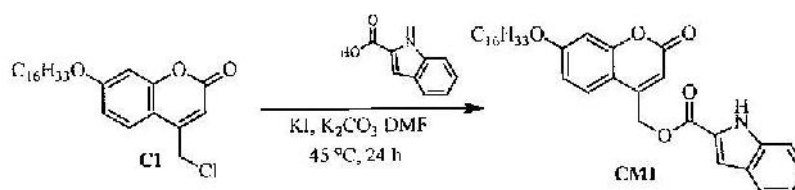
HRMS (ESI):

calculated for $\text{C}_{26}\text{H}_{40}\text{ClO}_3$ $[\text{M}+\text{H}^+] = 435.2666 \text{ m/z}$

found $[\text{M}+\text{H}^+] = 435.2666 \text{ m/z}$

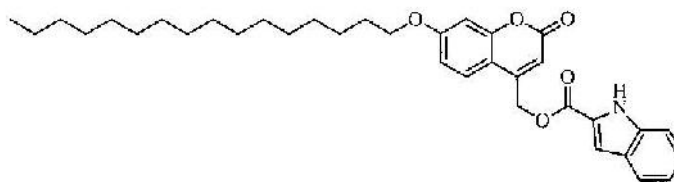
3.3.3 Esterification reaction

3.3.3.1 Synthesis of (7-(hexadecyloxy)-2-oxo-2H-chromen-4-yl)methyl 1H-indole-2-carboxylate (**CM1**)



Compound **CM1** was synthesized by esterification reaction. 7-Hexadecylcoumarin (**C1**) (0.1 g, 0.23 mmol) was dissolved in dry N,N -dimethylformamide (DMF) (6 ml). Potassium iodide (0.02 g, 0.12 mmol), potassium carbonate (0.064 g, 0.28 mmol) and 2-indolecarboxylic acid (0.037 g, 0.23 mmol) were added to the solution. The reaction mixture was stirred at 60°C for 2 h and monitored by TLC. After completion of the reaction, the crude residue was washed with brine and extracted with ethyl acetate. The organic layer was dried over Na_2SO_4 and evaporated under vacuum. The residue was separated by column chromatography using 50% EtOAc in hexane as eluent to give white solid photoresponsive coumarin **CM1** (40 mg, 24%).

Compound **CM1**: (7-(hexadecyloxy)-2-oxo-2*H*-chromen-4-yl)methyl 1*H*-indole-2-carboxylate



^1H NMR (300 MHz, CDCl_3):

δ = 8.92 (s, 1H, *NH*)
 7.73 (d, J = 8.2 Hz, 1H, Ar-*H*)
 7.52-7.37 (m, 4H, Ar-*H*)
 7.19 (t, J = 7.3 Hz, 1H, Ar-*H*)
 6.88 (m, 2H, Ar-*H*)
 6.47 (s, 1H, =CH)
 5.53 (s, 2H, -CH₂-O)
 4.03 (t, J = 6.4 Hz, 2H, OCH₂)
 1.82 (m, 2H, OCH₂CH₂)
 1.64 – 1.15 (m, 26H, (CH₂)₁₃)
 0.87 (t, J = 6.9 Hz, 3H, CH₃)

^{13}C NMR (75 MHz, CDCl_3):

δ = 162.5, 160.9, 155.6, 154.8, 143.9, 137.1, 127.5, 126.0, 125.9, 124.4,
 122.9, 121.1, 113.1, 111.9, 110.4, 110.0, 101.7, 68.7, 61.5, 31.8, 29.9-
 28.5(11C), 26.0, 22.4, 13.9

FT-IR (ATR):

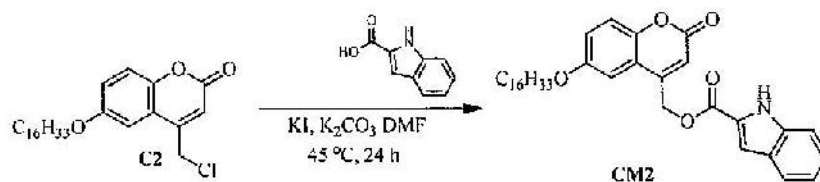
ν_{max} = 3287, 2915, 2849, 1693, 1624, 1296 cm^{-1}

HRMS (ESI):

calculated for $\text{C}_{35}\text{H}_{46}\text{NO}_5$ [$\text{M}+\text{H}^+$] = 560.3376 m/z

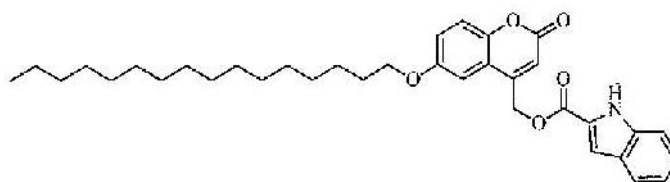
found [$\text{M}+\text{H}^+$] = 560.3376 m/z

3.3.3.7 Synthesis of (6-(hexadecyloxy)-2-oxo-2*H*-chromen-4-yl)methyl 1*H*-indole-2-carboxylate (**CM2**)



Compound **CM2** was carried out by simple esterification as follows: 6-hexadecylcoumarin (**C2**) (0.1 g, 0.23 mmol) was dissolved in dry *N,N*-dimethylformamide (DMF) (6 ml). Potassium iodide (0.02 g, 0.12 mmol), potassium carbonate (0.064 g, 0.28 mmol) and 2-indolecarboxylic acid (0.037 g, 0.23 mmol) were added to the solution. The reaction mixture was stirred at 60 °C for 2 h and monitored by TLC. After completion of the reaction, the crude residue was washed with brine and extracted with ethyl acetate. The organic layer was dried over Na_2SO_4 and evaporated under vacuum. The residue was separated by column chromatography using 50% EtOAc in hexane as eluent to give white solid photoresponsive coumarin **CM2** (78 mg, 44%).

Compound **CM2**: (6-(hexadecyloxy)-2-oxo-2*H*-chromen-4-yl)methyl 1*H*-indole-2-carboxylate



^1H NMR (300 MHz, CDCl_3):

- δ = 8.98 (s, 1H, *NH*)
- 7.73 (d, J = 8.1 Hz, 1H, Ar-*H*)
- 7.47 (d, J = 8.3 Hz, 1H, Ar-*H*)
- 7.42 – 7.29 (m, 3H, Ar-*H*)
- 7.18 (m, 2H, Ar-*H*)
- 6.99 (s, 1H, Ar-*H*)

6.66 (s, 1H, =CH)
 5.55 (s, 2H, -CH₂-OC=O)
 3.98 (t, *J* = 6.2 Hz, 2H, OCH₂)
 1.95–1.67 (m, 2H, OCH₂CH₂)
 1.36 (m, 26H, (CH₂)₁₃)
 0.87 (t, *J* = 6.5 Hz, 3H, CH₃)

¹³C NMR (75 MHz, CDCl₃):

δ = 160.9, 160.6, 155.7, 148.6, 147.9, 137.2, 127.3, 126.1, 125.7, 122.8,
 121.2, 119.9, 118.3, 117.4, 113.6, 111.9, 110.1, 106.9, 68.9, 61.4,
 31.9, 29.7–29.1(11C), 25.9, 22.6, 14.1

FT-IR (ATR):

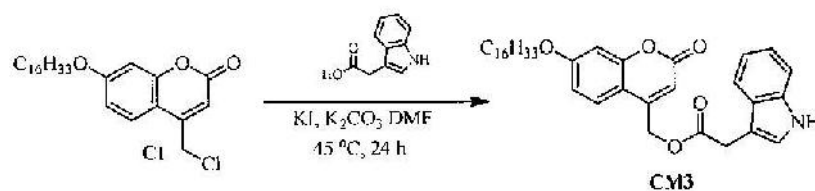
ν_{max} = 3280, 2915, 2848, 1712, 1578, 1248 cm⁻¹

HRMS (ESI):

calculated for C₃₅H₄₆NO₅ [M+H⁺] = 560.3376 m/z

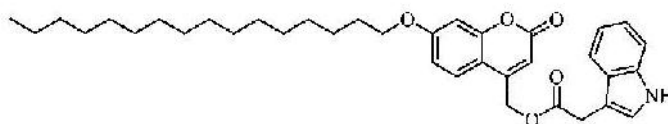
found [M+H⁺] = 560.3376 m/z

3.3.3.2 Synthesis of (7-(hexadecyloxy)-2-oxo-2*H*-chromen-4-yl)methyl 2-(1*H*-indol-3-yl)acetate (**CM3**)



Compound **CM3** was synthesized using a similar route as used for the synthesis of **CM1**, except 3-indoleacetic acid was used instead of 2-indolecarboxylic acid to give photoresponsive coumarin **CM3** (73 mg, 40 %).

Compound **CM3**: (7-(hexadecyloxy)-2-oxo-2H-chromen-4-yl)methyl 2-(1H-indol-3-yl) acetate



^1H NMR (300 MHz, CDCl_3):

δ = 8.17 (s, 1H, NH)
 7.62 (d, J = 7.8 Hz, 1H, Ar- H)
 7.39 (d, J = 8.0 Hz, 1H, Ar- H)
 7.34 – 7.06 (m, 4H, Ar- H)
 6.80 (s, 1H, Ar- H)
 6.75 (d, J = 8.9 Hz, 1H)
 6.24 (s, 1H, =CH)
 5.26 (s, 2H, $\text{CH}_2\text{-OC=O}$)
 3.99 (t, J = 6.4 Hz, 2H, OCH_2)
 3.92 (s, 2H, $-\text{CH}_2\text{-C=O}$)
 1.87 – 1.68 (m, 2H, OCH_2CH_2)
 1.65 – 1.08 (m, 26H, $(\text{CH}_2)_{13}$)
 0.87 (t, J = 6.3 Hz, 3H, CH_3)

^{13}C NMR (75 MHz, CDCl_3):

δ = 171.1, 162.4, 161.0, 155.4, 149.2, 136.1, 127.0, 124.4, 123.2, 122.4,
 119.8, 118.6, 112.9, 111.3, 110.3, 109.8, 107.6, 101.6, 68.6, 61.5,
 31.9, 31.2, 29.6-28.9(11C), 25.9, 22.6, 14.1

FT-IR (ATR):

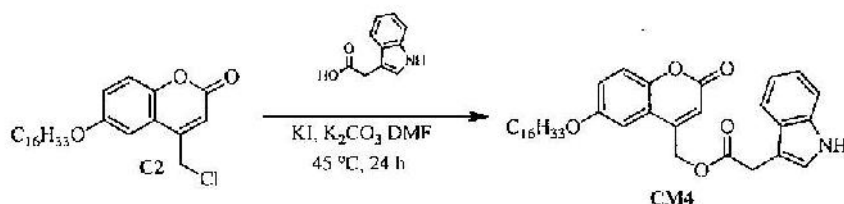
ν_{max} = 3396, 2916, 2852, 1723, 1698, 1620, 1300 cm^{-1}

HRMS (ESI):

calculated for $\text{C}_{36}\text{H}_{48}\text{NO}_5$ $[\text{M}+\text{H}^+] = 573.3532$ m/z

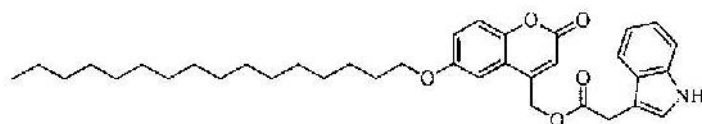
found $[\text{M}+\text{H}^+] = 573.3535$ m/z

3.3.3.8 Synthesis of (6-(hexadecyloxy)-2-oxo-2*H*-chromen-4-yl)methyl 2-(1*H*-indol-3-yl)acetate (**CM4**)



Compound **CM4** was synthesized using a similar route as used for the synthesis of **CM2**, except 3-indoleacetic acid was used instead of 2-indolecarboxylic acid to give photoresponsive coumarin **CM4** (42 mg, 23%).

Compound **CM4**: (6-(hexadecyloxy)-2-oxo-2*H*-chromen-4-yl)methyl 2-(1*H*-indol-3-yl)acetate



^1H NMR (300 MHz, CDCl_3):

- δ = 8.17 (s, 1H, NH)
- 7.62 (d, $J = 7.5$ Hz, 1H, Ar-*H*)
- 7.39 (d, $J = 7.9$ Hz, 1H, Ar-*II*)
- 7.24-7.13 (m = 5H, Ar-*H*)
- 6.84 (s, 1H, Ar-*H*)
- 6.41 (s, 1H, =CH)
- 5.28 (s, 2H, $\text{CH}_2\text{-OC=O}$)
- 3.94 (s, 2H, $\text{CH}_2\text{-C=O}$)
- 3.88 (t, 2H, OCH_2)
- 1.76 (m, 2H, OCH_2CH_2)
- 1.43-1.25 (m, 26H, $(\text{CH}_2)_{13}$)
- 0.88 (t, $J = 6.4$ Hz, 3H, CH_3)

^{13}C NMR (75 MHz, CDCl_3):

δ = 171.1, 160.6, 155.6, 148.7, 147.8, 136.1, 127.0, 123.2, 122.4, 119.9,
119.8, 118.6, 118.2, 117.4, 113.4, 111.3, 107.6, 106.8, 68.8, 61.3,
31.9, 31.2, 29.6-29.1(11C), 25.9, 22.6, 14.1

FT-IR (ATR):

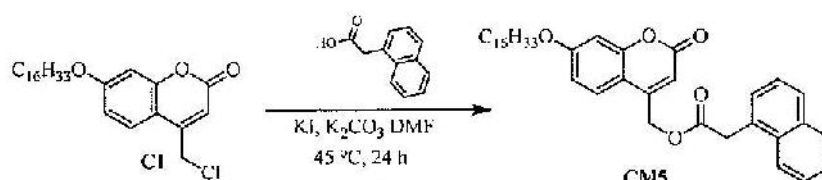
ν_{max} = 3360, 2921, 2851, 1723, 1249 cm^{-1}

HRMS (ESI):

calculated for $\text{C}_{36}\text{H}_{48}\text{NO}_5$ $[\text{M}+\text{H}^+]$ = 574.3532 m/z

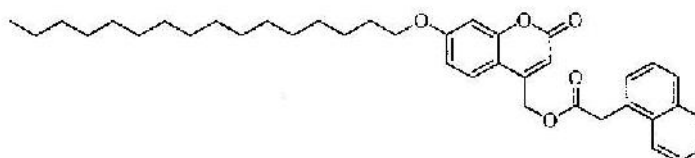
found $[\text{M}+\text{H}^+]$ = 574.3533 m/z

3.3.3.3 Synthesis of (7-(hexadecyloxy)-2-oxo-2*H*-chromen-4-yl)methyl 2-(naphthalen-1-yl)acetate (**CM5**)



Compound **CM5** was synthesized using a similar route as used for the synthesis of **CM1**, except 1-naphthaleneacetic acid was used instead of 2-indolecarboxylic acid to give photoresponsive coumarin **CM5**. (82 mg, 48%).

Compound **CM5**: (7-(hexadecyloxy)-2-oxo-2*H*-chromen-4-yl)methyl 2-(naphthalene-1-yl)acetate



^1H NMR (300 MHz, CDCl_3):

δ = 7.98 (d, J = 8.0 Hz, 1H, Ar-*H*)
7.85 (dd, J = 18.4, 5.9 Hz, 2H, Ar-*H*)
7.65–7.49 (m, 4H, Ar-*H*)

7.46 (d, $J = 4.3$ Hz, 1H, Ar-*H*)
 7.21 (d, $J = 8.8$ Hz, 2H, Ar-*H*)
 6.78 (s, 1H, Ar-*H*)
 6.71 (d, $J = 8.3$ Hz, 1H, Ar-*H*)
 6.17 (s, 1H, =CH)
 5.23 (s, 2H, CH₂-OC=O)
 4.21 (s, 2H, Ar-CH₂-C=O)
 3.99 (t, $J = 6.3$ Hz, 2H, OCH₂)
 1.91–1.65 (m, 2H, OCH₂CH₂)
 1.59–1.16 (m, 26H, (CH₂)₁₃)
 0.87 (d, $J = 6.8$ Hz, 3H, CH₃)

¹³C NMR (75 MHz, CDCl₃):

δ = 170.7, 162.3, 160.7, 155.4, 148.8, 133.8, 131.9, 129.6, 128.8, 128.4,
 128.2, 126.5, 125.9, 125.5, 124.3, 123.4, 112.8, 110.3, 110.1, 101.6,
 68.6, 61.8, 39.0, 31.9, 29.6–28.9 (11C), 25.9, 22.6, 14.1

FT-IR (ATR):

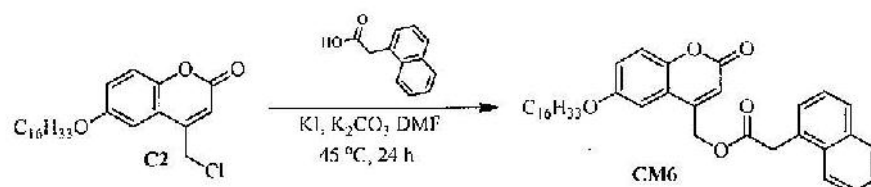
ν_{max} = 2917, 2850, 1730, 1615, 1511, 1261 cm⁻¹

HRMS (ESI):

calculated for C₃₈H₄₉O₅ [M+H⁺] = 585.3580 m/z

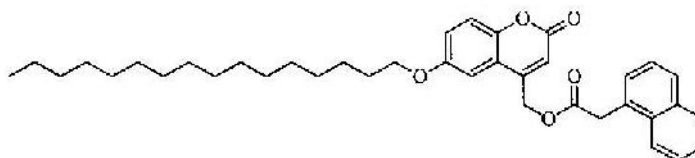
found [M+H⁺] = 585.3587 m/z

3.3.3.9 Synthesis of (6-(hexadecyloxy)-2-oxo-2*H*-chromen-4-yl)methyl 2-(naphthalen-1-yl)acetate (**CM6**)



Compound **CM6** was synthesized using a similar route as used for the synthesis of **CM2**, except 1-naphthaleneacetic acid was used instead of 2-indolecarboxylic acid to give photoresponsive coumarin **CM6** (130 mg, 47%).

Compound **CM6**: (6-(hexadecyloxy)-2-oxo-2*H*-chromen-4-yl)methyl 2-(naphthalene-1-yl)acetate



^1H NMR (300 MHz, CDCl_3):

δ = 7.97 (d, J = 7.2 Hz, 1H, Ar-*H*)
 7.94 – 7.69 (m, 2H, Ar-*H*)
 7.69 – 7.36 (m, 3H, Ar-*H*)
 7.25 (d, J = 8.9 Hz, 2H, Ar-*H*)
 7.08 (dd, J = 8.9 Hz, 1H, Ar-*H*)
 6.76 (s, 1H), 6.33 (s, 1H, Ar-*H*)
 5.25 (s, 2H, $\text{CH}_2\text{-OC=O}$)
 4.21 (s, 2H, Ar- $\text{CH}_2\text{-C=O}$)
 3.82 (t, J = 6.2 Hz, 2H, OCH_2)
 1.83–1.57 (m, 2H, OCH_2CH_2)
 1.51–1.15 (m, 26H, $(\text{CH}_2)_{13}$)
 0.87 (t, J = 6.6 Hz, 3H, CH_3)

^{13}C NMR (75 MHz, CDCl_3):

δ = 170.7, 160.4, 155.6, 148.3, 147.8, 133.8, 131.9, 129.6, 128.8, 128.4,
 128.1, 126.5, 125.9, 125.5, 123.4, 119.8, 118.1, 117.3, 113.8, 106.7,
 68.7, 61.5, 39.0, 31.9, 29.6–29.1 (11C), 25.9, 22.6, 14.1

FT-IR (ATR):

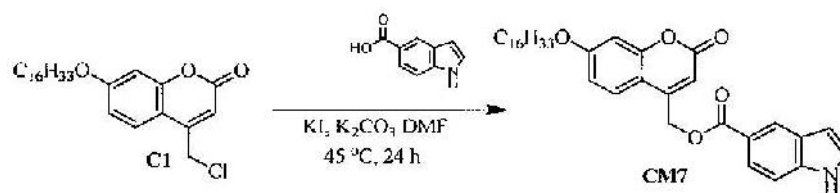
ν_{max} = 2919, 2850, 1737, 1717, 1570, 1255 cm^{-1}

HRMS (ESI):

calculated for $\text{C}_{38}\text{H}_{49}\text{O}_5$ [$\text{M} + \text{H}^+$] = 585.3580 m/z

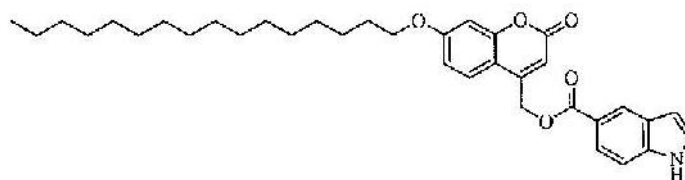
found [$\text{M} + \text{H}^+$] = 585.3583 m/z

3.3.3.4 Synthesis of (7-(hexadecyloxy)-2-oxo-2*H*-chromen-4-yl)methyl 1*H*-indole-5-carboxylate (**CM7**)



Compound **CM7** was synthesized using a similar route as used for the synthesis of **CM1**; except indole-5-carboxylic acid was used instead of 2-indolecarboxylic acid to give photoresponsive coumarin **CM7** (55 mg, 34%).

Compound **CM7**: (7-(hexadecyloxy)-2-oxo-2*H*-chromen-4-yl)methyl 1*H*-indole-5-carboxylate



^1H NMR (300 MHz, CDCl_3):

- δ = 8.50 (m, 2H, NH)
- 7.97 (d, J = 8.6 Hz, 1H, Ar-*Id*)
- 7.51 (d, J = 8.6 Hz, 1H, Ar-*H*)
- 7.46 (d, J = 8.6 Hz, 1H, Ar-*H*)
- 7.32 (s, 1H, Ar-*Id*)
- 6.88 (m, 2H, Ar-*H*)
- 6.70 (s, 1H, Ar-*H*)
- 6.53 (s, 1H, =CH)
- 5.53 (s, 2H, $\text{CH}_2\text{-OC=O}$)
- 4.03 (t, J = 6.4 Hz, 2H, OCH_2)
- 1.93–1.71 (m, J = 14.1, 6.7 Hz, 2H, OCH_2CH_2)
- 1.54 – 1.10 (m, J = 63.6 Hz, 26H, $(\text{CH}_2)_{13}$)

0.88 (t, $J = 6.3$ Hz, 3H, CH_3)

^{13}C NMR (75 MHz, CDCl_3):

$\delta = 166.7, 162.4, 161.2, 155.5, 149.9, 138.7, 127.6, 125.8, 124.4, 124.2, 123.5, 120.7, 113.0, 111.0, 110.6, 109.7, 104.2, 101.7, 68.7, 61.3, 31.9, 29.6\text{--}28.9(11\text{C}), 25.9, 22.6, 14.1$

FT-IR (ATR):

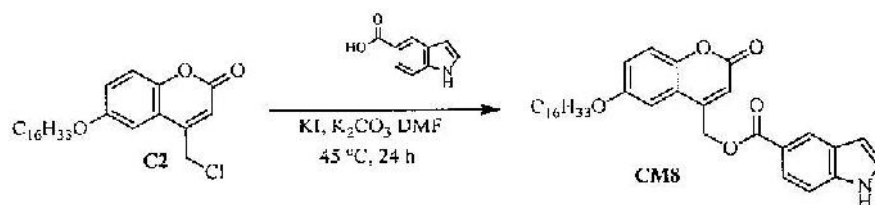
$\nu_{\text{max}} = 3329, 2916, 1850, 1702, 1519, 1149 \text{ cm}^{-1}$

HRMS (ESI):

calculated for $\text{C}_{35}\text{H}_{46}\text{NO}_5$ $[\text{M} + \text{H}^+] = 560.3376 \text{ m/z}$

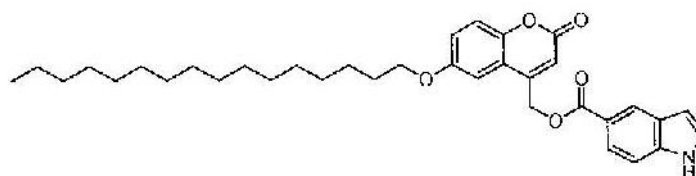
found $[\text{M} + \text{H}^+] = 560.3370 \text{ m/z}$

3.3.3.10 Synthesis of (6-(hexadecyloxy)-2-oxo-2H-chromen-4-yl)methyl 1H-indole-5-carboxylate (**CM8**)



Compound **CM8** was synthesized using a similar route as used for the synthesis of **CM2**, except indole-5-carboxylic acid was used instead of 2-indolecarboxylic acid to give photoresponsive coumarin **CM8** (49 mg, 30%).

Compound **CM8**: (6-(hexadecyloxy)-2-oxo-2H-chromen-4-yl)methyl 1H-indole-5-carboxylate



^1H NMR (300 MHz, CDCl_3):

δ = 8.51 (s, 1H, Ar-H)
 8.46 (s, 1H, NH)
 7.98 (d, J = 9.0 Hz, 1H, Ar-H)
 7.46 (d, J = 8.6 Hz, 1H, Ar-H)
 7.38–7.28 (m, 2H, Ar-H)
 7.15 (m, 1H, Ar-H)
 7.02 (m, 2H, Ar-H)
 6.71 (s, 2H, Ar-H)
 5.55 (s, 2H, $\text{CH}_2\text{-OC=O}$)
 3.98 (t, J = 6.4 Hz, 2H, OCH_2)
 1.97–1.65 (m, 2H, OCH_2CH_2)
 1.53–1.05 (m, 26H, $(\text{CH}_2)_{13}$)
 0.88 (t, J = 6.3 Hz, 3H, CH_3)

^{13}C NMR (75 MHz, CDCl_3):

δ = 166.7, 160.8, 155.7, 149.4, 147.9, 138.7, 127.6, 125.8, 124.2, 123.5,
 120.6, 119.9, 118.2, 117.6, 113.3, 111.0, 106.8, 104.2, 68.9, 61.2,
 31.9, 29.6–29.1(11C), 25.9, 22.6, 14.1

FT-IR (ATR):

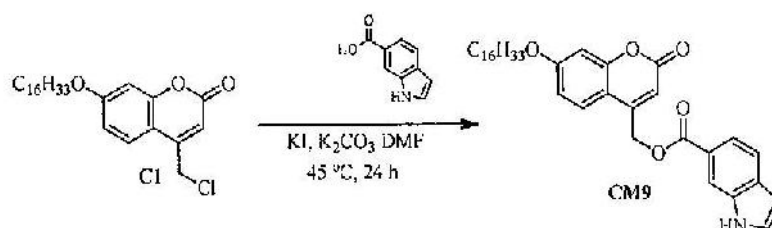
ν_{max} = 3320, 2916, 2849, 1713, 1575, 1264 cm^{-1}

HRMS (ESI):

calculated for $\text{C}_{35}\text{H}_{46}\text{NO}_5$ $[\text{M}+\text{H}^+] = 560.3376$ m/z

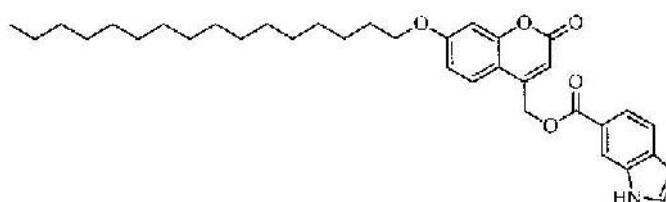
found $[\text{M}+\text{H}^+] = 560.3372$ m/z

3.3.3.5 Synthesis of (7-(hexadecyloxy)-2-oxo-2H-chromen-4-yl)methyl 1H-indole-6-carboxylate (CM9)



Compound **CM9** was synthesized using a similar route as used for the synthesis of **CM1**, except indole-6-carboxylic acid was used instead of 2-indolecarboxylic acid to photoresponsive coumarin **CM9**. (41 mg, 25%).

Compound **CM9**: (7-(hexadecyloxy)-2-oxo-2H-chromen-4-yl)methyl 1H-indole-6-carboxylate



¹H NMR (300 MHz, CDCl₃):

- δ = 8.56 (s, 1H, NH)
- 8.24 (s, 1H, Ar-H)
- 7.88 (d, J = 7.9 Hz, 1H, Ar-H)
- 7.70 (d, J = 8.0 Hz, 1H, Ar-H)
- 7.50 (d, J = 8.3 Hz, 1H, Ar-H)
- 7.43 (s, 1H, Ar-H)
- 6.88 (m, 2H, Ar-H)
- 6.64 (s, 1H, Ar-H)
- 6.52 (s, 1H, =CH)
- 5.53 (s, 2H, CH₂-OC=O)
- 4.02 (t, J = 6.4 Hz, 2H, OCH₂)

1.98 – 1.71 (m, 2H, OCH₂CH₂)

1.58 – 1.10 (m, $J = 60.3$ Hz, 26H, (CH₂)₁₃)

0.88 (t, $J = 6.3$ Hz, 3H, CH₃)

¹³C NMR (75 MHz, CDCl₃):

δ = 166.6, 162.5, 161.2, 155.5, 149.8, 135.1, 132.1, 128.0, 124.4, 122.3,
121.0, 120.6, 113.7, 113.1, 110.5, 109.7, 103.2, 101.7, 68.7, 61.4,
31.9, 29.6-29.3(10C), 28.9, 25.9, 22.6, 14.1

FT-IR (ATR):

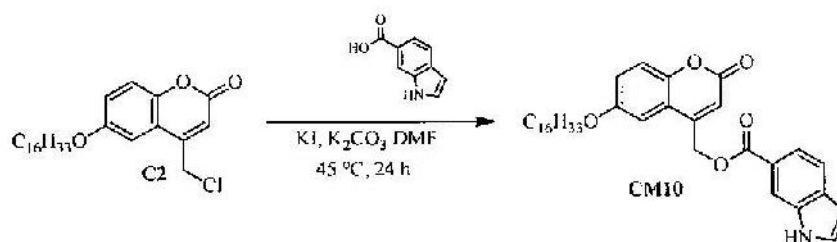
ν_{max} = 3415, 2916, 2850, 1715, 1698, 1520 cm⁻¹

HRMS (ESI):

calculated for C₃₅H₄₆NO₅ [M+H⁺] = 560.3376 m/z

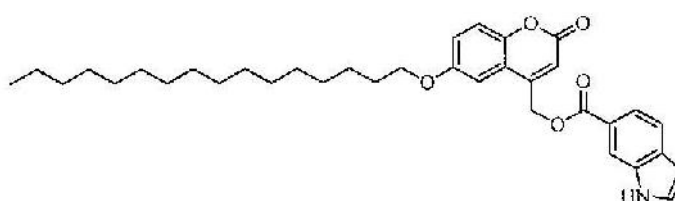
found [M+H⁺] = 560.3370 m/z

3.3.3.11 Synthesis of (6-(hexadecyloxy)-2-oxo-2*H*-chromen-4-yl)methyl 1*H*-indole-6-carboxylate (**CM10**)



Compound **CM10** was synthesized using a similar route as used for the synthesis of **CM2**, except indole-6-carboxylic acid was used instead of 2-indolecarboxylic acid to give photoresponsive coumarin **CM10** (33 mg, 20%).

Compound **CM10**: (6-(hexadecyloxy)-2-oxo-2*H*-chromen-4-yl)methyl 1*H*-indole-6-carboxylate



^1H NMR (300 MHz, CDCl_3):

δ = 8.59 (s, 1H, NH)
 8.25 (s, 1H, Ar-H)
 7.89 (d, J = 8.3 Hz, 1H, Ar-H)
 7.71 (d, J = 8.3 Hz, 1H, Ar-H)
 7.44 (s, 1H, Ar-H)
 7.32 (d, J = 8.9 Hz, 1H, Ar-H)
 7.14 (d, J = 8.8 Hz, 1H, Ar-H)
 7.01 (s, 1H, Ar-H)
 6.70 (s, 1H, Ar-H)
 6.64 (s, 1H, =CH)
 5.54 (s, 2H, $\text{CH}_2\text{-OC-O}$)
 3.97 (t, J = 6.2 Hz, 2H, OCH_2)
 1.95–1.70 (m, 2H, OCH_2CH_2)
 1.56–1.10 (m, 26H, $(\text{CH}_2)_{13}$)
 0.87 (t, J = 6.3 Hz, 3H, CH_3)

^{13}C NMR (75 MHz, CDCl_3):

δ = 166.6, 160.8, 155.7, 149.4, 147.9, 135.1, 132.2, 128.1, 122.2, 121.0,
 120.6, 119.9, 118.3, 117.5, 113.7, 113.3, 106.8, 103.2, 68.9, 61.3,
 31.9, 29.6–29.1(11C), 25.9, 22.6, 14.1

FT-IR (ATR):

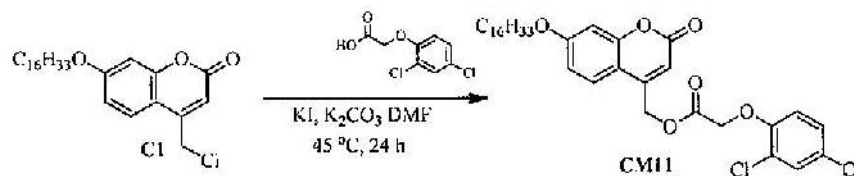
ν_{max} = 3325, 2915, 2849, 1710, 1299 cm^{-1}

HRMS (ESI):

calculated for $\text{C}_{35}\text{H}_{46}\text{NO}_5$ $[\text{M}+\text{H}^+]$ = 560.3376 m/z

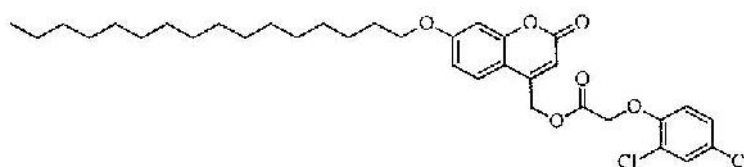
found $[\text{M}+\text{H}^+]$ = 560.3377 m/z

3.3.3.6 Synthesis of (7-(hexadecyloxy)-2-oxo-2*H*-chromen-4-yl)methyl 2-(2,4-dichlorophenoxy)acetate (**CM11**)



Compound **CM11** was synthesized using a similar route as used for the synthesis of **CM1**, except 2,4-dichlorophenoxyacetic acid was used instead of 2-indolecarboxylic acid to give photoresponsive coumarin **CM11** (80 mg, 44%).

Compound **CM11**: (7-(hexadecyloxy)-2-oxo-2*H*-chromen-4-yl)methyl 2-(2,4-dichlorophenoxy)acetate



^1H NMR (300 MHz, CDCl_3):

- δ = 7.55 – 7.29 (m, 2H, Ar-*H*)
- 7.14 (d, J = 8.6 Hz, 1H, Ar-*H*)
- 6.94 – 6.66 (m, 3H, Ar-*H*)
- 6.31 (s, 1H, =C*H*)
- 5.37 (s, 2H, $\text{CH}_2\text{-OC=O}$)
- 4.82 (s, 2H, $\text{OCH}_2\text{-C-O}$)
- 4.01 (t, J = 6.2 Hz, 2H, OCH_2)
- 1.82 (m, 2H, OCH_2CH_2)
- 1.55 – 1.03 (m, J = 62.6 Hz, 26H, $(\text{CH}_2)_{13}$)
- 0.87 (t, J = 6.6 Hz, 3H, CH_3)

^{13}C NMR (75 MHz, CDCl_3):

δ = 167.4, 162.6, 160.6, 155.6, 152.0, 147.9, 130.5, 127.5, 124.3, 114.7,
113.1, 110.6, 110.1, 101.7, 68.7, 66.2, 62.1, 31.9, 29.6-29.3(12C),
28.9, 25.9, 22.6, 14.1

FT-IR (ATR):

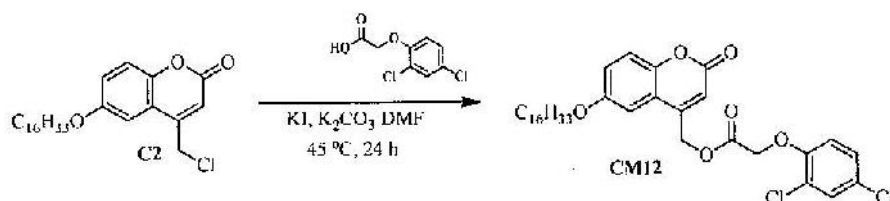
ν_{max} = 2918, 2850, 1767, 1710, 1610, 1227 cm^{-1}

HRMS (ESI):

calculated for $\text{C}_{34}\text{H}_{45}\text{Cl}_2\text{O}_5$ [$\text{M}^+ \text{H}^+$] = 619.2593 m/z

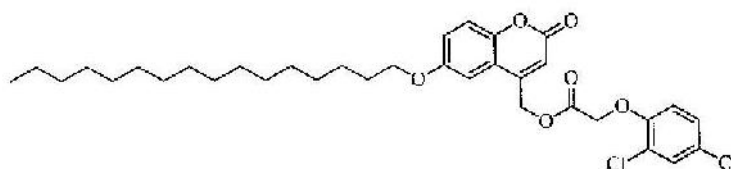
found [$\text{M}+\text{H}^+$] = 619.2593 m/z

3.3.3.12 Synthesis of (6-(hexadecyloxy)-2-oxo-2*H*-chromen-4-yl)methyl 2-(2,4-dichlorophenoxy)acetate (**CM12**)



Compound **CM12** was synthesized using a similar route as used for the synthesis of **CM2**, except 2,4-dichlorophenoxyacetic acid was used instead of 2-indolecarboxylic acid to give photoresponsive coumarin **CM12** (58 mg, 32%).

Compound **CM12**: (6-(hexadecyloxy)-2-oxo-2*H*-chromen-4-yl)methyl 2-(2,4-dichlorophenoxy)acetate



^1H NMR (300 MHz, CDCl_3):

δ = 7.38 (1H, Ar-H)
 7.29 (d, J = 9.1 Hz, 1H, Ar-H)
 7.13 (d, J = 8.8 Hz, 2H, Ar-H)
 6.87 (s, 1H, Ar-H)
 6.77 (d, J = 8.8 Hz, 1H, Ar-H)
 6.49 (s, 1H, =CH)
 5.38 (s, 2H, $\text{CH}_2\text{-OC=O}$)
 4.83 (s, 2H, $\text{O-CH}_2\text{-C=O}$)
 3.94 (t, J = 6.4 Hz, 2H, OCH_2)
 1.95–1.70 (m, 2H, OCH_2CH_2)
 1.67–1.04 (m, 26H, $(\text{CH}_2)_{13}$)
 0.87 (t, J = 6.2 Hz, 3H, CH_3)

^{13}C NMR (75 MHz, CDCl_3):

δ = 167.4, 160.3, 155.7, 152.0, 147.8, 147.4, 130.5, 127.5, 124.4, 119.7,
 118.3, 117.2, 114.7, 114.4, 107.0, 68.8, 66.3, 61.9, 31.9, 29.6-
 29.2(^{12}C), 26.0, 22.6, 14.1

FT-IR (ATR):

ν_{max} = 3216, 2849, 1758, 1720, 1573, 1242 cm^{-1}

HRMS (ESI):

calculated for $\text{C}_{34}\text{H}_{44}\text{Cl}_2\text{O}_5$ $[\text{M}+\text{H}^+] = 618.2515$ m/z

found $[\text{M}+\text{H}^+] = 618.2510$ m/z

3.4 Preparation of photoresponsive coumarin CM1-CM12 nanoemulsion

Photoresponsive compounds were dissolved in chloroform and varied the concentration of 0.15 - 0.25 wt.%. Poly(vinyl alcohol) (PVA) was dissolved in water to make aqueous solutions the concentration of 0 - 5 wt.%. Sodium dodecyl sulfate (SDS) was used as a surfactant and dissolved in aqueous PVA solutions at the concentration of 0 - 5 wt.% to form an oil-in-water emulsion. Then the photoresponsive solution was added into the aqueous PVA-SDS solution drop wise while stirring at room temperature. The volume ratio of oil phase to aqueous phase in the emulsions was 75:25.

3.4.1 Particle size and zeta potential analysis of photoresponsive coumarin CM1-CM12 nanoemulsion

Measurements of particle size distribution and zeta potential of nanoformulation prepared from target photoresponsive coumarin were conducted after the removal of chloroform. Measurements were done using a dynamic light scattering particle size analyzer (DLS) by using 600 ppm of formulation.

3.4.1 Wettability properties of photoresponsive coumarin CM1-CM12 nanoemulsion on the plant leaf surface

The contact angle analysis of 600 ppm photoresponsive nanoformulation were studied on the *Cassia fistula* leaves. The contact angle between droplet and plant leaf surface were measured by contact angle and droplet size analyzer.

3.4.2 Photolysis of photoresponsive coumarin CM1-CM12 nanoemulsion

A suspension of 200 ppm of CM1-CM12 were irradiated under UV light (365 nm) and sunlight for 7 hours daily for 5 days. The fluorescence decay of photoresponsive coumarin CM1-CM2 were monitored by UV-vis and fluorescence spectroscopy.

CHAPTER 4

RESULTS AND DISSCUSSIONS

4.1 Synthesis and characterization of novel photoresponsive coumarin

The photoresponsive coumarins (CM1-CM12) were prepared by using 3 steps synthesis as shown in Figure 4.1. The first step is Williamson ether synthesis reaction of resorcinol or hydroquinone with bromohexadecane to give 1A and 1B. The second step, coumarin intermediates (C1 and C2) were synthesized by Pechmann cyclization reaction of 1A or 1B. The last step is esterification reaction with plant hormones or herbicide to give CM1-CM12.

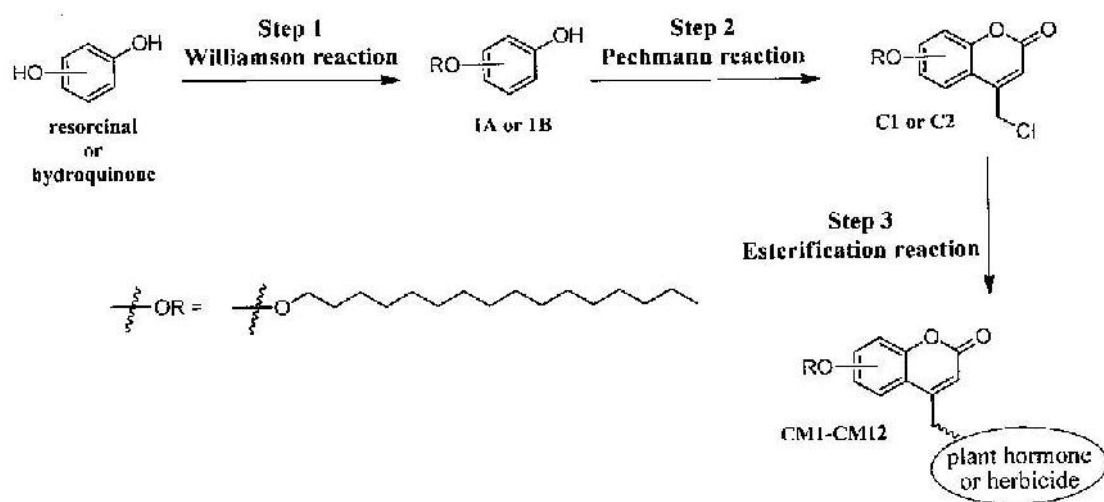


Figure 4.1 Synthetic route of the photoresponsive coumarin

4.1.1 Williamson ether synthesis reaction

The 3-(hexadecyloxy)phenol (**1A**) and 4-(hexadecyloxy)phenol (**1B**) were synthesized by the Williamson ether synthesis of resorcinol or hydroquinone with 1-bromohexadecane in the presence of sodium hydrogen carbonate as a base to get the resulting **1A** and **1B** products as a white solid in 31% and 25% yield, respectively shown in Figure 4.2.

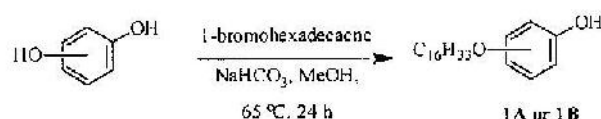


Figure 4.2 Synthetic method of 1A and 1B

The mechanism of the Williamson reaction of resorcinol is presented in Figure 4.3. The sodium phenoxide was generated by NaHCO_3 and followed by ether formation with hexadecyl bromide to obtain the target compounds as white solid. The results showed low yields (~30%) of monosubstituted as it can further form the disubstituted products with the recovery of resorcinol and hydroquinone.

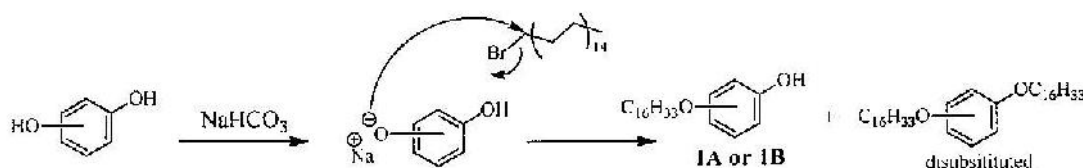


Figure 4.3 The mechanism of Williamson ether synthesis reaction

The chemical structure of **1A** was confirmed by ^1H NMR as it is shown in Figure 4.4. The spectra in CDCl_3 showed the chemical shift at 7.12 (1H), 6.48 (1H) and 6.44 – 6.34 (2H) ppm assigned as proton of phenol ring. The chemical shift at 3.92 (2H, OCH_2), 1.87 – 1.67 (2H, OCH_2CH_2), 1.41 – 1.26 (26H, $(\text{CH}_2)_{13}$) and 0.88 (t, $J = 6.4$ Hz, 3H, CH_3) ppm were assigned as the protons of the hexadecyloxy group. The chemical structure was confirmed by ^{13}C NMR with 16 alkyl and 6 aromatic carbons (Figure A.1, Appendix). Mass spectrum of the compound **1A** showed the peaks at 335.2952 m/z is assigned to $\text{M} + \text{H}^+$.

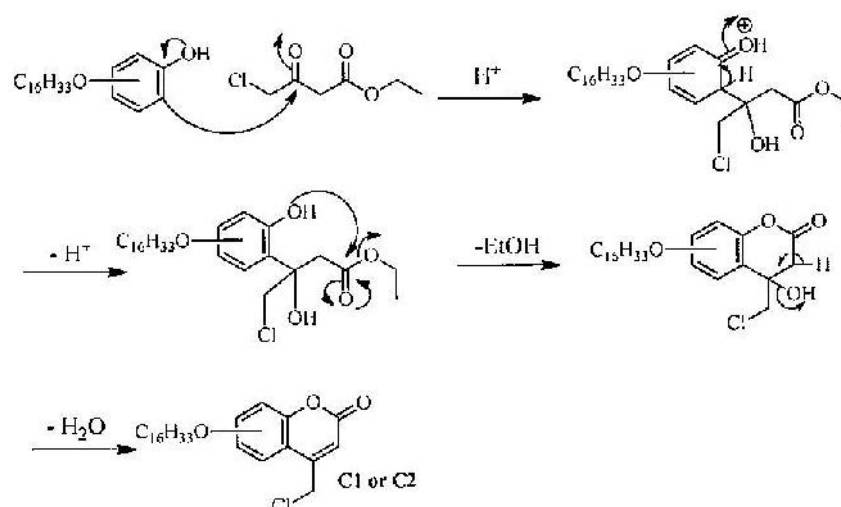


Figure 4.6 The mechanism of Pechmann coumarin synthesis

The products were characterized by ^1H , ^{13}C NMR and IR spectra. The ^1H NMR of **C1** in CDCl_3 show 9 signals of 39 protons (Figure 4.7). The two singlets signal at 6.84 and 6.39 ppm were assigned as H^8 and H^3 , respectively. The two doublets signal at 7.55 and 6.88 ppm were assigned to H^5 and H^6 , respectively. The H^5 showed in the downfield region due to conjugation with carbonyl group. The coupling constant of H^5 and H^6 was observed about 8.8 Hz. The singlet signal at 4.62 ppm (2H) was allyl methylene proton. The long alkyl chain was observed at 4.02 ppm (t, 2H), 1.92 ppm (m, 2H), 1.46-1.26 (m, 26H) and 0.88 (t, 3H). The ^{13}C spectra of this structure showed 26 carbons from 9 coumarin carbons, one signal of methylene group and alkoxy carbons. Furthermore, **C1** showed the IR peaks at $2,918\text{ cm}^{-1}$ from C-H stretching, $1,702\text{ cm}^{-1}$ from C=O vibration of lactone, $1,282\text{ cm}^{-1}$ from C-O stretching and 769 cm^{-1} from C-Cl signal. The molecular weight was confirmed by mass spectroscopy which showed the peaks at m/z 435.2666 assigned to $\text{M}+\text{H}^+$ (Figure A.5 and A.6, Appendix).

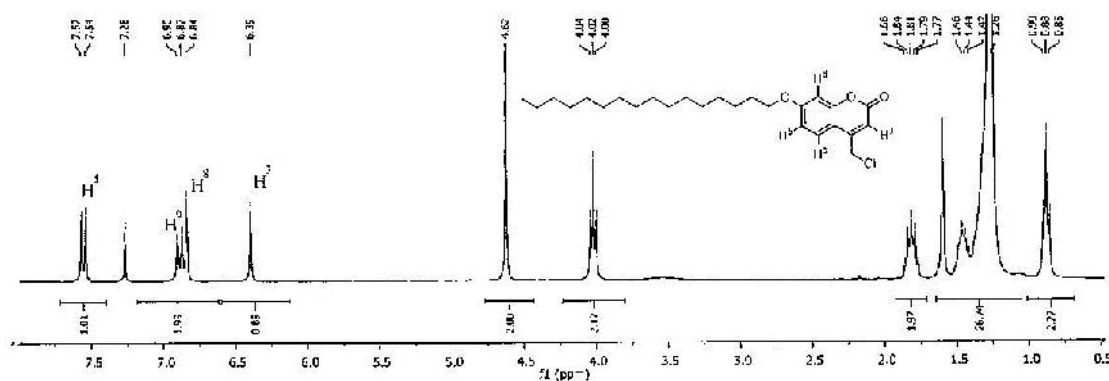


Figure 4.7 ^1H NMR spectrum of C1 in CDCl_3

^1H NMR spectra of C2 in Figure 4.8 gave 9 signals of 39 protons in molecule. The alkoxy protons were found similar to C1, whereas the protons of coumarin core chemical were observed as singlet signal at 6.58 ppm and doublet signal at 7.30 ppm assigning as proton H^1 and H^8 , respectively. Moreover, the H^5 and H^7 were assigned to singlet and doublet signals at 7.08 and 7.13 ppm, respectively. Mass spectrum showed the peaks at 435.2666 (m/z) assigning to $\text{M}+\text{H}^+$ (Figure A.7 and A.8, Appendix).

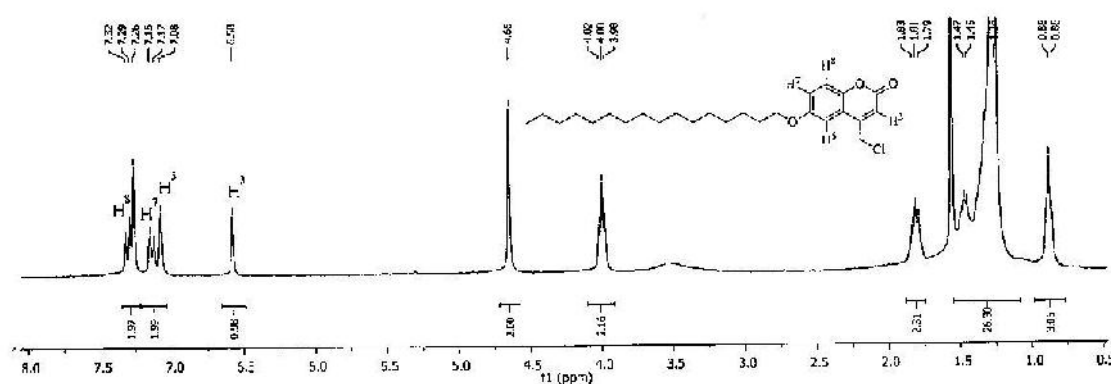


Figure 4.8 ^1H NMR spectrum of C2 in CDCl_3

4.1.3 Esterification reaction

The photoresponsive coumarins were successfully formed in Figure 4.9. **CM1-CM12** were synthesized by esterification reaction of plant hormones with coumarin **C1** or **C2** in the presence of potassium iodide (KI) and K_2CO_3 in dimethyl formamide (DMF).

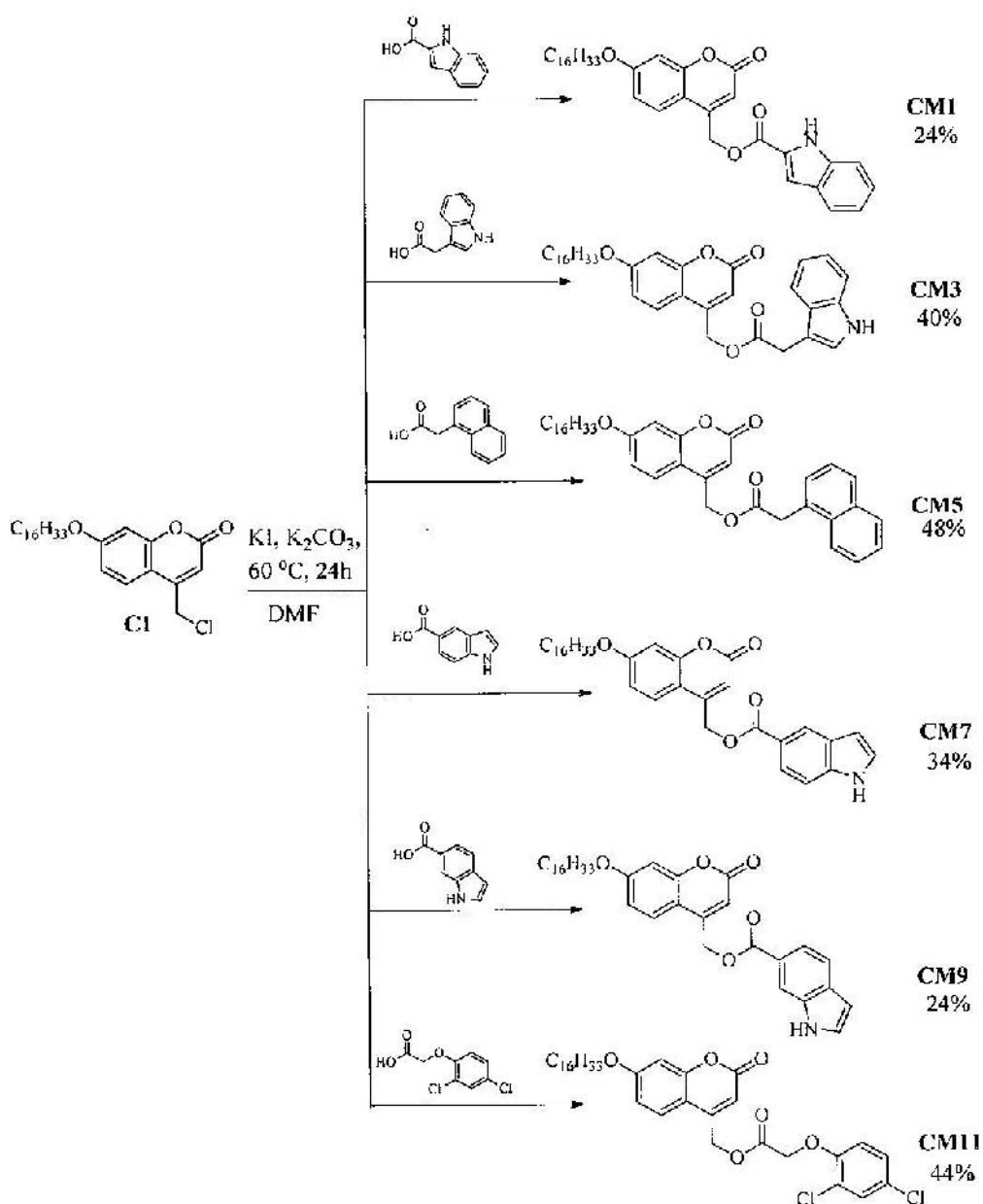


Figure 4.9 Synthetic route of photoresponsive coumarins (**CM1-CM2**)

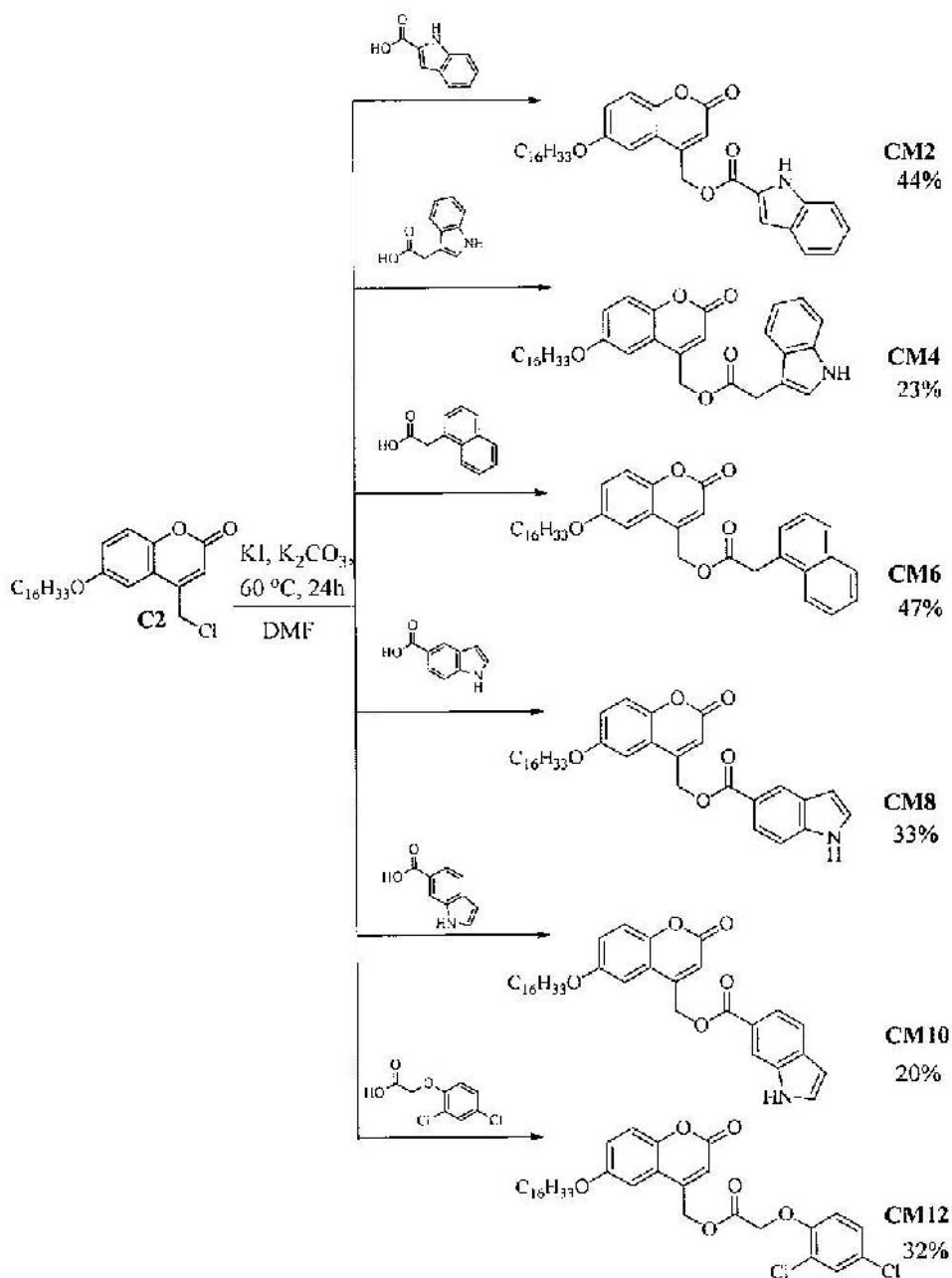


Figure 4.9 Synthetic route of photoresponsive coumarin CM1-CM2 (continued)

Figure 4.10 showed the mechanism of esterification. The carboxyl groups of plant hormones and herbicide were deprotonated by base K₂CO₃ to form potassium carboxylate. The activated electrophile was induced by the adding of KI. Then, the nucleophilic substitution was performed at active methylene carbon of coumarin.

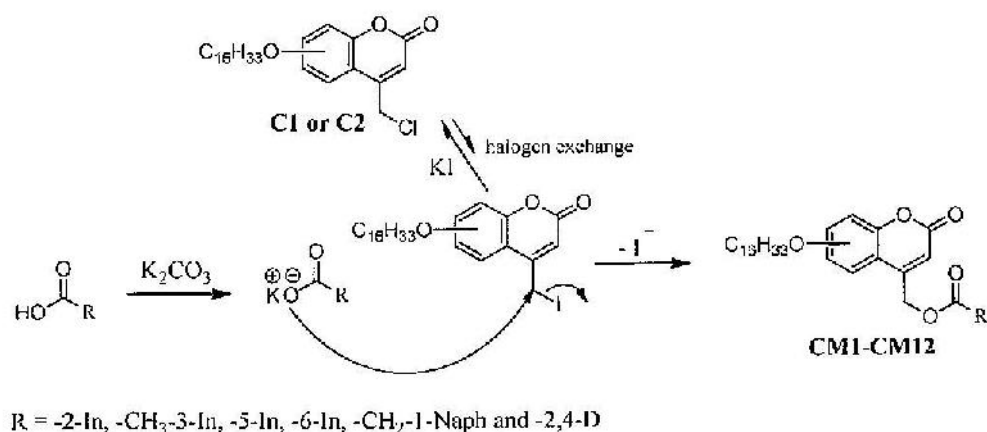


Figure 4.10 The mechanism of esterification synthesis

The ^1H NMR spectra of CM1 shown two singlet and two doublet signals at 6.47 (s), 6.87 (s), 6.88 (d) and 7.72 (d) ppm from H^3 , H^8 , H^6 and H^5 , respectively. In addition, indole protons denoted as $\text{H}^{3'}$, $\text{H}^{4'}$, $\text{H}^{5'}$, $\text{H}^{6'}$ and $\text{H}^{7'}$ were found around 7.0-7.7 ppm as it is shown in Figure 4.11. The singlet signal at 5.53 ppm (2H) was allyl methylene proton. The long alkyl chain was observed at 4.03 ppm (t, 2H), 1.82 ppm (m, 2H), 1.52-1.26 (m, 26H) and 0.87 (t, 3H).

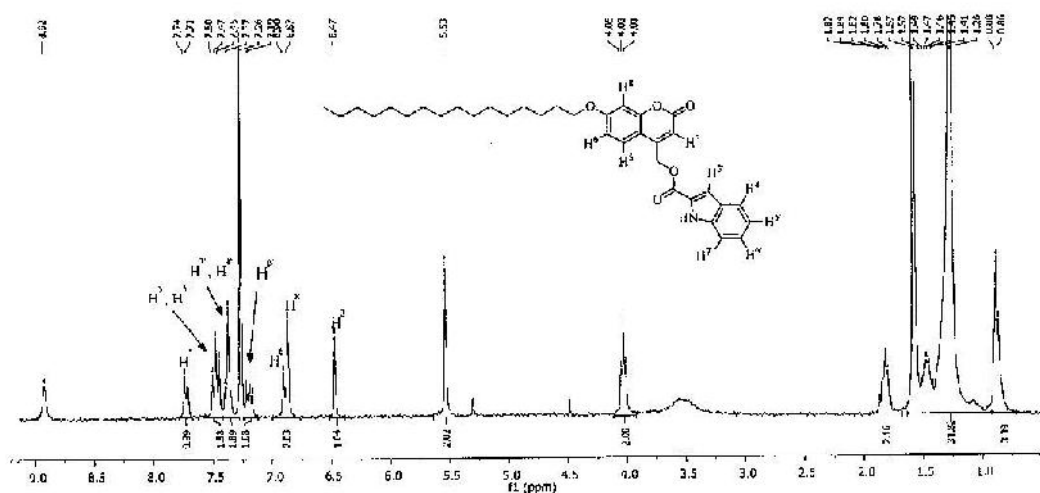


Figure 4.11 ^1H NMR spectrum of CM1 in CDCl_3

Comparison of ^1H NMR spectra of **CM1** and **CM2** in Figure 4.12, the singlet proton of H^3 was shifted from 6.47 ppm to 6.66 ppm because of the low electron density from alkoxy chain at position 6 on coumarin unit. In addition, H^5 of **CM1** was observed doublet signal at 7.49 ppm instead of singlet signal at 7.00 ppm for **CM2**. The singlet signal at 6.87 ppm and doublet signal at 7.15 ppm of H^8 were assigned to proton on **CM1** and **CM2**, respectively. While indole protons showed similar ^1H NMR pattern.

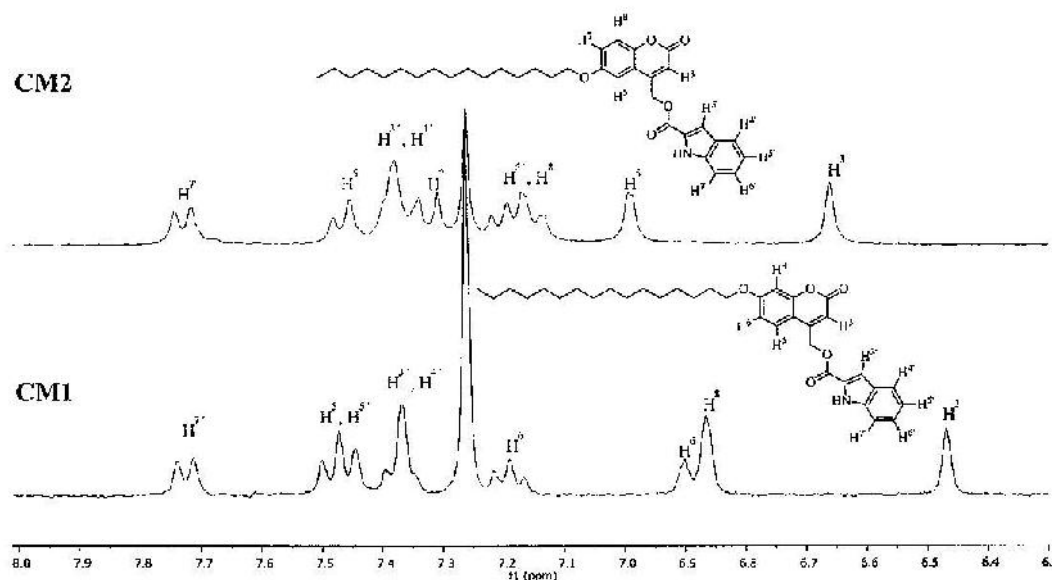


Figure 4.12 ^1H NMR spectrum of **CM1** and **CM2** in CDCl_3

The chemical structure of **CM1**, **CM7** and **CM9** were synthesized by using **C1** as coumarin core structure and varied substituted position of carboxylate on indole ring; 2-indolecarboxylic acid, indole-5-carboxylic acid, and indole-6-carboxylic acid, respectively. Therefore the ^1H NMR spectra of these compounds in CDCl_3 were shown in a similar pattern proton signals of coumarin core and alkoxy group. In aromatic region as it shown in Figure 4.13, the **CM1** appeared singlet proton of $\text{H}^{3'}$ at 7.36 ppm in low field compared to **CM7** and **CM9** because of the effect of electron withdrawing carbonyl group. In the same way, the singlet proton H^4 at 8.50 ppm of **CM7** was observed at lower low field compared to **CM1** and **CM9**. Moreover, singlet proton of **CM9** ($\text{H}^{7'}$) was appeared at 8.24 ppm shown at lower field compared to **CM1** and **CM7**.

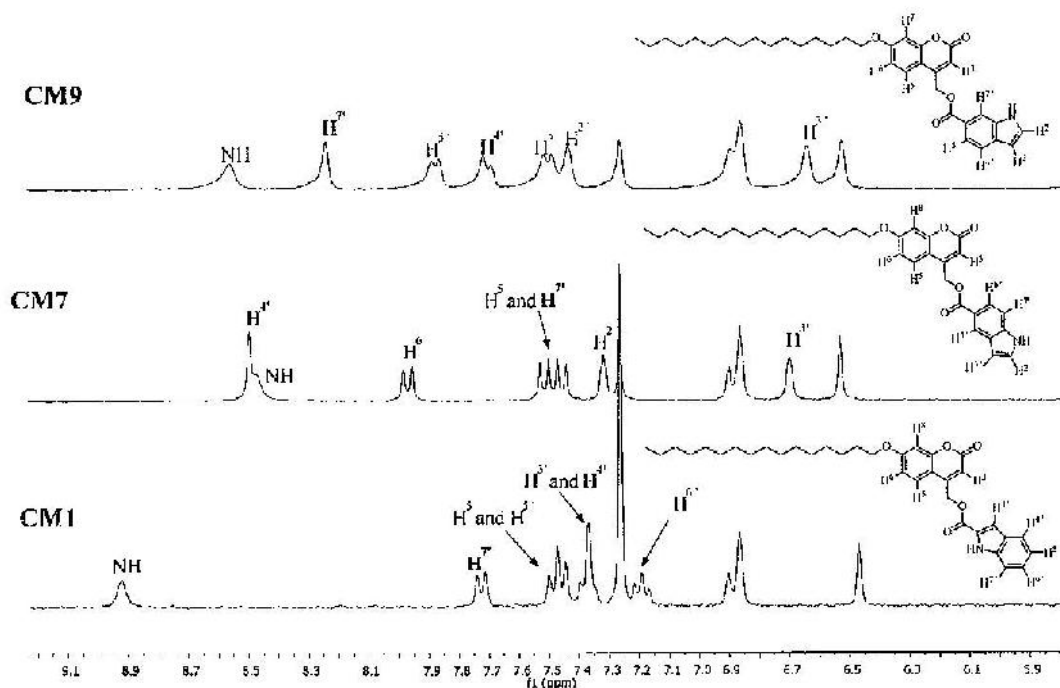


Figure 4.13 ^1H NMR spectrum of CM1, CM7 and CM9 in CDCl_3

Similarly, the chemical structure of **CM3**, **CM5** and **CM11** were synthesized by using **C1** as coumarin core structure and varied aromatic unit with acetate linkage; 3-indoleacetic acid, 1-naphthaleneacetic acid, and 2,4-dichlorophenoxyacetic acid, respectively. Accordingly, the spectra of these compounds in CDCl_3 were shown similar proton signal of alkoxy and coumarin core as mentions above. However, the spectra appeared new singlet signal of 2 protons methylene of acetate linkage at chemical shift 3.92 ppm, 4.20 ppm and 4.81 ppm, respectively. Moreover, integration numbers of aromatic protons were shown differently at aromatic region as shown in Figure 4.14.

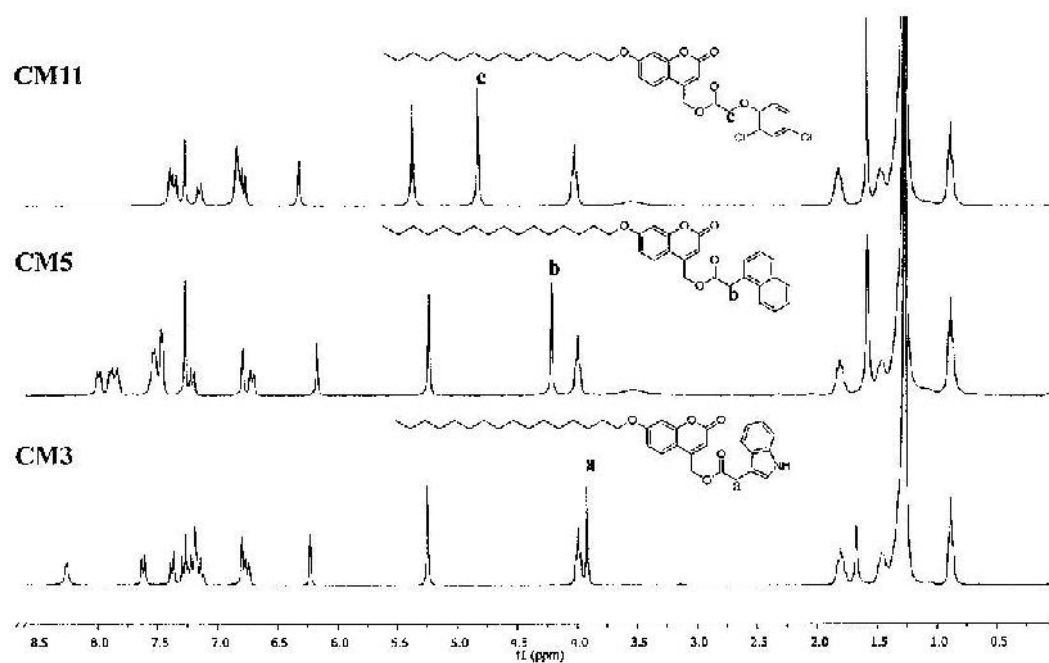









Figure 4.14 ^1H NMR spectrum of CM3, CM5 and CM11 in CDCl_3

4.2 Nanoformulation and characterization of photoresponsive coumarin CM1-CM12

4.2.1 Nanoformulation, particle size and zeta potential analysis

In this study, CM1 was used to study the optimized condition for nanoformulation. The photoresponsive compound in chloroform solvent was emulsified by using 75:25 of oil phase to aqueous phase with PVA as a stabilizer and SDS as a surfactant.

Table 4.1 The result for optimization condition

Condition	CM1 (wt%)	PVA (wt%)	SDS (wt%)	Nanoformulation image
1	0.15	0	5	
2	0.15	2	5	
3	0.15	3	5	
4	0.15	5	0	
5	0.15	3	1	
6	0.2	3	1	
7	0.25	3	1	

The PVA and SDS were dissolved the different concentrations (0 - 5 wt%) to make aqueous solutions. The loading compound was studied by varying the

concentration 0.15 - 0.25 wt%. The preparation conditions are shown in Table 4.1. It was found that the use of PVA and SDS were crucial in order to obtain a stable nanoemulsions. The pictures of condition 1 and 4 showed the precipitation after formulation.

The study of PVA concentration was prepared by using 5 wt% SDS and 0.15 wt% loading. The results showed that using 3 wt% PVA gave a stable milky solution without precipitate. Therefore, the reduced SDS concentrations were performed with 1 wt% SDS. The homogeneous emulsion also observed as shown in condition 5. Then, the organic loadings were optimized which gave the maximum concentration at 0.2 wt% (in condition 6). From the nanoformulation study, we summarized that the use of 3 wt% PVA 1 wt% SDS and 0.2 wt% CM1 was an optimum condition.

Table 4.2 Characteristics of the CM1-CM12 nanoemulsion

Compound	*Mean particle diameter (nm)	*Zata potential (mV)
CM1	321.7 ± 5.1	-24.5 ± 0.1
CM2	346.7 ± 6.1	-28.4 ± 0.3
CM3	378.6 ± 5.6	-29.8 ± 0.9
CM4	389.5 ± 6.3	-30.9 ± 0.6
CM5	368.6 ± 6.2	-29.5 ± 0.8
CM6	388.8 ± 5.4	-30.1 ± 1.2
CM7	292.5 ± 4.4	-25.0 ± 1.0
CM8	302.1 ± 6.1	-21.7 ± 0.8
CM9	306.5 ± 4.5	-24.4 ± 0.4
CM10	311.2 ± 4.8	-27.4 ± 0.8
CM11	397.1 ± 2.4	-25.7 ± 1.1
CM12	403.3 ± 5.0	-27.0 ± 0.7

* Values are given as means ± standard deviation from two measurement was run in triplicate

Particle size analysis of the nanoformulation were studied by dynamic light scattering (DLS) in Table 4.1. The nanoformulation give average particle diameters about 292.5-403.3 nm which was referred to as nanoemulsion [26].

The nanoemulsions showed the high negative charge values due to the stable particles in the presence of sulfate anion [27], which were reported from zeta potential values (Table 4.1). On the other hand, there is no significant difference of zeta potential values among the nanodispersions made from different target compounds.

4.2.2 Contact angle measurement

The optimized **CM1-CM12** nanoemulsions at concentration 600 ppm on the *Cassia fistula* leaf were investigated. The wettability of nanoemulsions indicated a strong hydrophobicity with contact angle less than 57°, compared with pure water (91°) and PVA/DDS additive (73°) in Figure 4.15. The data showed no significant difference of contact angle values from various photoresponsive materials.

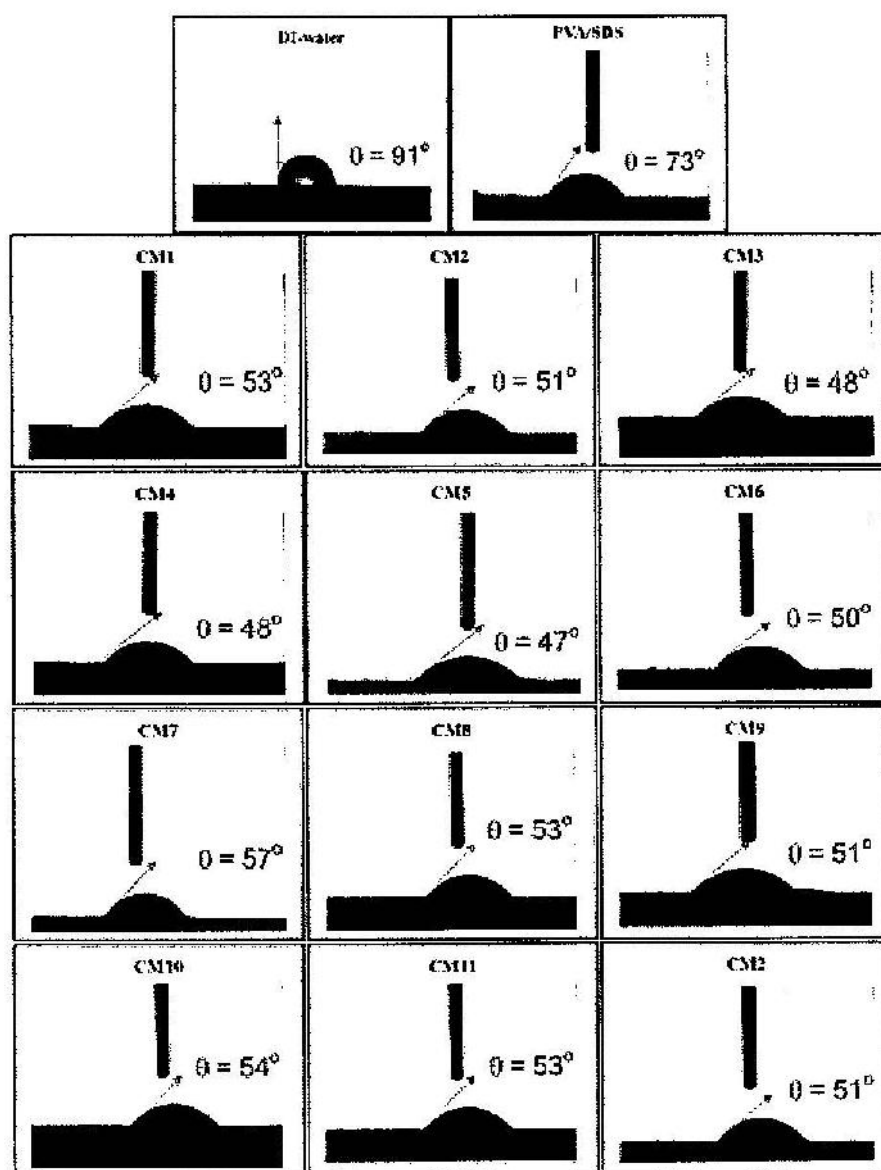


Figure 4.15 Image of droplets and contact angle (θ) of pure DI-water, mixed additive (PVA/SDS) and nonaformulation photoresponsive coumarin on *Cassia fistula* leaf

4.2.3 Photophysical properties of nanoemulsion

The photophysical properties of nanoemulsions were investigated. It was found that both **CM1** and **CM2** show a similar UV-vis absorption spectra (see Figure 4.16 (a)). Absorption spectra of both compound showed three maxima absorption bands around 350, 300 and 250 nm. The first two peaks originated from coumarin chromophore and the last peak from indole core.

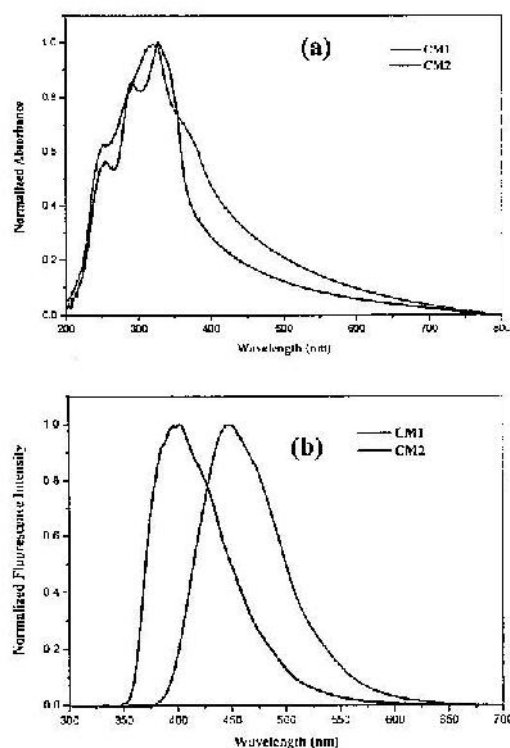


Figure 4.16 (a) Absorption and (b) emission spectra of nanoformulation photoresponsive CM1 and CM2

Whereas, the emission spectra showed a blue shifted for **CM1** compared to **CM2** (Figure 4.16 (b)). This result can be explained by description of frontier orbital theory (DFT) calculation [28] (showed in Figure 4.17). We found that the lowest unoccupied molecular orbital (LUMO) of coumarin localized at position 7. Therefore, alkoxy side chain (donating group) of **CM1** gave a destabilization of the LUMO level that affected to a wide energy gap.

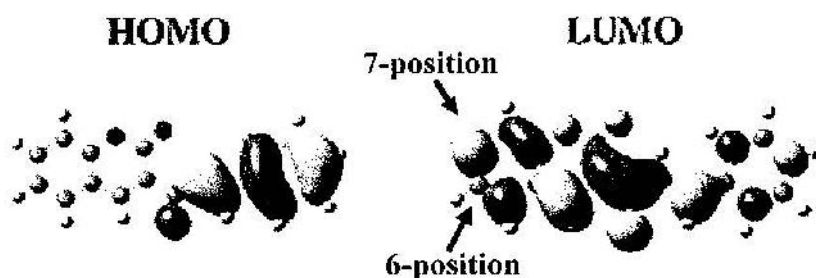


Figure 4.17 HOMO and LUMO distributions calculated for coumarin-chalcone hybrids by Xue and coworker

The absorption spectra of varied positions on indole ring (**CM1**, **CM7** and **CM9**) showed the different intensities around 250 nm. The high intensity (**CM7** and **CM9** in Figure 4.18 (a)) originated from the conjugation of ester group linkage and indole unit, as shown in Figure 4.18 (b). However all three compounds gave similar emission which occurred from the emission of coumarin core.

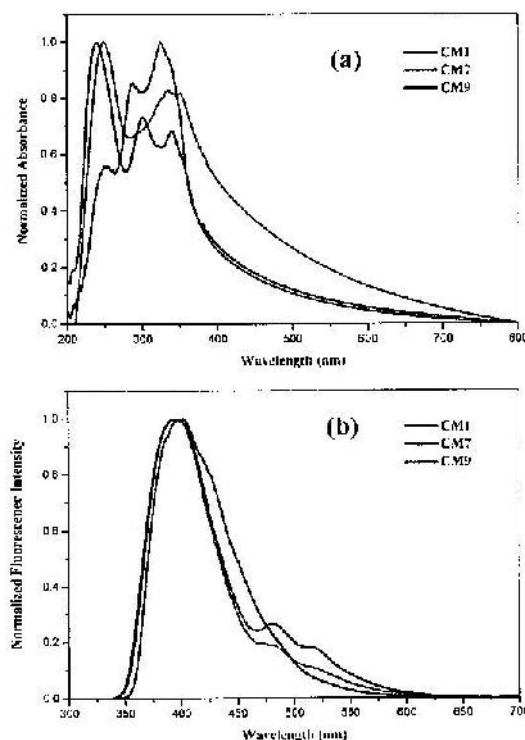


Figure 4.18 (a) Absorption and (b) emission spectra of nanoformulation photoresponsive **CM1**, **CM7** and **CM9**

4.2.4 Photolysis of photoresponsive coumarin nanoemulsion

Irradiations of nanoformulation photoresponsive compounds in DI water with specific wavelength (365 nm) and sunlight were followed. We also monitored the photolysis both UV-vis absorption and emission of **CM1**. Data are shown in Figure 4.19 and Figure 4.20. The results showed that reduced intensities were observed with increasing irradiation times. It should be noted that the induced sunlight showed a dramatically decreased within five days.

The mechanism of the photolysis of the photoresponsive compounds initiated by photo irradiation to cleave C-O bond at benzylic position was occurred *via* photo-SN₁ mechanism. The ion pairs of coumarinyl methyl carbocation and carboxylate anion of plant hormone were formed (Figure 4.21). After that ion pair was trapped by water molecule to yield 4-hydroxymethyl coumarin.

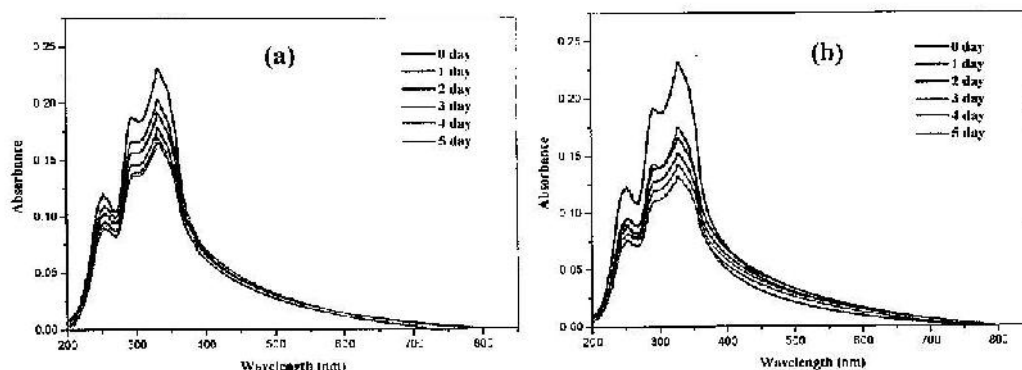


Figure 4.19 Absorption spectra of CM1 under (a) 365 nm and (b) sunlight

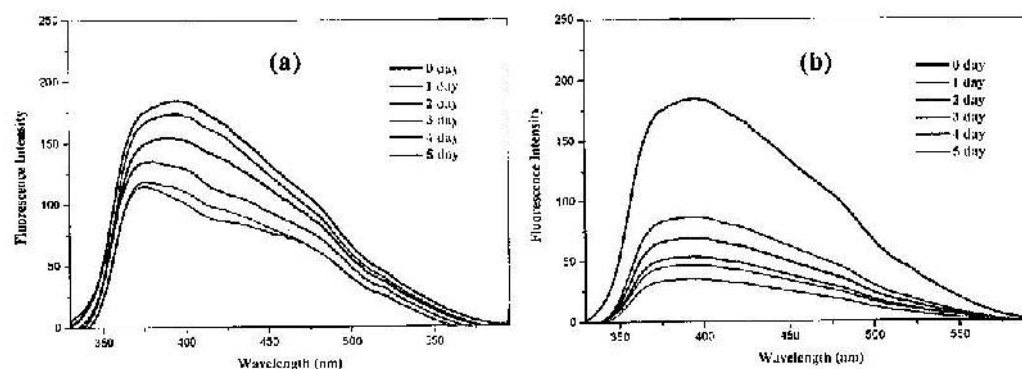


Figure 4.20 Emission spectra of CM1 under (a) 365 nm and (b) sunlight

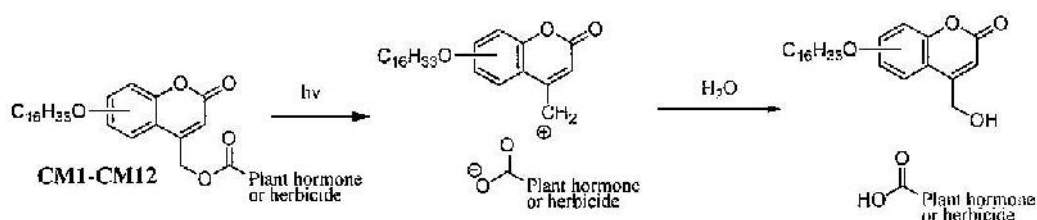


Figure 4.21 Mechanism of the photolysis of photoresponsive coumarin (CM1-CM12) to release plant hormone and herbicide

The summarization of the photolysis rate of **CM1** is shown in Figure 4.22. The result showed that only 30% hormone releasing under specific light (365 nm) within five days. On the other hand, the saturated releasing (>60%) was detected under sunlight condition only in three days.

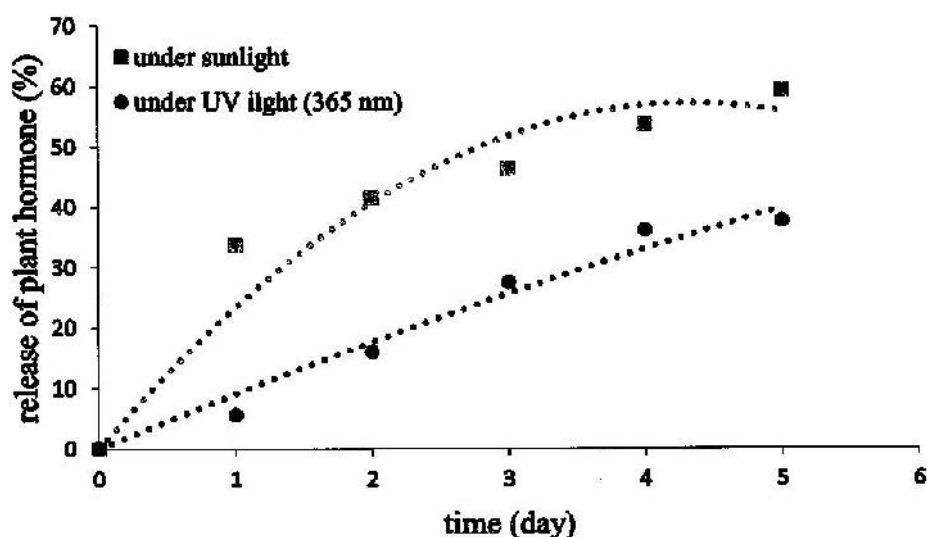


Figure 4.22 Photolysis emission spectra rate of CM1 at 365 nm and under sunlight

On the effect of alkoxy position in coumarin core on the release of plant hormones, we found that the different substituents at the 6-position and 7-position of the coumarin moiety have great influence on the active compound ability release. The fast photolysis rate of **CM1** was observed with 35% (Figure 4.23). This result can be

explained by the stabilized carbocation from alkoxy side chain as an electron donor group at position 7. The intermediates of CM1 and CM2 are shown in Figure 4.24.

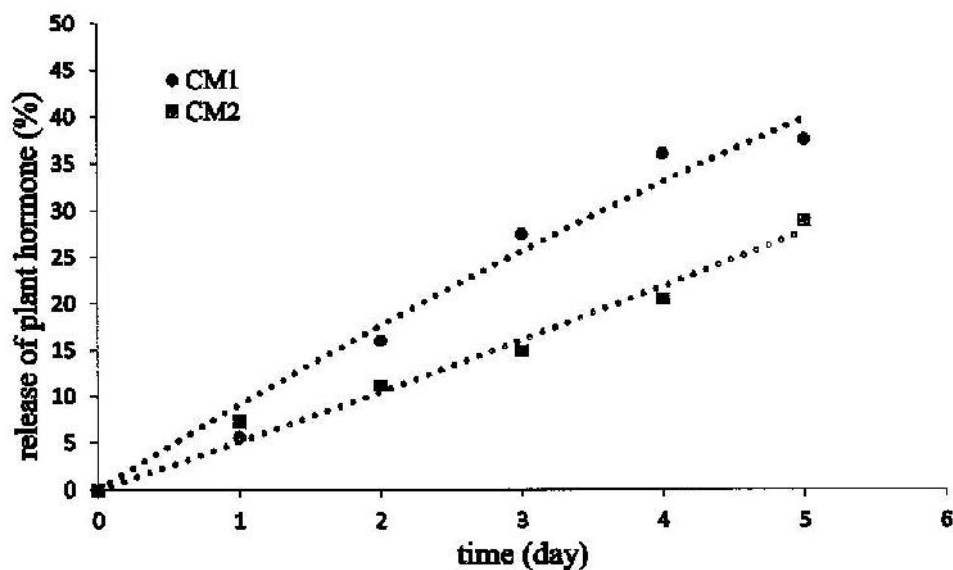


Figure 4.23 Photolysis emission spectra rate of CM1 and CM2 at 365 nm

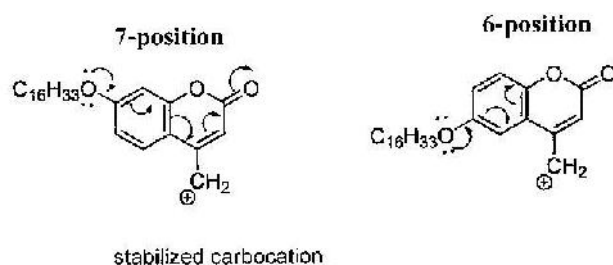


Figure 4.24 The intermediates of the CM1 and CM2

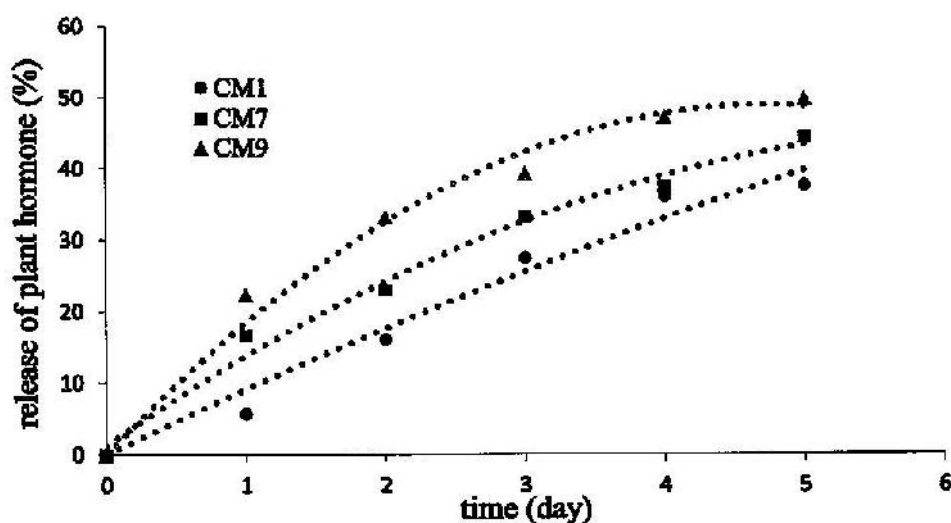


Figure 4.25 Photolysis emission spectra rate of CM1, CM7 and CM9 at 365 nm

In the case of varying the positions of indole, the slow releasing of plant hormone from **CM1** was observed compared with **CM7** and **CM9** in Figure 4.25. The results can be clarified by the intermediate in Figure 4.26. The unstable carboxylate anion was generated from negative repulsion of anion and lone pair electron on nitrogen atom. Moreover, the photolysis rate of **CM7** was reduced compared to **CM9** because of the unstable carboxylate anion.

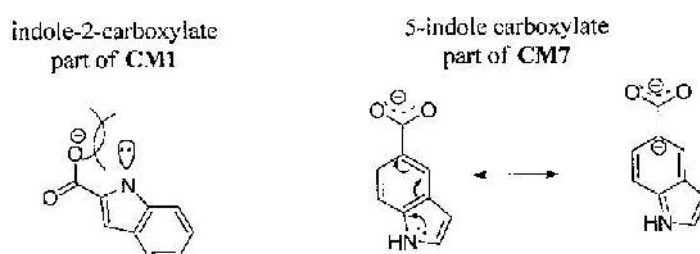


Figure 4.26 The electronic effect of the CM1 and CM7 intermediates

CHAPTER 5

CONCLUSIONS

Novel photoresponsive plant hormones and herbicide coumarins attached with a long alkoxy chain ($-\text{OC}_{16}\text{H}_{33}$) to enhance adhesive property on the plant leaves were successfully synthesized and characterized. The target compounds were synthesized *via* three step reactions specifically Williamson reaction, Pechmann condensation, and esterification reaction, respectively. All compounds were characterized by means of ^1H NMR, ^{13}C NMR, FTIR, and mass spectroscopy.

The nanoemulsion in aqueous solution was obtained by using PVA and SDS as the stabilizer and surfactant, respectively. The optimized condition was 3 wt% PVA and 1 wt% SDS with sample loading of 0.2 wt%. The nanoemulsion showed a high negative zeta potential value corresponding to the stability with the particle size in a range of 292.5-403.3 nm. Moreover, the long alkoxy chain showed a beneficial with a strong hydrophobicity which reduced the contact angle on the leaf surface to less than 57 degree.

The photolysis of nanoemulsions under specific wavelength (365 nm) and sunlight were monitored by UV-vis absorption and emission techniques. From the result, we found that the photolysis rate obviously depended on the substituted position of alkoxy on coumarin ring and substituted position of carboxylate ester linkage on indole. The efficiency of the photoresponsive compounds for release plant hormone would increase as the alkoxy electron-donating character of the substituent at the 7-position of the coumarin moiety showed higher value of photolysis compared to photoresponsive coumarin with an alkoxy at the 6-position. In the case of various indole derivatives, we found that the electronic effect of 2-position carboxylate on indole affect to rate of photolysis.

REFERENCES

REFERENCES

- [1] Sermsuk, S. "Agricultural chemicals imported to Thailand", **Department of Agriculture**. <http://www.doa.go.th/ard>. October 2, 2015.
- [2] Melotto, M. and et al. "Role of stomata in plant innate immunity and foliar bacterial diseases", **Annu Rev Phytopathol**. 46: 101-122; September, 2008.
- [3] Riggle, B. and et al. "The use of controlled-release technology for herbicides", **Reviews of Weed Science**. 5: 1-14; January, 1990.
- [4] Davis, T. and et al. "Chemical control of adventitious root formation in cuttings", **Quarterly-PGRSA (USA)**. 12: 121-198; October, 1990.
- [5] Riggle, B. and et al. "The use of controlled-release technology for herbicides", **Reviews of Weed Science**. 5: 1-14; July, 1990.
- [6] Ellis-Davies, GC. "Caged compounds: photorelease technology for control of cellular chemistry and physiology", **Nature methods**. 4(8): 619-628; August, 2007.
- [7] Goeldner, M. and et al. "Dynamic studies in biology: phototriggers, photoswitches and caged biomolecules", **John Wiley & Sons**. 21: 756-779; November, 2006.
- [8] Mayer, G. and et al. "Biologically active molecules with a light switch", **Angewandte Chemie International Edition**. 45(30): 4900-4921; July, 2006.
- [9] Pelliccioli, AP. and et al. "Photoremovable protecting groups: reaction mechanisms and applications", **Photochemical & photobiological sciences**. 1(7): 441-458; January, 2002.
- [10] Yu, H. and et al. "Chemistry and biological applications of photo-labile organic molecules", **Chemical Society Reviews**. 39(2): 464-473; September, 2010.
- [11] Banerjee, A. and et al. "Toward the development of new photolabile protecting groups that can rapidly release bioactive compounds upon photolysis with visible light", **The Journal of organic chemistry**. 68(22): 8361-8367; October, 2003.

REFERENCES (CONTINUED)

- [12] Grewer, C. and et al. "A new photolabile precursor of glycine with improved properties: A tool for chemical kinetic investigations of the glycine receptor", **Biochemistry**. 39(8): 2063-2070; February, 2000.
- [13] Singh, A.K. and et al. "3-Nitro-2-naphthalenemethanol: a photocleavable protecting group for carboxylic acids", **Tetrahedron**. 61(42): 10007-10012; October, 2005.
- [14] Givens, R.S. and et al. "New phototriggers 9: p-hydroxyphenacyl as a C-terminal photoremovable protecting group for oligopeptides", **Journal of the American Chemical Society**. 122(12): 2687-2697; March, 2000.
- [15] Singh, A.K. and et al. "Anthracene-9-methanol a novel fluorescent phototrigger for biomolecular caging", **Tetrahedron letters**. 46(33): 5563-5566; August, 2005.
- [16] Zhu, Y. and et al. "8-Bromo-7-hydroxyquinoline as a photoremovable protecting group for physiological use: mechanism and scope", **Journal of the American Chemical Society**. 128(13): 4267-4276; March, 2006.
- [17] Furuta, T. and et al. "Brominated 7-hydroxycoumarin-4-ylmethyls: photolabile protecting groups with biologically useful cross-sections for two photon photolysis", **Proceedings of the National Academy of Sciences**. 96(4): 1193-1200; February, 1999.
- [18] Pérez-de-Luque, A. and et al. "Nanotechnology for parasitic plant control", **Pest management science**. 65(5): 540-545; March, 2009.
- [19] Subramaniam, R. and et al. "Light-mediated and H-bond facilitated liposomal release: the role of lipid head groups in release efficiency", **Tetrahedron letters**. 51(3): 529-532; January, 2010.
- [20] Lin, Q. and et al. "7-Amino coumarin based fluorescent phototriggers coupled with nano/bio-conjugated bonds: Synthesis, labeling and photorelease", **Journal of Materials Chemistry**. 22(14): 6680-6688; February, 2012.

REFERENCES (CONTINUED)

- [21] Atta, S. and et al. "Fluorescent caged compounds of 2, 4-dichlorophenoxyacetic acid (2, 4-D): photorelease technology for controlled release of 2, 4-D", **Journal of agricultural and food chemistry**. 58(22): 11844-11851; October, 2010.
- [22] Ilagen, V. and et al. "[8-[Bis (carboxymethyl) aminomethyl]-6-bromo-7-hydroxycoumarin-4-yl] methyl Moieties as Photoremovable Protecting Groups for Compounds with COOH, NH₂, OH, and C=O Functions", **The Journal of organic chemistry**. 75(9): 2790-2797; March, 2010.
- [23] Atta, S. and et al. "Application of photoremovable protecting group for controlled release of plant growth regulators by sunlight", **Journal of Photochemistry and Photobiology B: Biology**. 111: 39-49; June, 2012.
- [24] Zhang, H. and et al. "Formation and enhanced biocidal activity of water-dispersable organic nanoparticles", **Nature nanotechnology**. 3(8): 506-511; July, 2008.
- [25] Herrmann, A. "Controlled release of volatiles under mild reaction conditions: from nature to everyday products", **Angewandte Chemie International Edition**. 46(31): 5836-5863; July, 2007.
- [26] Weiss, J. and et al. "Functional materials in food nanotechnology", **Journal of food science**. 71(9): R107-R116; November, 2006.
- [27] Grant, N. and et al. "Poorly water-soluble drug nanoparticles via an emulsion-freeze-drying approach", **Journal of colloid and interface science**. 356(2): 573-578; April, 2011.
- [28] Xue, Y. and et al. "Structure and electronic spectral property of coumarin-chalcone hybrids: A comparative study using conventional and long-range corrected hybrid functionals", **Computational and Theoretical Chemistry**. 981: 90-99; February, 2012.

APPENDICES

APPENDIX A
Characterization data

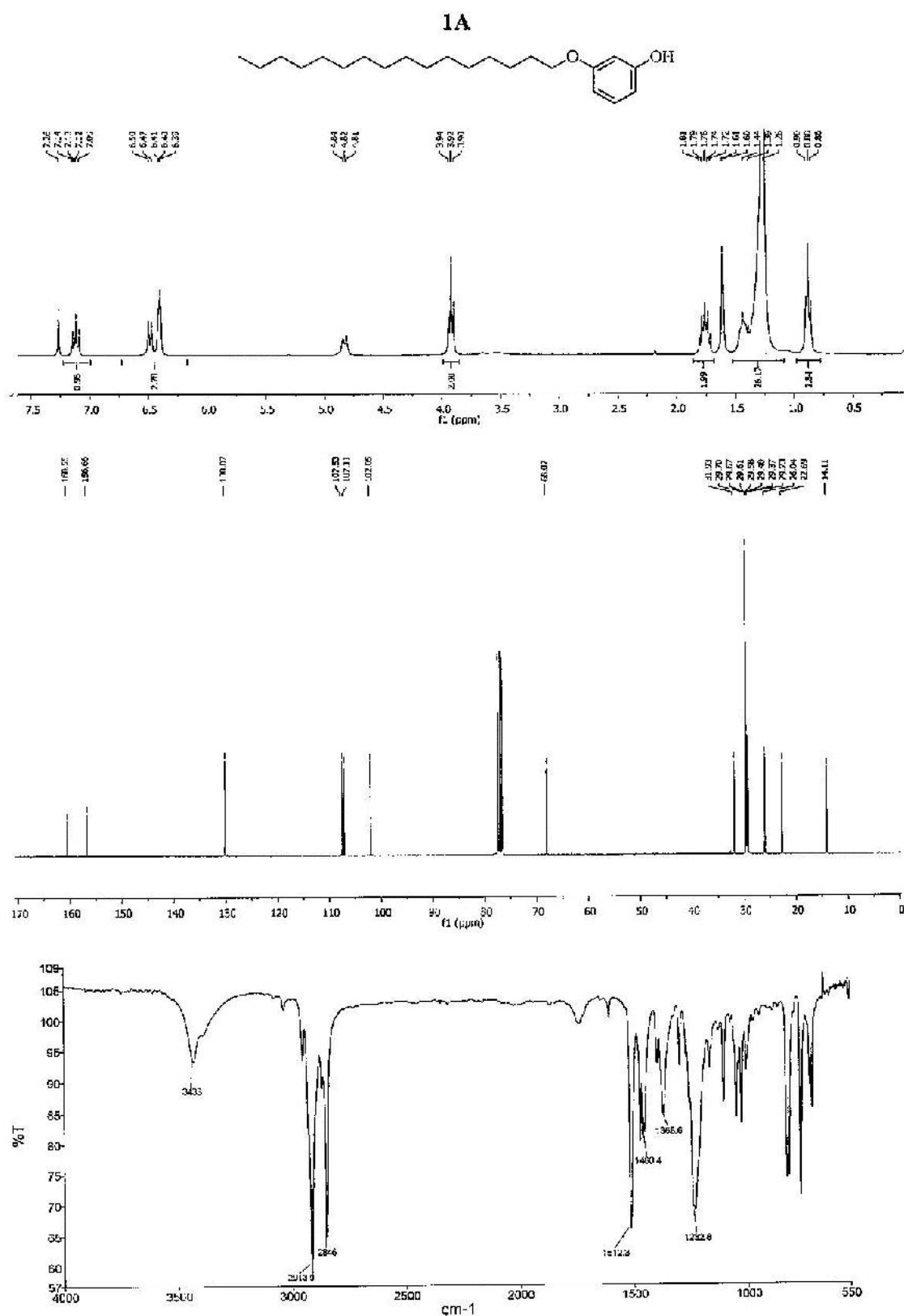


Figure A.1 ^1H , ^{13}C NMR in CDCl_3 and ATR-FTIR of 1A

Method tune_low_APCI_PEG.m
Sample Name
Comment

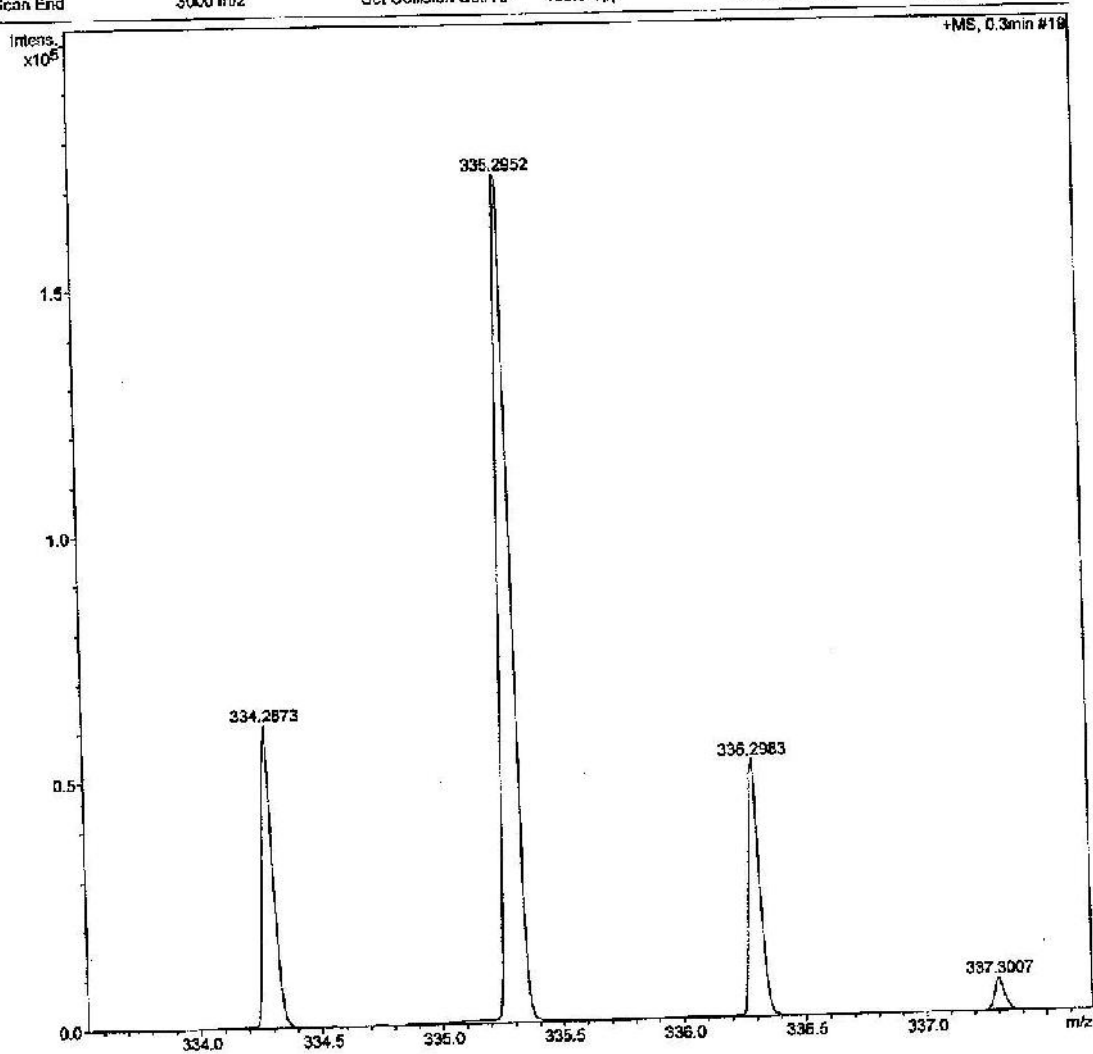
Instrument microOTOF-Q II 10414

Acquisition Parameter

Source Type APCI
Focus Not active
Scan Begin 50 m/z
Scan End 3000 m/z

Ion Polarity Positive
Set Capillary 4500 V
Set End Plate Offset -500 V
Set Collision Cell RF 150.0 Vpp

Set Nebulizer 1.5 Bar
Set Dry Heater 200 °C
Set Dry Gas 8.0 l/min
Set Divert Valve Waste



Bruker Compass DataAnalysis 4.0

printed: 5/18/2017 4:17:18 PM

Page 1 of 1

Figure A.2 Mass spectroscopy of 1A

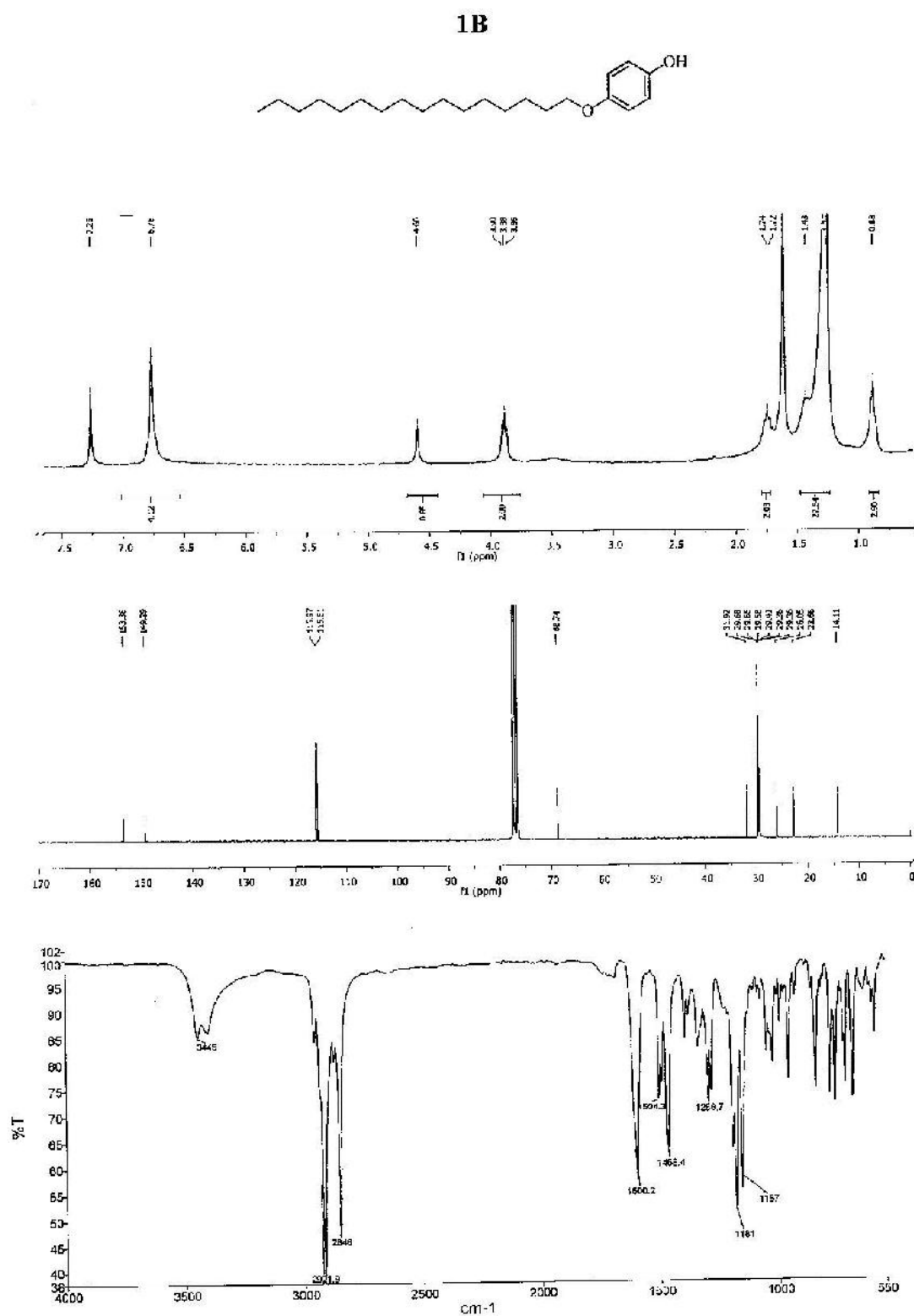


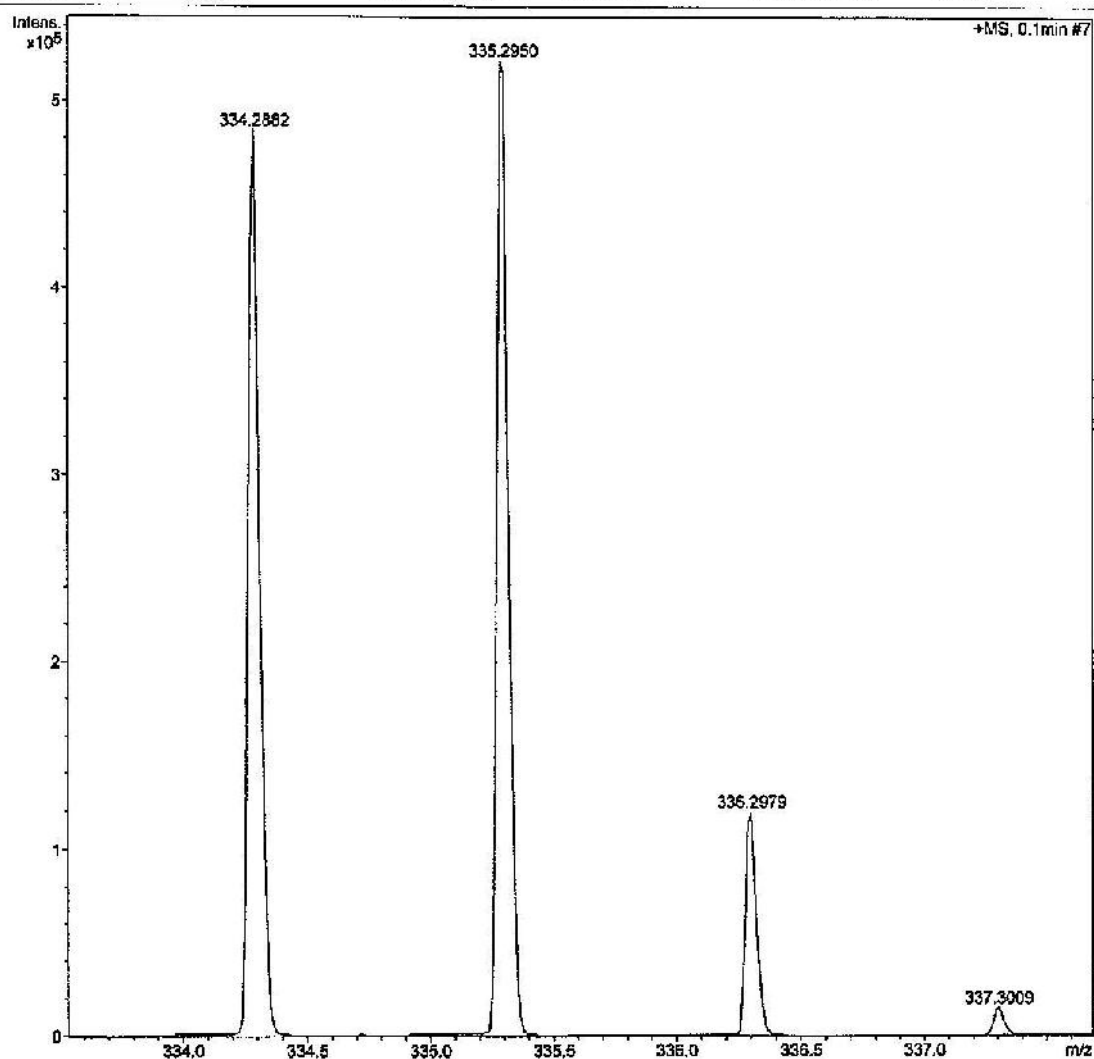
Figure A.3 ^1H , ^{13}C NMR in CDCl₃ and ATR-FTIR of 1B

Method tune_low_APCI_FEG.m
Sample Name
Comment

Operator CTB
Instrument micrOTOF-Q II 10414

Acquisition Parameter

Source Type	APCI	Ion Polarity	Positive	Set Nebulizer	1.6 Bar
Focus	Not active	Set Capillary	4500 V	Set Dry Heater	200 °C
Scan Begin	50 m/z	Set End Plate Offset	-500 V	Set Dry Gas	8.0 l/min
Scan End	3000 m/z	Set Collision Cell RF	150.0 Vpp	Set Divert Valve	Waste

**Figure A.4 Mass spectroscopy of 1B**

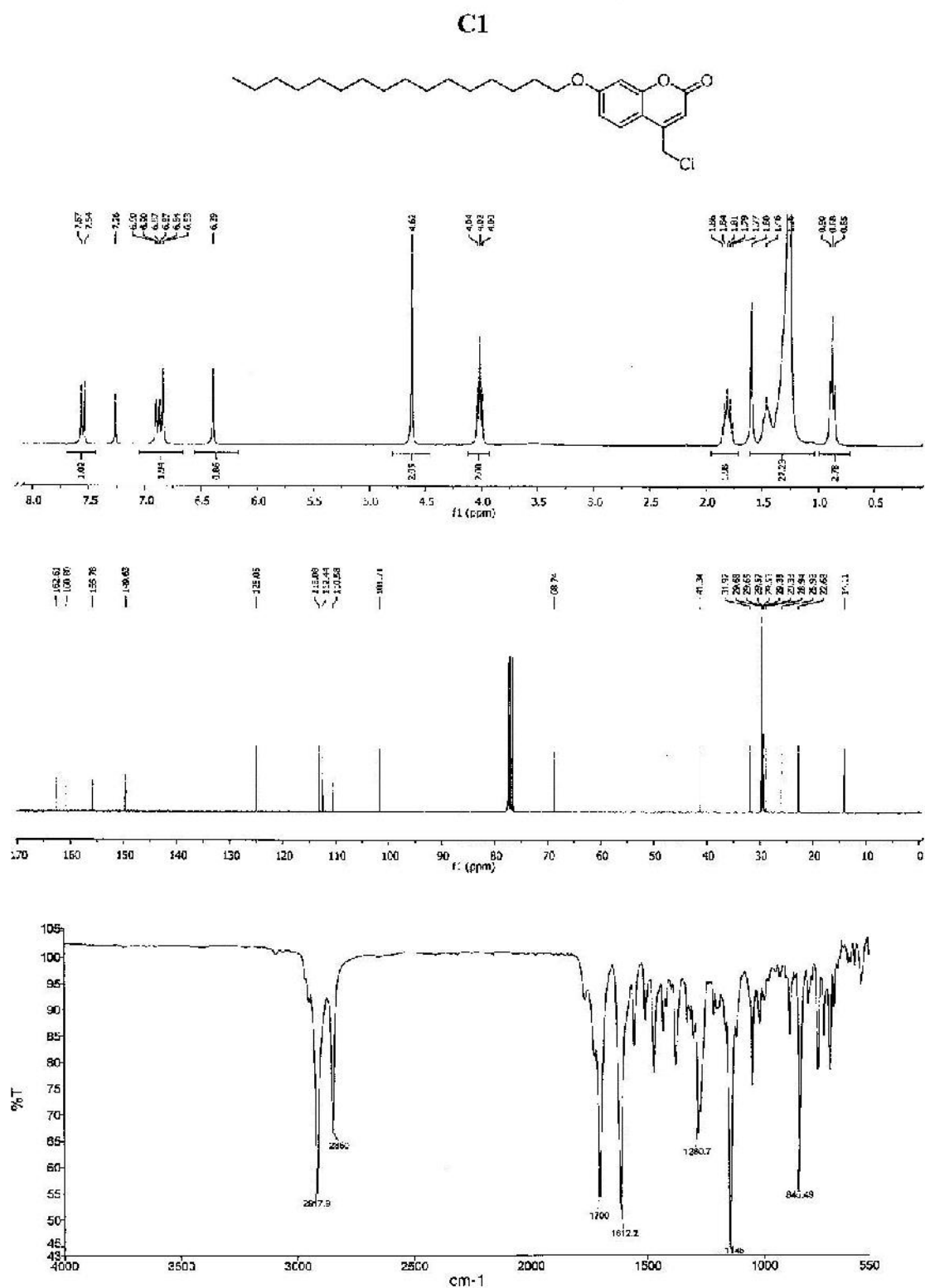


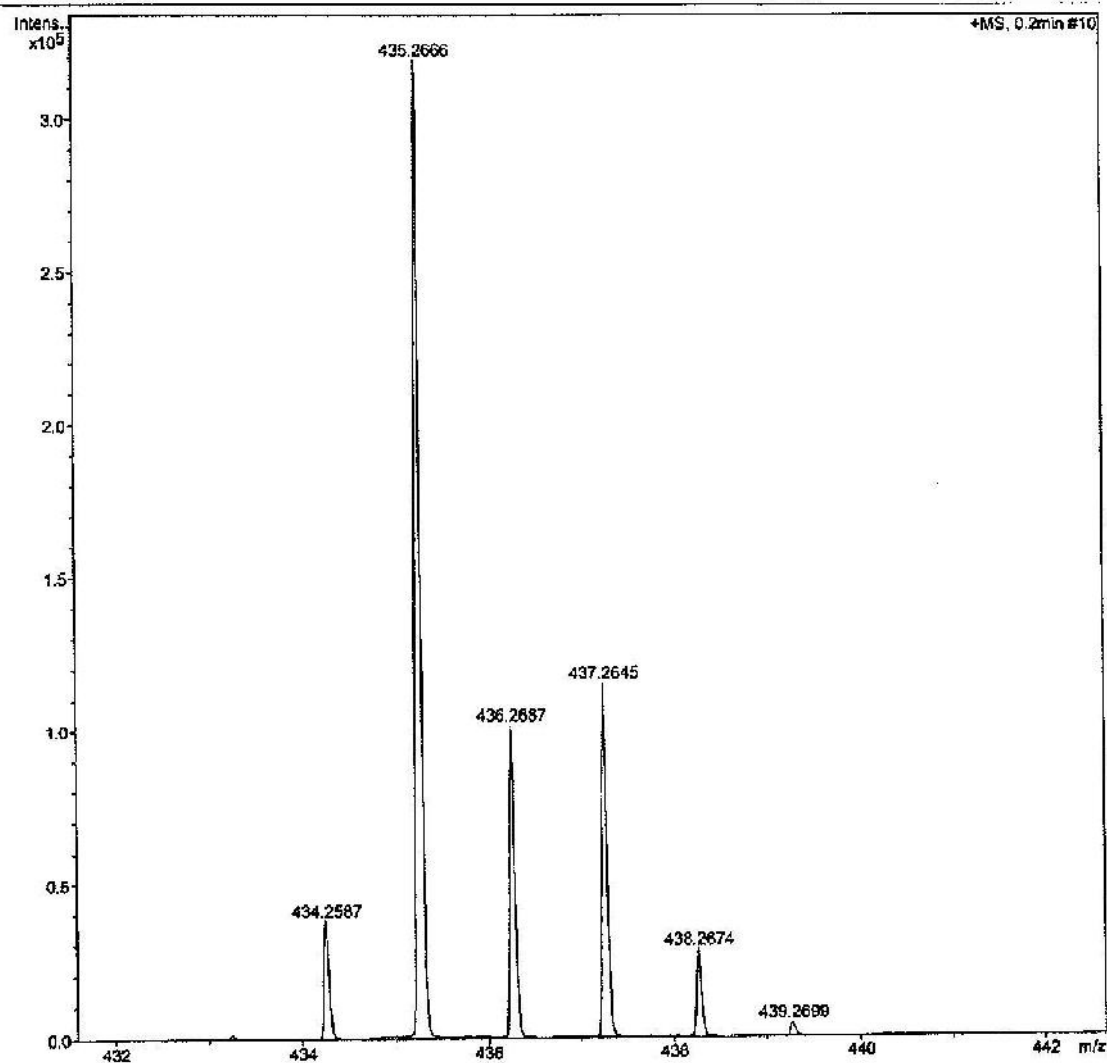
Figure A.5 ¹H, ¹³C NMR in CDCl₃ and ATR-FTIR of C1

Method tune_low_APCI_PEG.m
Sample Name
Comment

Operator CTB
Instrument micrOTOF-Q II 10414

Acquisition Parameter

Source Type	APCI	Ion Polarity	Positive	Set Nebulizer	1.6 Bar
Focus	Not active	Set Capillary	4500 V	Set Dry Heater	200 °C
Scan Begin	50 m/z	Set End Plate Offset	-800 V	Set Dry Gas	8.0 l/min
Scan End	3000 m/z	Set Collision Cell RF	150.0 Vpp	Set Divert Valve	Waste



Bruker Compass DataAnalysis 4.0

printed: 6/18/2017 4:19:36 PM

Page 1 of 1

Figure A.6 Mass spectroscopy of C1

C2

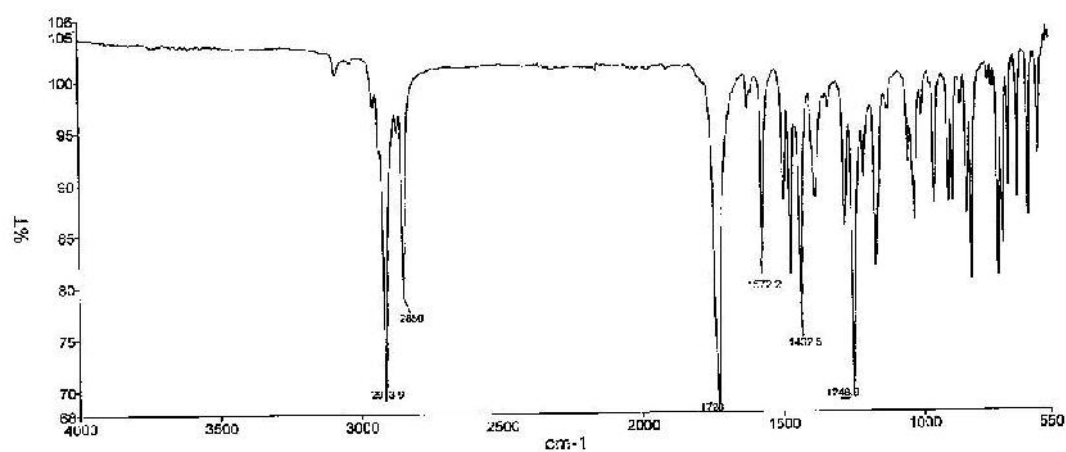
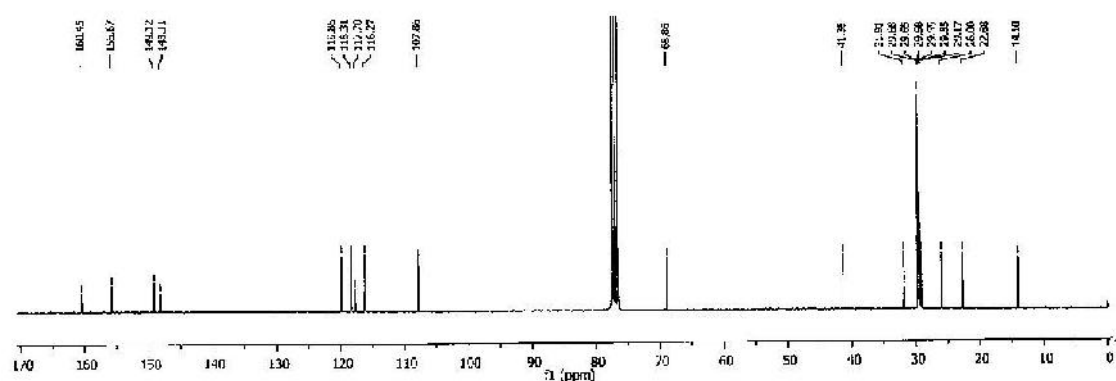
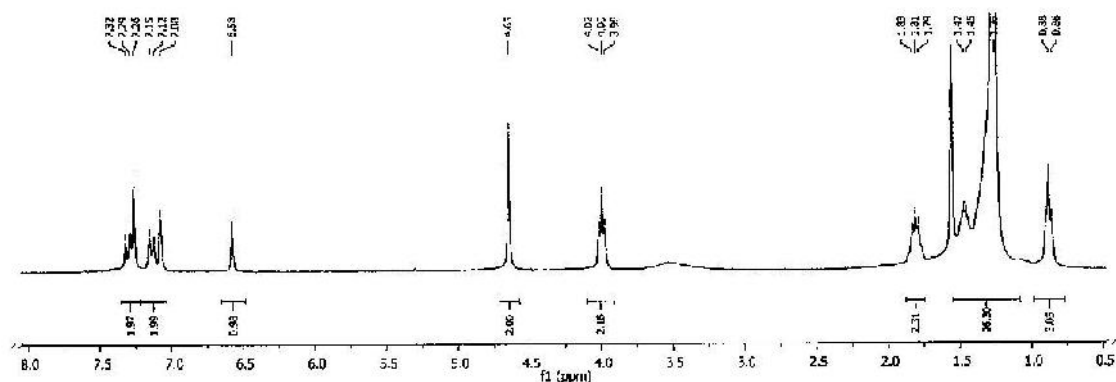
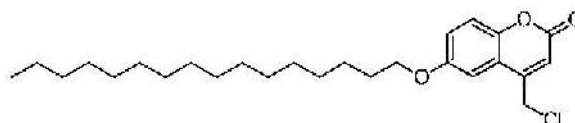


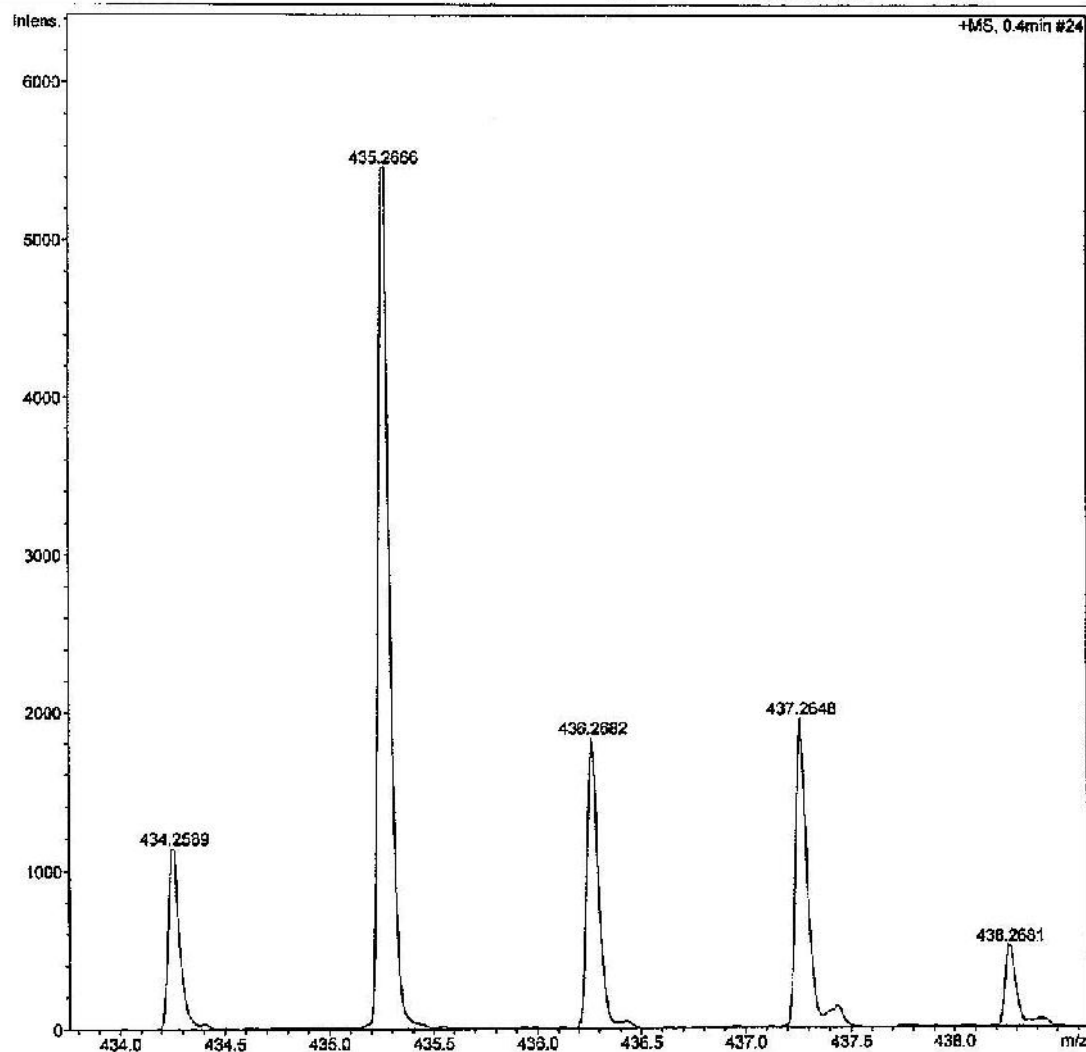
Figure A.7 ¹H, ¹³C NMR in CDCl₃ and ATR-FTIR of C2

Method tune_low_APCI_PEG.m
Sample Name
Comment

Operator CTB
Instrument micrOTOF-Q II 10414

Acquisition Parameter

Source Type	APCI	Ion Polarity	Positive	Set Nebulizer	1.6 Bar
Focus	Not active	Set Capillary	4500 V	Set Dry Heater	200 °C
Scan Begin	50 m/z	Set End Plate Offset	-500 V	Set Dry Gas	8.0 l/min
Scan End	3000 m/z	Set Collision Cell RF	150.0 Vpp	Set Divert Valve	Waste



Bruker Compass DataAnalysis 4.0

printed: 5/18/2017 4:20:34 PM

Page 1 of 1

Figure A.8 Mass spectroscopy of C2

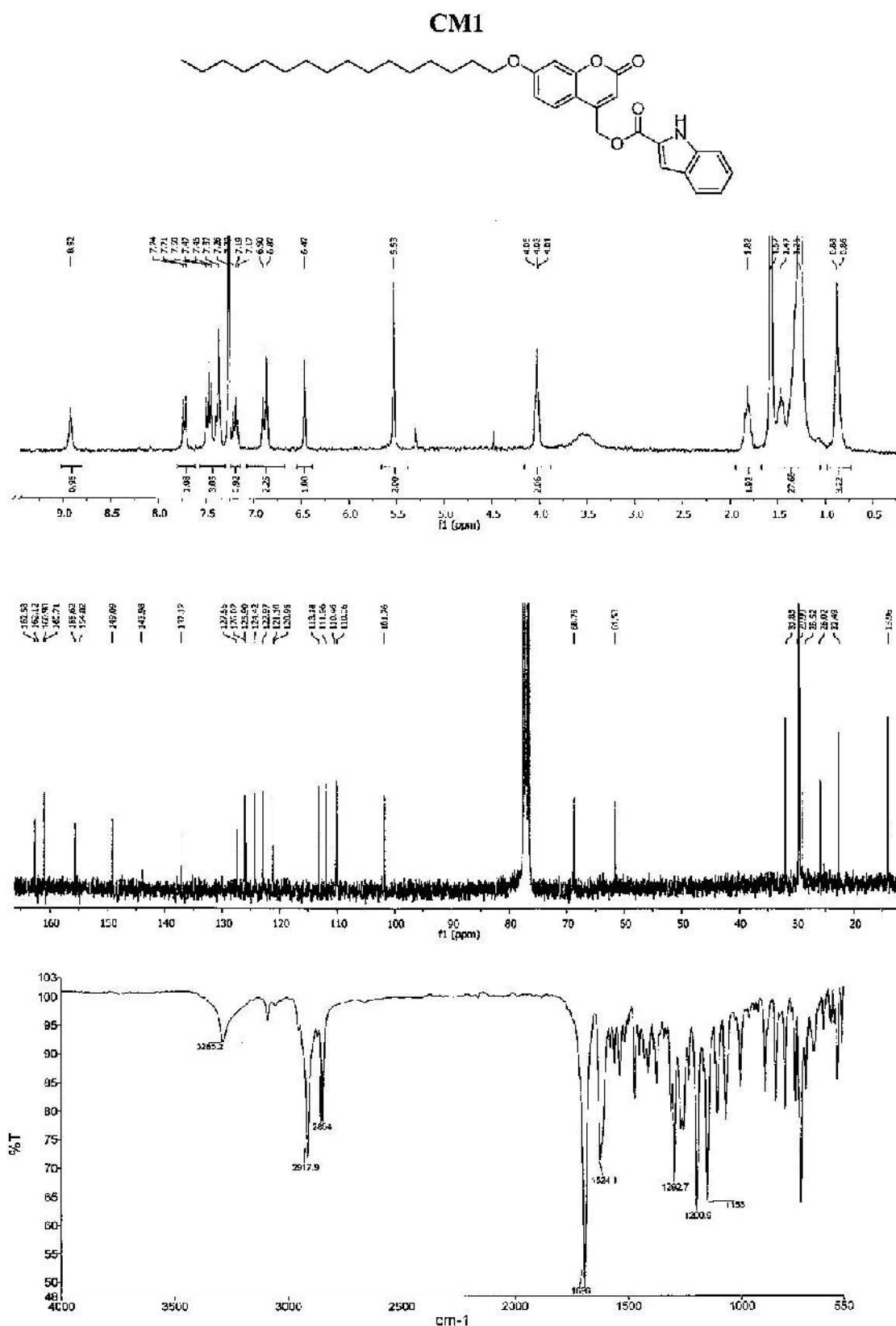


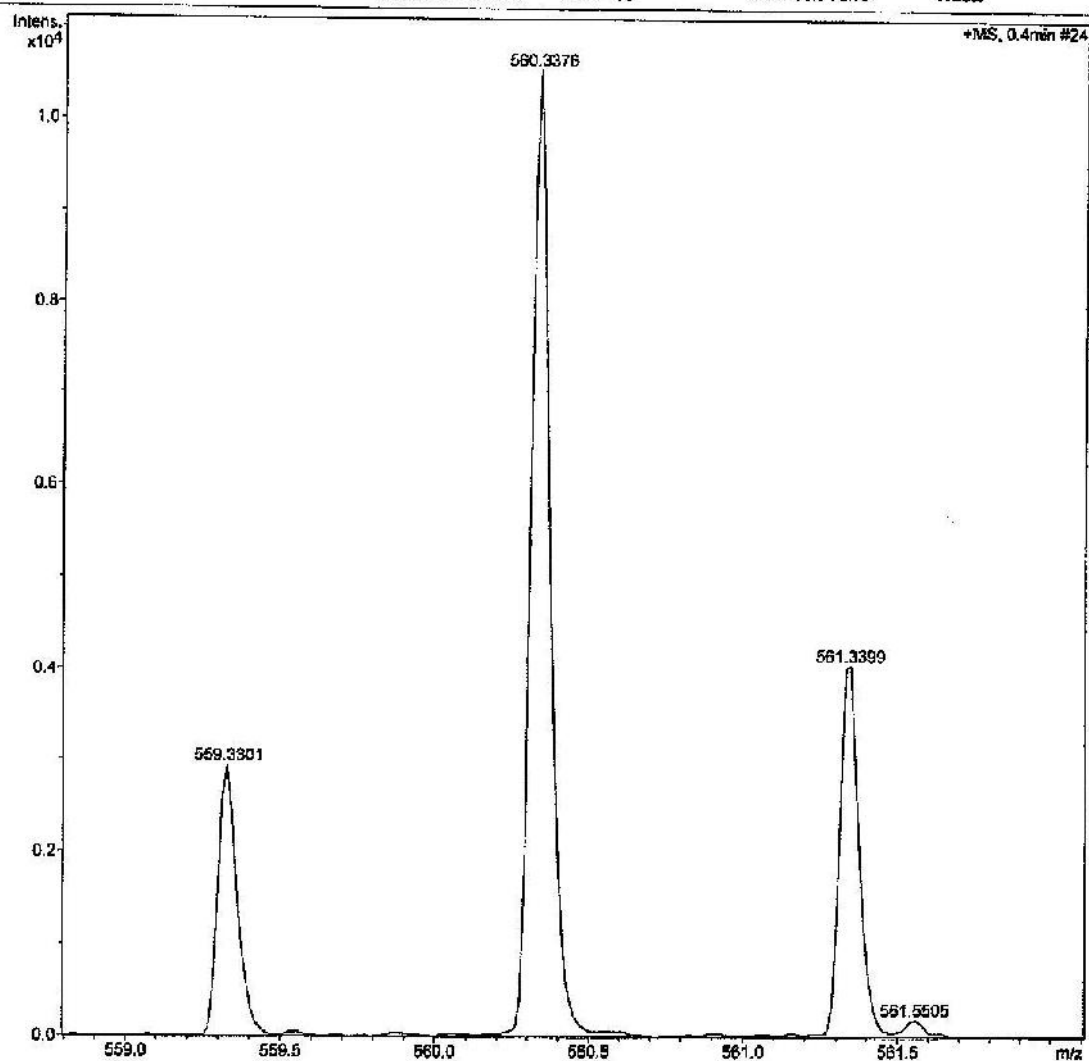
Figure A.9 ^1H , ^{13}C NMR in CDCl_3 and ATR-FTIR CM1

Method tune_low_APCI_PEG.m
Sample Name
Comment

Operator CTB
Instrument microTOF-Q II 10414

Acquisition Parameter

Source Type	APCI	Ion Polarity	Positive	Set Nebulizer	1.6 Bar
Focus	Not active	Set Capillary	4500 V	Set Dry Heater	200 °C
Scan Begin	50 m/z	Set End Plate Offset	-500 V	Set Dry Gas	8.0 l/min
Scan End	3000 m/z	Set Collision Cell RF	150.0 Vpp	Set Divert Valve	Waste



Bruker Compass DataAnalysis 4.0

Printed: 5/18/2017 5:21:30 PM

Page 1 of 1

Figure A.10 Mass spectroscopy of CMI

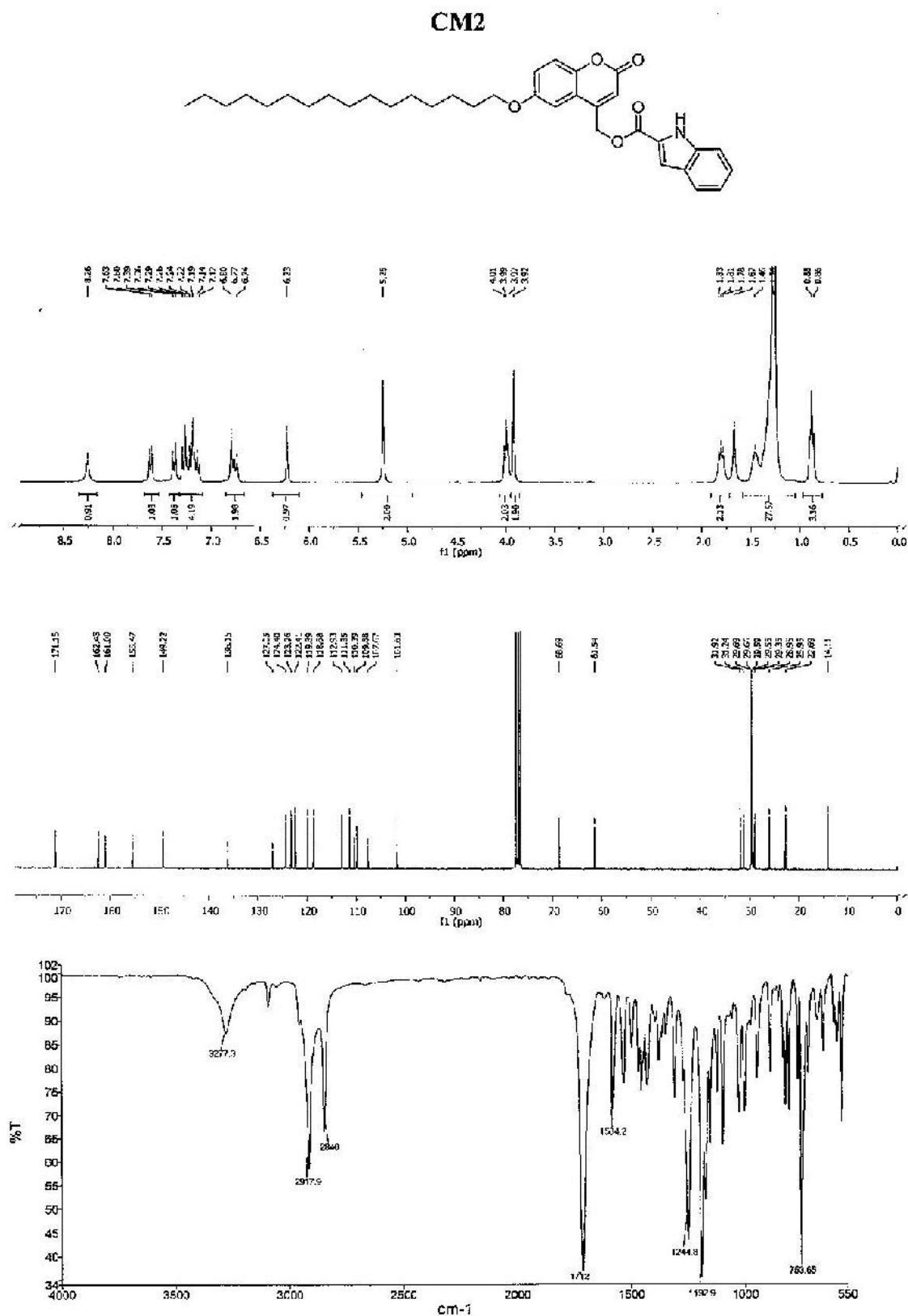


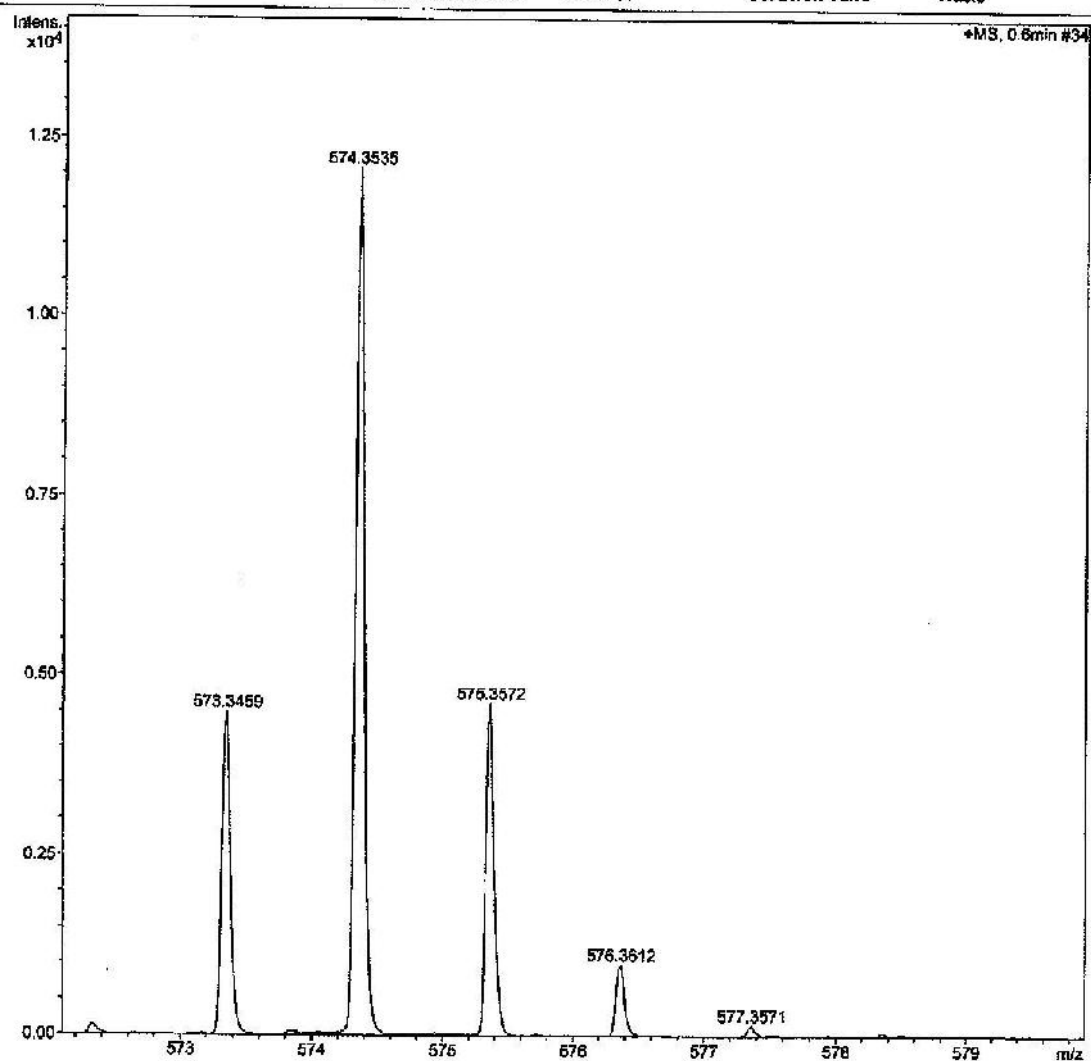
Figure A.11 ^1H , ^{13}C NMR in CDCl_3 and ATR-FTIR of CM2

Method tune_low_APCI_PEG.m
Sample Name
Comment

Operator CTB
Instrument micrOTOF-Q II 10414

Acquisition Parameter

Source Type	APCI	Ion Polarity	Positive	Set Nebulizer	1.6 Bar
Focus	Not active	Set Capillary	4500 V	Set Dry Heater	200 °C
Scan Begin	50 m/z	Set End Plate Offset	-500 V	Set Dry Gas	8.0 l/min
Scan End	3000 m/z	Set Collision Cell RF	150.0 Vpp	Set Divert Valve	Waste

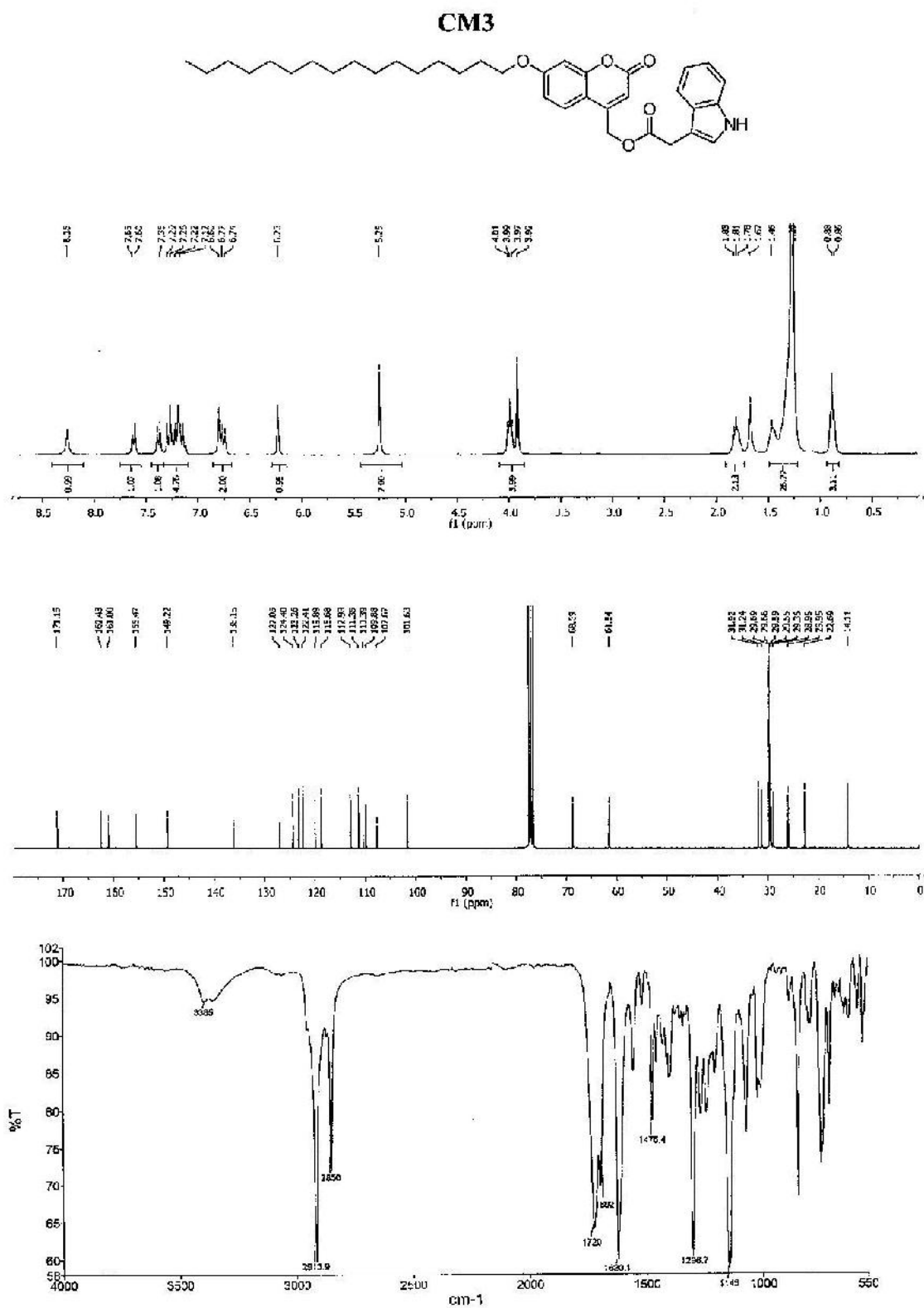


Bruker Compass DataAnalysis 4.0

printed: 5/18/2017 3:50:57 PM

Page 1 of 1

Figure A.12 Mass spectroscopy of CM2

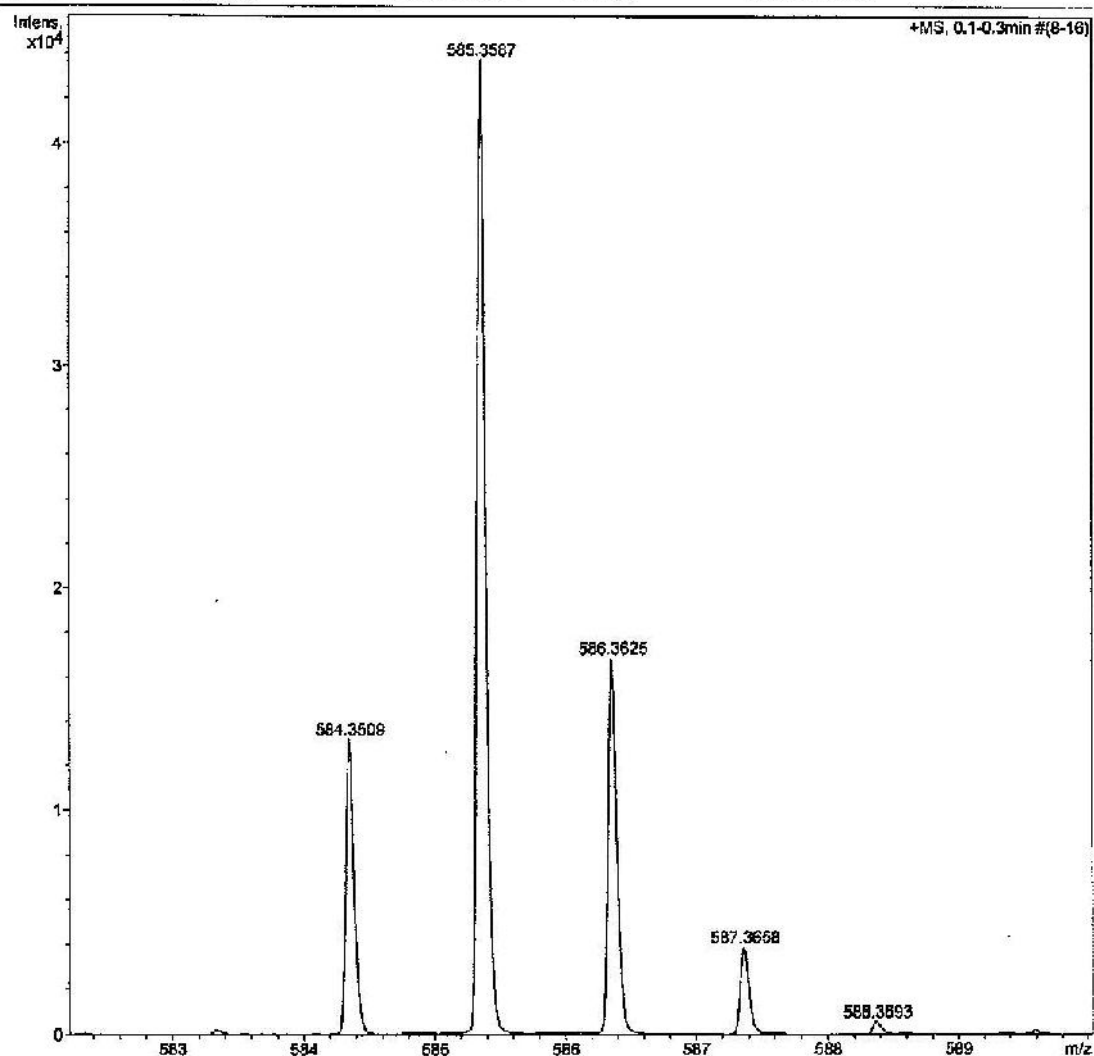


Method tune_low_APCI_PEG.m
Sample Name
Comment

Operator CTB
Instrument microTOF-Q II 10414

Acquisition Parameter

Source Type	APCI	Ion Polarity	Positive	Set Nebulizer	1.6 Bar
Focus	Not active	Set Capillary	4500 V	Set Dry Heater	200 °C
Scan Begin	50 m/z	Set End Plate Offset	-500 V	Set Dry Gas	8.0 l/min
Scan End	3000 m/z	Set Collision Cell RF	150.0 Vpp	Set Divert Valve	Waste



Bruker Compass DataAnalysis 4.0

printed: 5/18/2017 3:52:14 PM

Page 1 of 1

Figure A.14 Mass spectroscopy of CM3

CM4

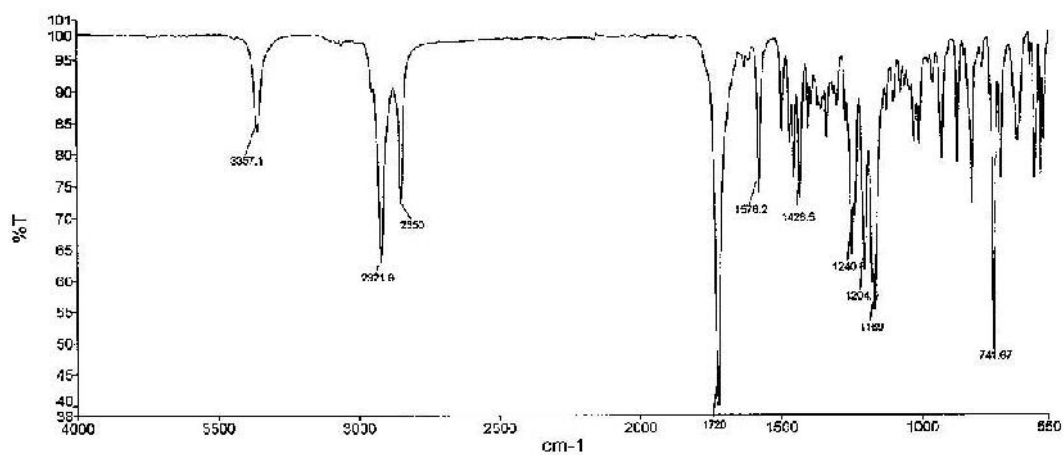
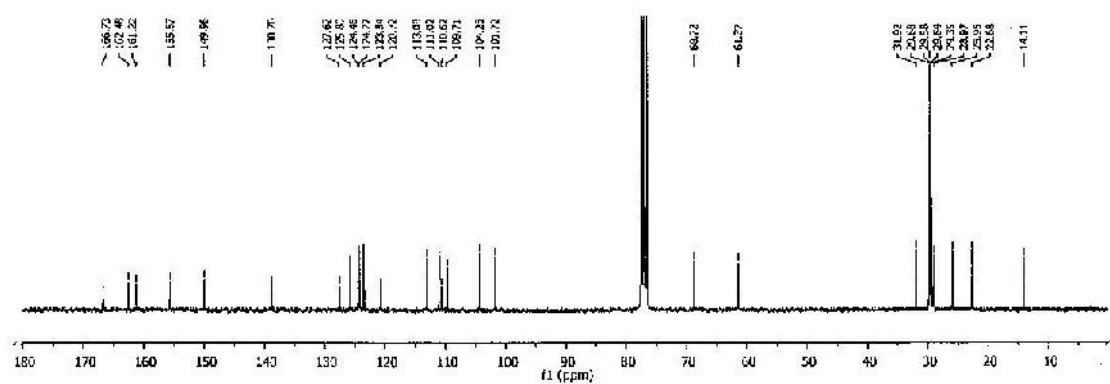
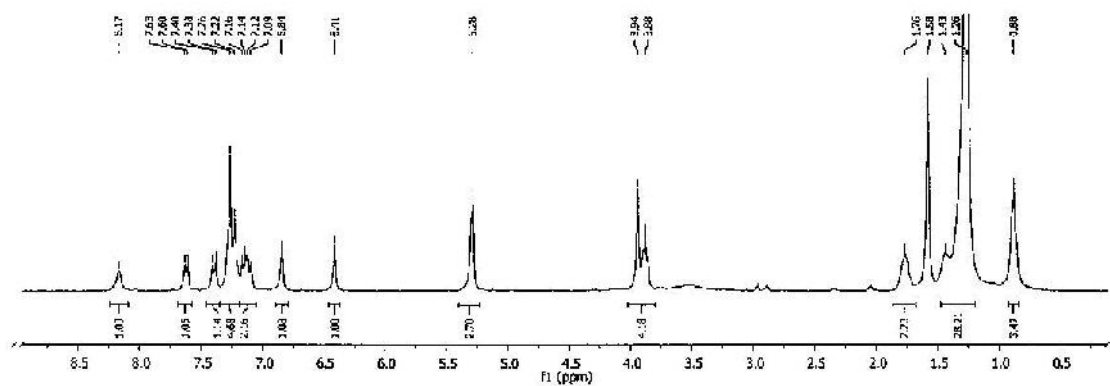
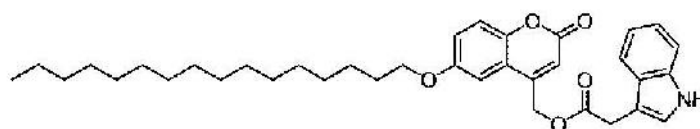


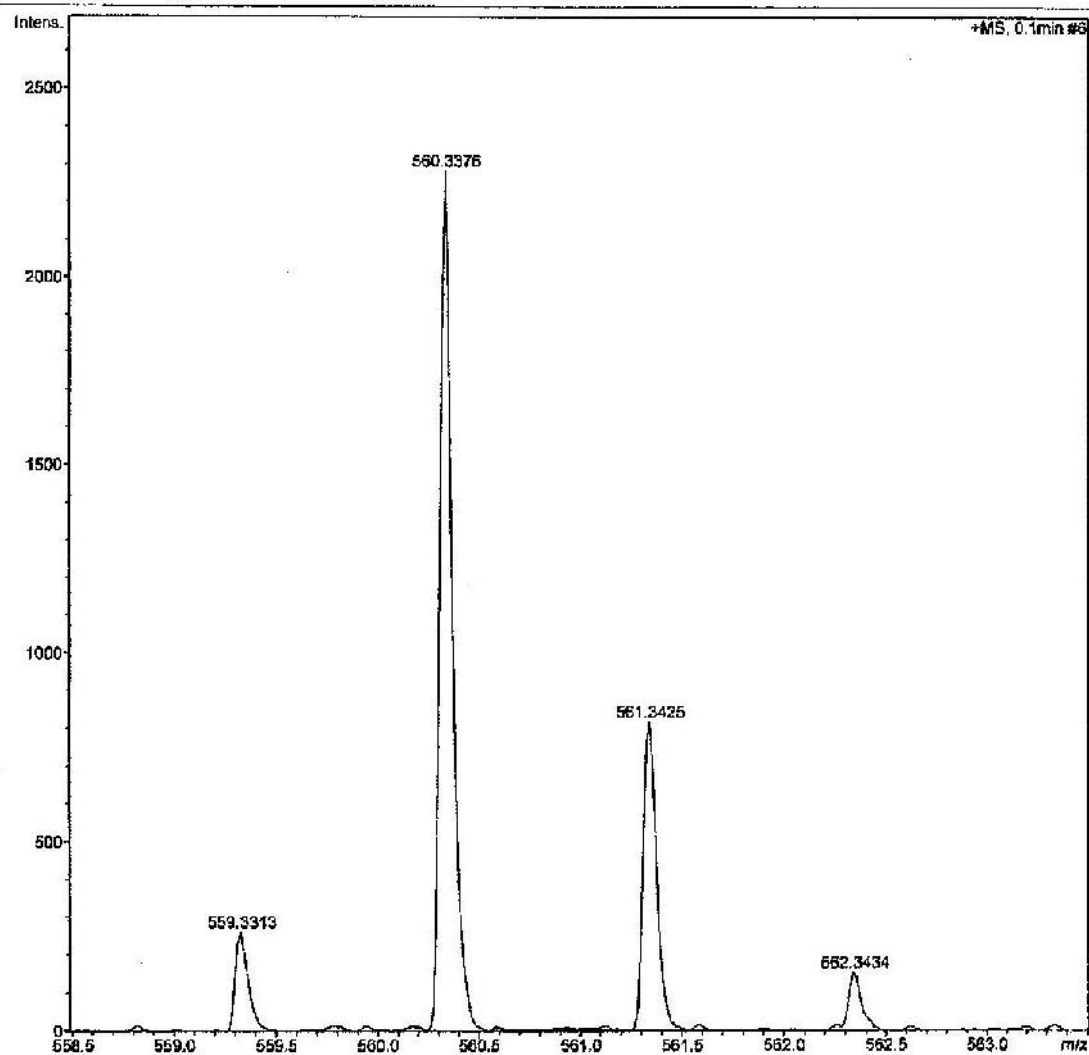
Figure A.15 ^1H , ^{13}C NMR in CDCl_3 and ATR-FTIR of CM4

Method tune_low_APCI_PEG.m
Sample Name
Comment

Operator CTB
Instrument microTOF-Q II 10414

Acquisition Parameter

Source Type	APCI	Ion Polarity	Positive	Set Nebulizer	1.6 Bar
Focus	Not active	Set Capillary	4500 V	Set Dry Heater	200 °C
Scan Begin	50 m/z	Set End Plate Offset	-500 V	Set Dry Gas	8.0 l/min
Scan End	3000 m/z	Set Collision Cell RF	150.0 Vpp	Set Divert Valve	Waste



Bruker Compass DataAnalysis 4.0

printed: 5/18/2017 3:59:03 PM

Page 1 of 1

Figure A.16 Mass spectroscopy of CM4

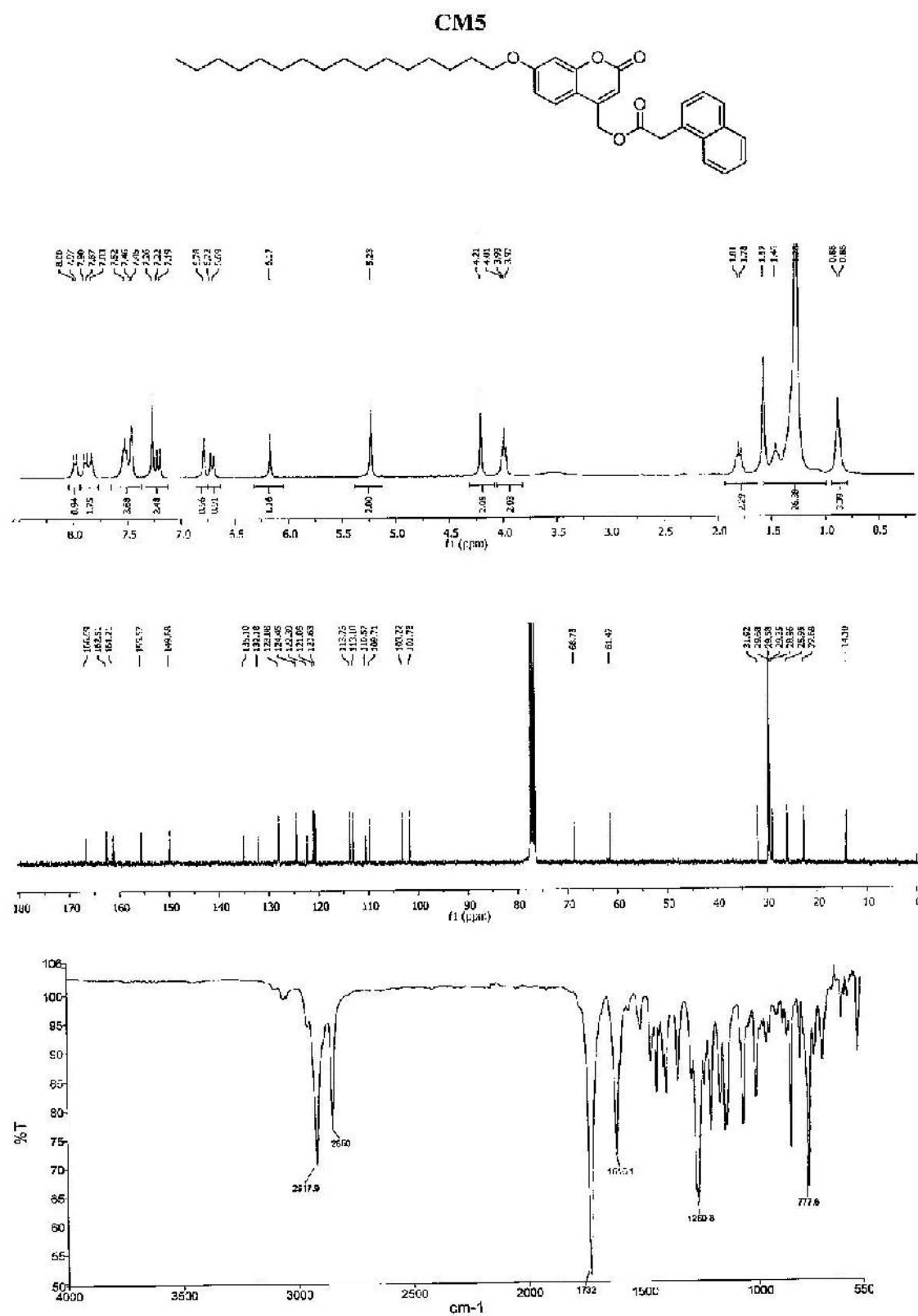


Figure A.17 ¹H, ¹³C NMR in CDCl₃ and ATR-FTIR of CM5

Method tune_low_APCI_PEG.m
Sample Name
Comment

Operator CTB
Instrument microQTOF-Q11 10414

Acquisition Parameter

Source Type	APCI	Ion Polarity	Positive	Set Nebulizer	1.6 Bar
Focus	Not active	Set Capillary	4500 V	Set Dry Heater	200 °C
Scan Begin	50 m/z	Set End Plate Offset	-500 V	Set Dry Gas	8.0 l/min
Scan End	3000 m/z	Set Collision Cell RF	150.0 Vpp	Set Divert Valve	Waste

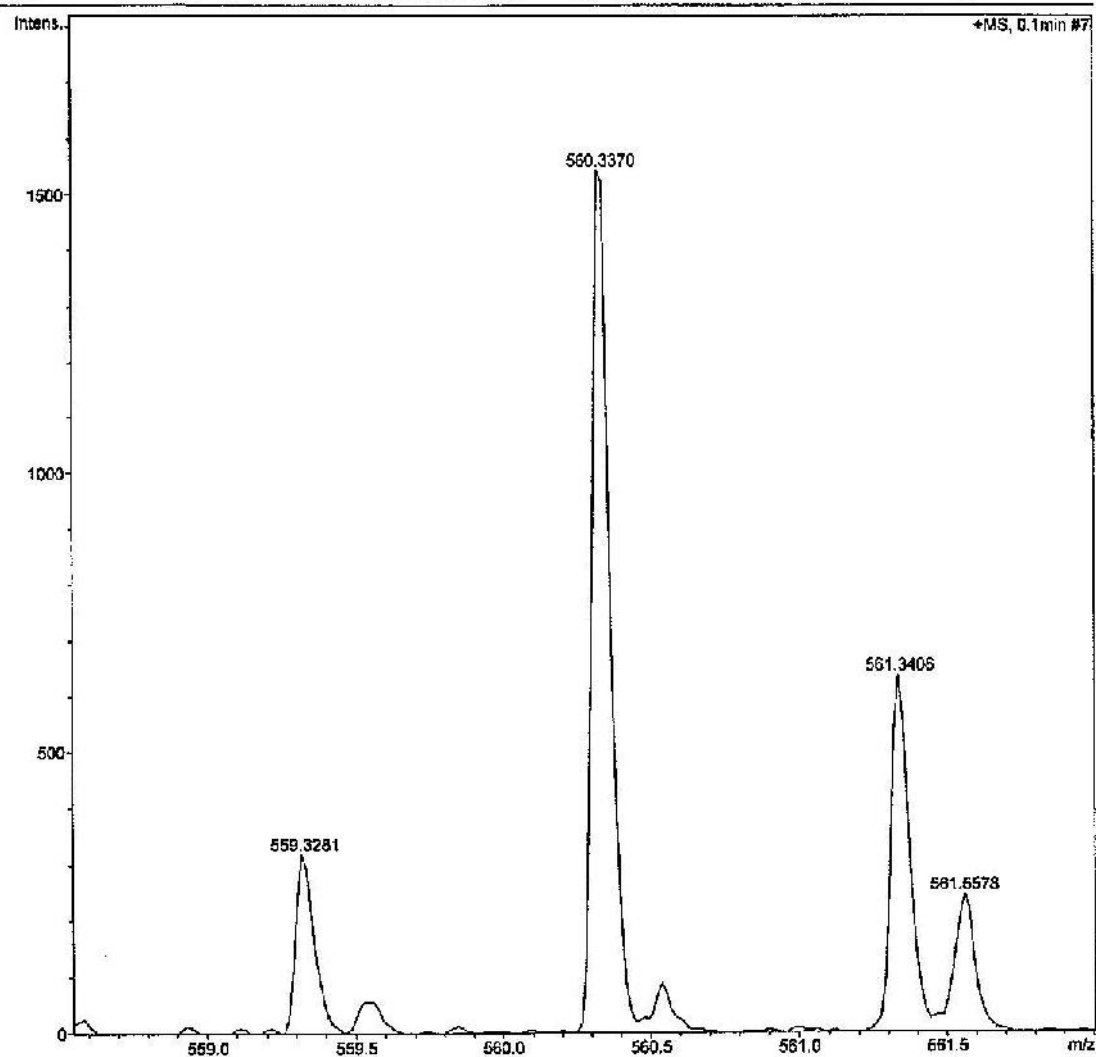
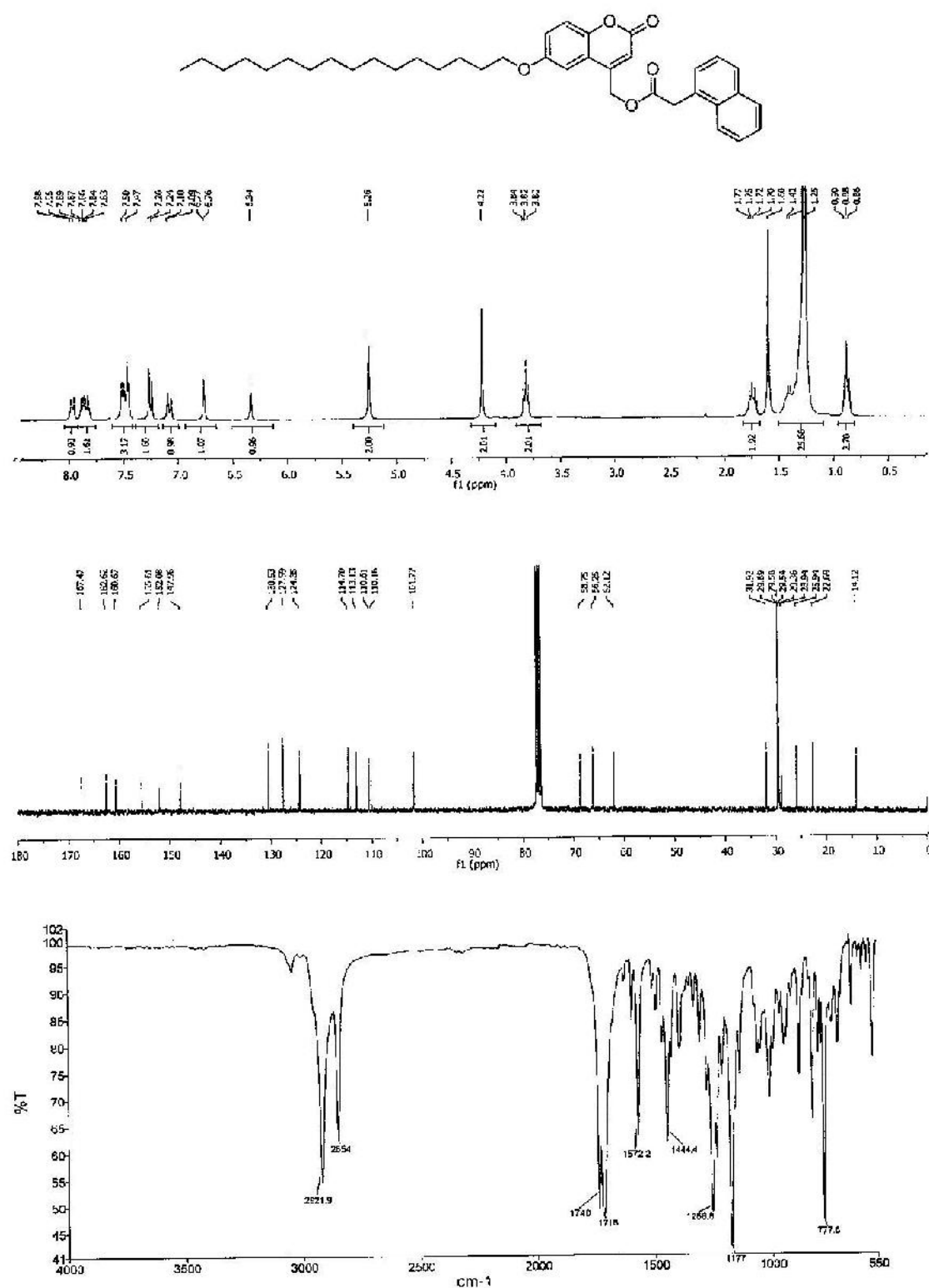


Figure A.18 Mass spectroscopy of CM5

CM6

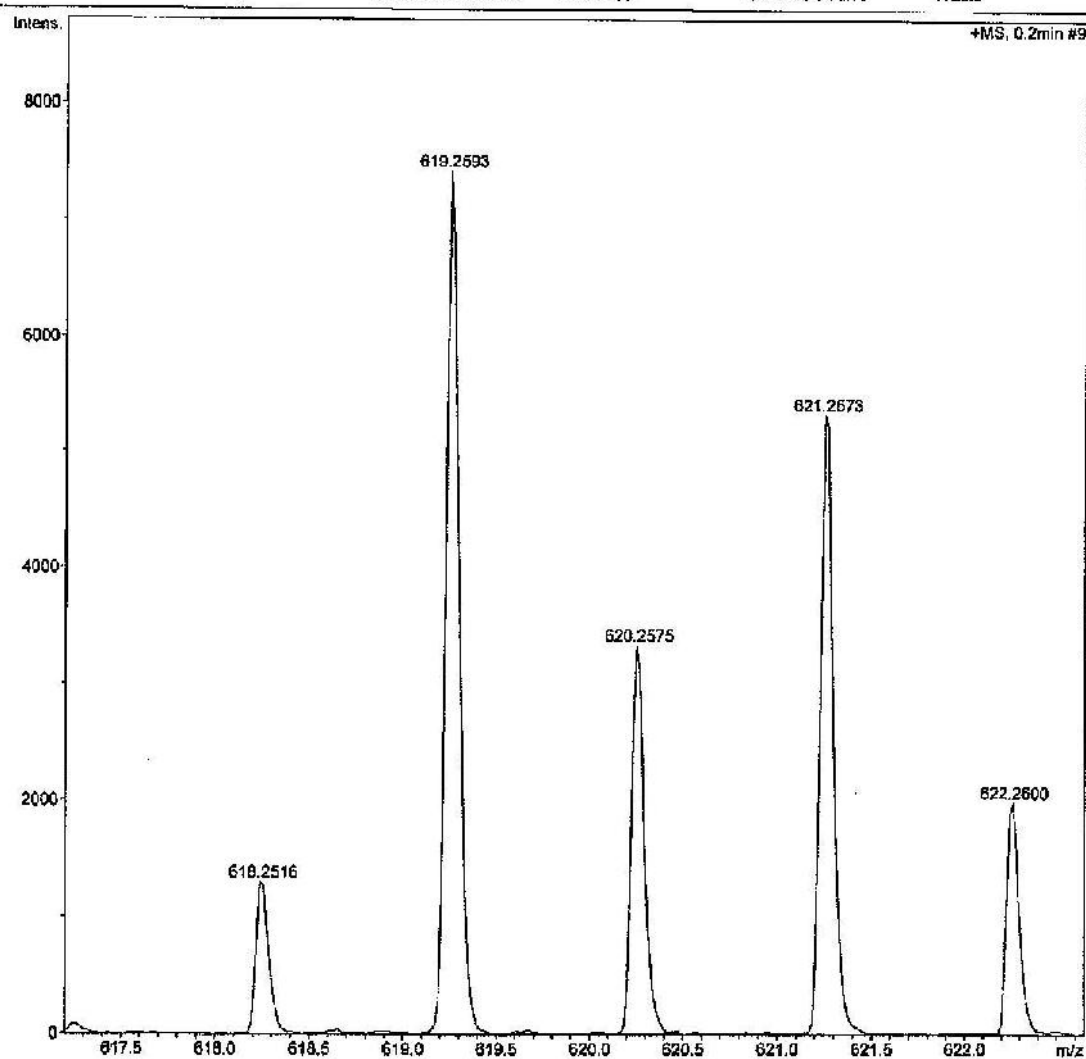
Figure A.19 ^1H , ^{13}C NMR in CDCl₃ and ATR-FTIR of CM6

Method tune_low_APCI_PEG.m
Sample Name
Comment

Operator CTB
Instrument micrOTOF-Q II 10414

Acquisition Parameter

Source Type	APCI	Ion Polarity	Positive	Set Nebulizer	1.6 Bar
Focus	Not active	Set Capillary	4500 V	Set Dry Heater	200 °C
Scan Begin	50 m/z	Set End Plate Offset	-500 V	Set Dry Gas	6.0 L/min
Scan End	3000 m/z	Set Collision Cell RF	160.0 Vpp	Set Divert Valve	Waste

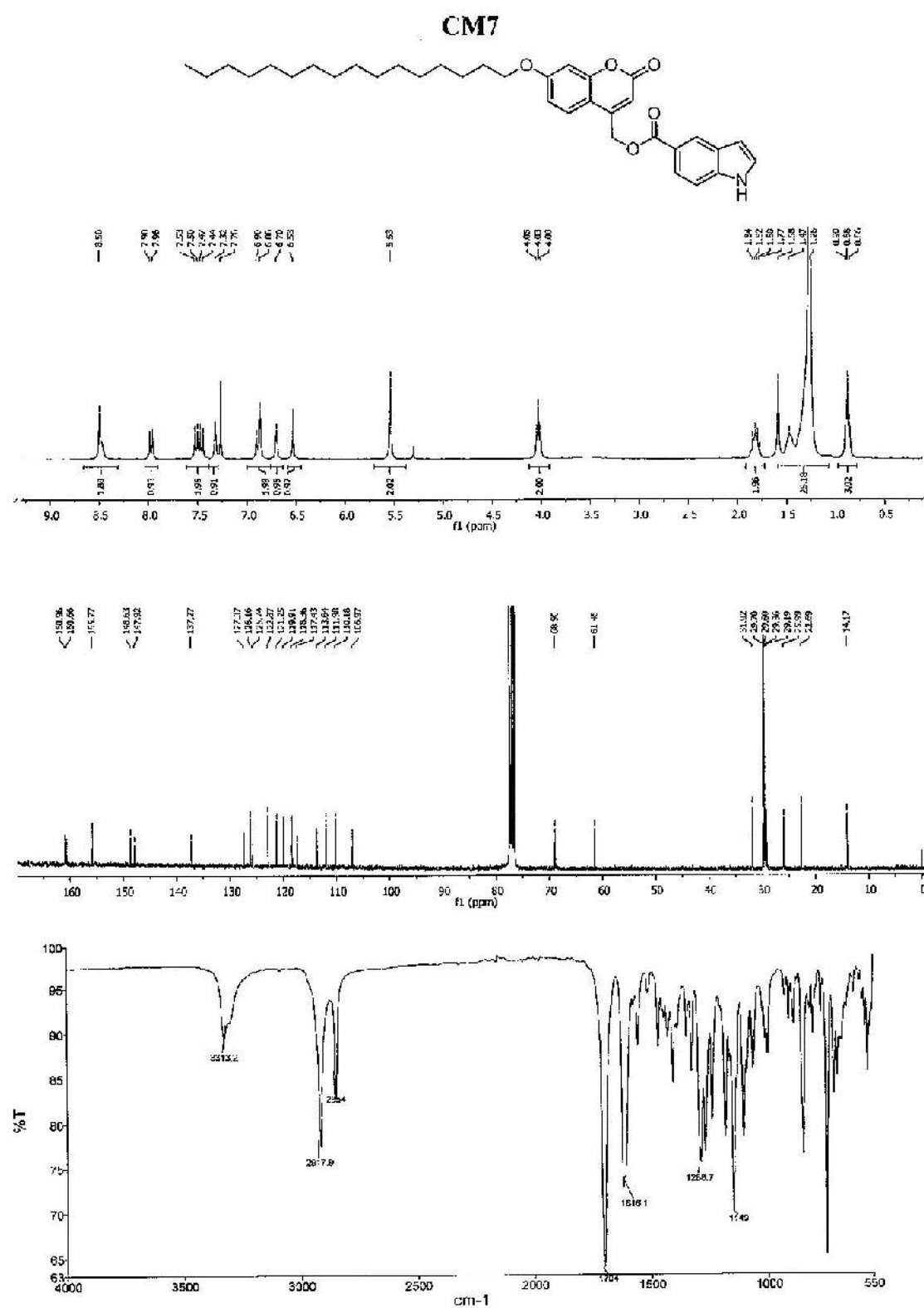


Bruker Compass DataAnalysis 4.0

printed: 5/18/2017 3:57:31 PM

Page 1 of 1

Figure A.20 Mass spectroscopy of CM6

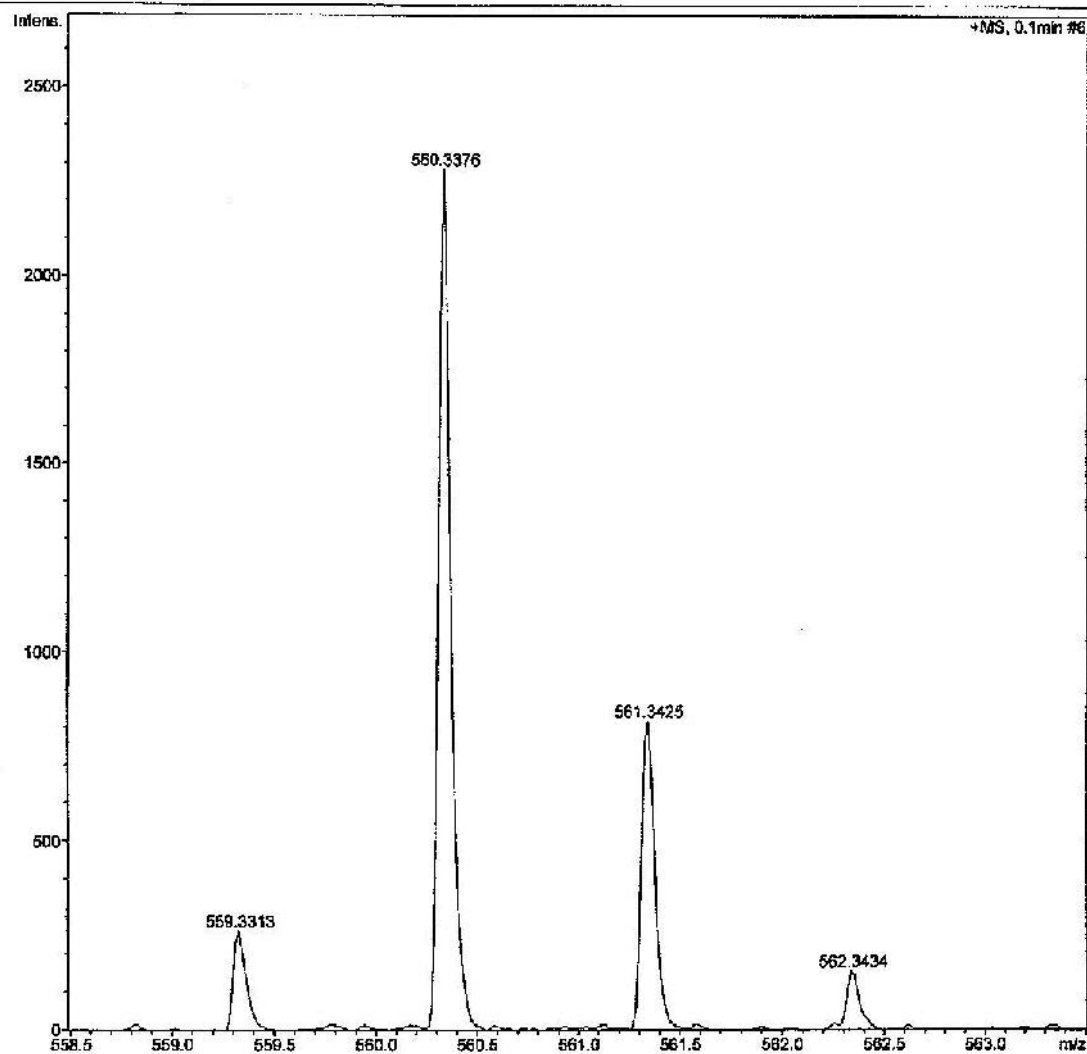


Method tune_low_APCI_PEG.m
Sample Name
Comment

Operator CTB
Instrument micrOTOF-Q II 10414

Acquisition Parameter

Source Type	APCI	Ion Polarity	Positive	Set Nebulizer	1.6 Bar
Focus	Not active	Set Capillary	4500 V	Set Dry Heater	200 °C
Scan Begin	50 m/z	Set End Plate Offset	-500 V	Set Dry Gas	8.0 l/min
Scan End	3000 m/z	Set Collision Cell RF	150.0 Vpp	Set Divert Valve	Waste



Bruker Compass DataAnalysis 4.0

printed: 5/18/2017 3:59:03 PM

Page 1 of 1

Figure A.22 Mass spectroscopy of CM7

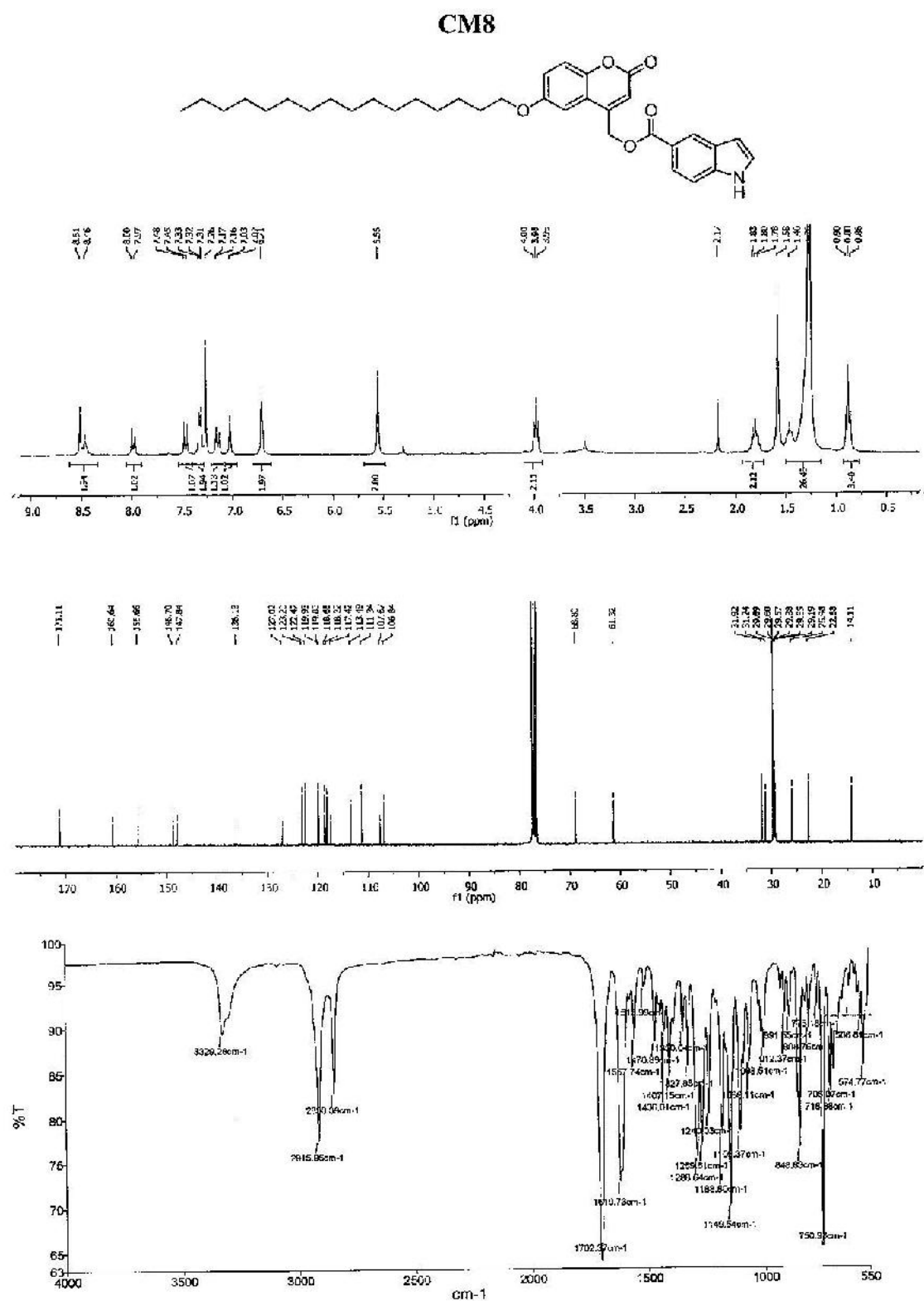


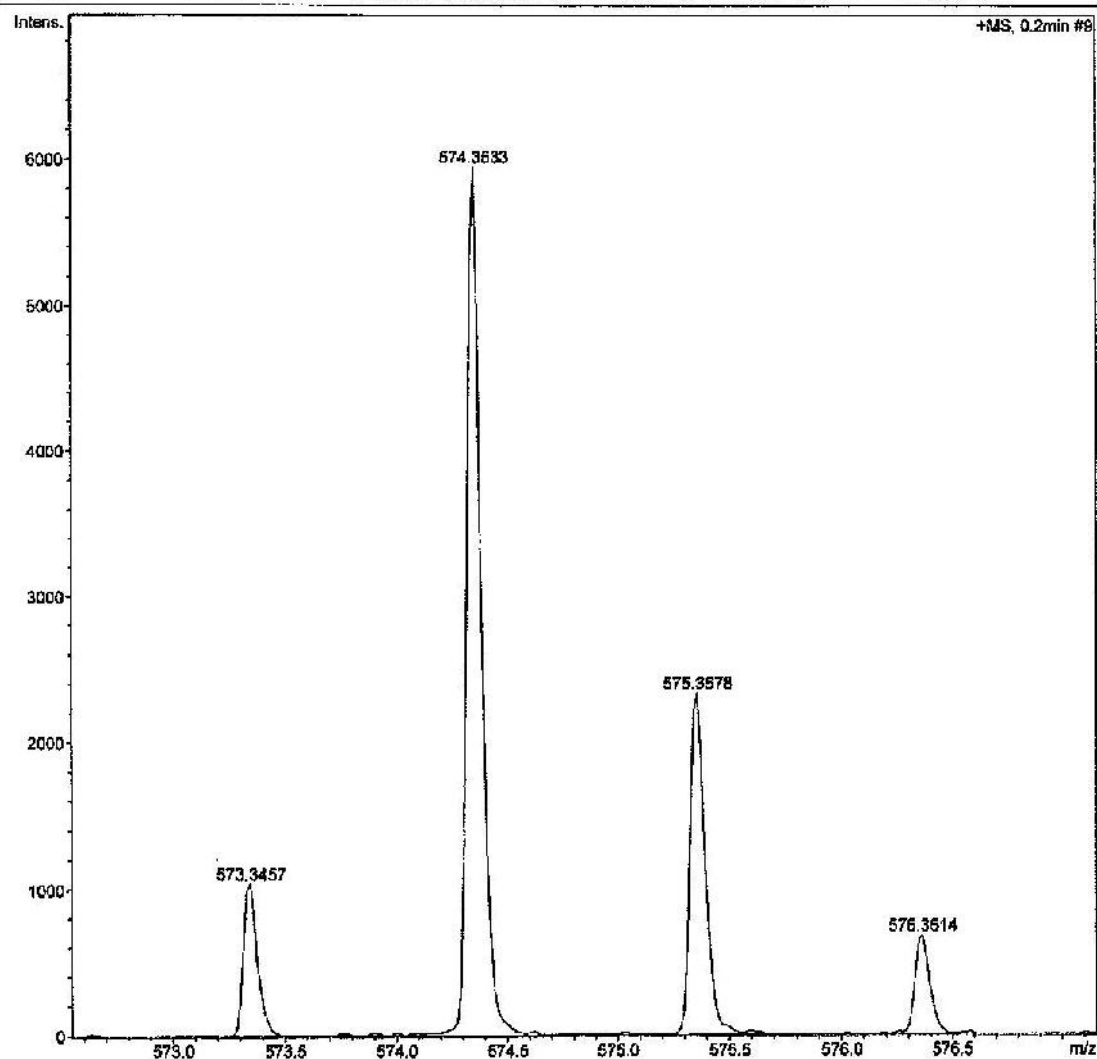
Figure A.23 ^1H , ^{13}C NMR in CDCl_3 and ATR-FTIR of CM8

Method tune_low_APCI_PEG.m
Sample Name
Comment

Operator CTB
Instrument microTOF-Q II 10414

Acquisition Parameter

Source Type	APCI	Ion Polarity	Positive	Set Nebulizer	1.6 Bar
Focus	Not active	Set Capillary	4500 V	Set Dry Heater	200 °C
Scan Begin	50 m/z	Set End Plate Offset	-500 V	Set Dry Gas	8.0 l/min
Scan End	3000 m/z	Set Collision Cell RF	150.0 Vpp	Set Divert Valve	Waste



Bruker Compass DataAnalysis 4.0

printed: 5/18/2017 4:00:26 PM

Page 1 of 1

Figure A.24 Mass spectroscopy of CM8

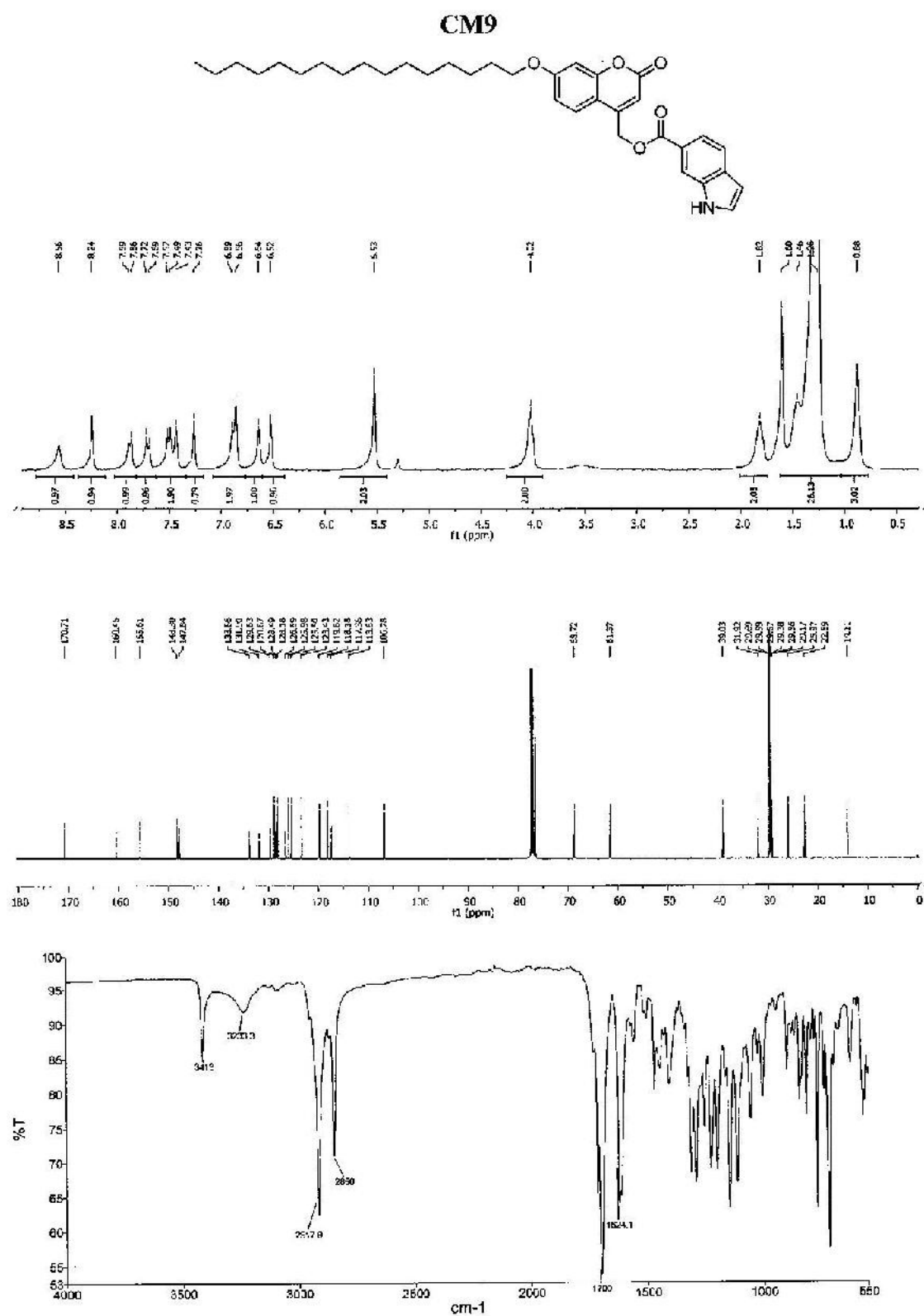


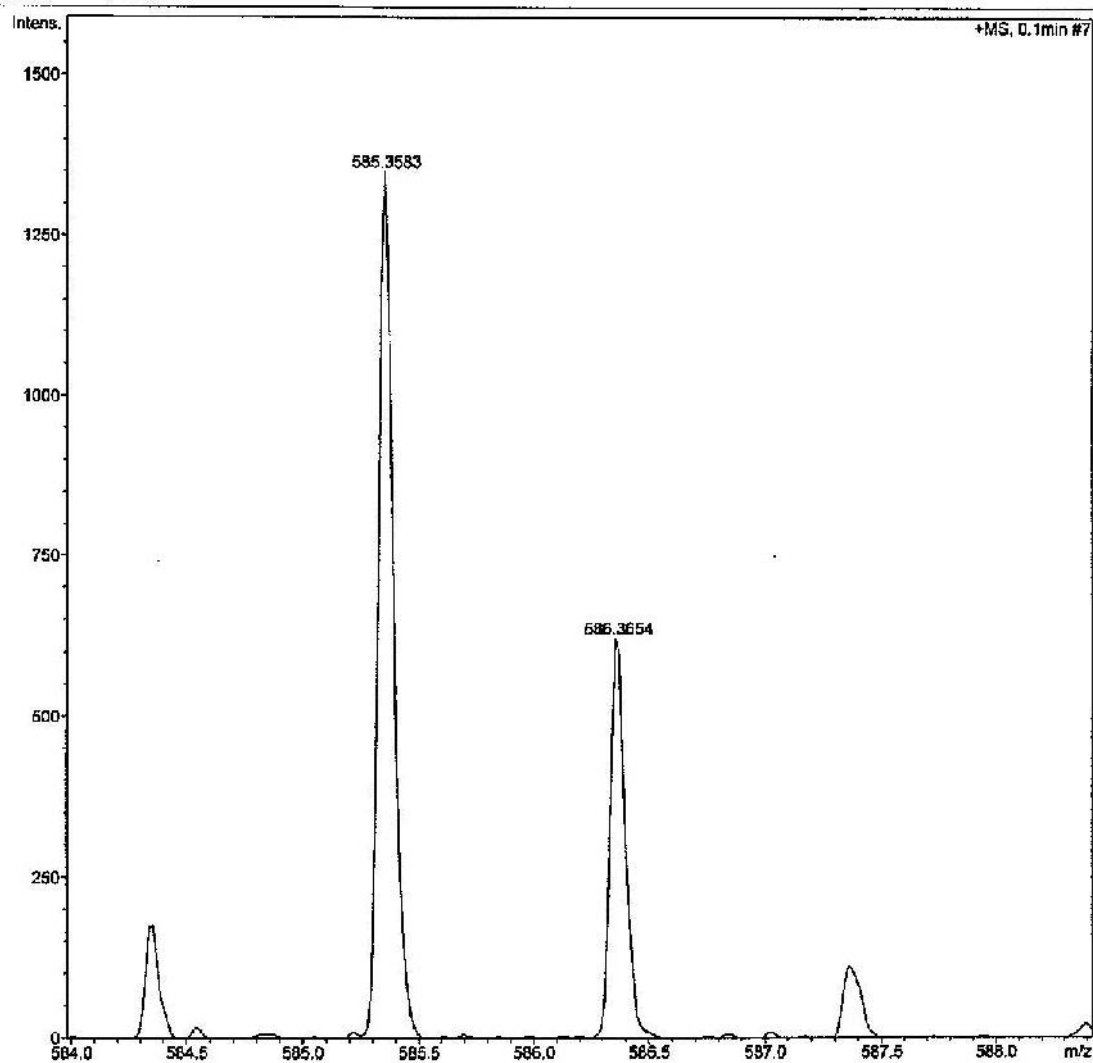
Figure A.25 ^1H , ^{13}C NMR in CDCl_3 and ATR-FTIR of CM9

Method tune_low_APCI_PEG.m
Sample Name
Comment

Operator CTB
Instrument micrOTOF-Q II 10414

Acquisition Parameter

Source Type	APCI	Ion Polarity	Positive	Set Nebulizer	1.6 Bar
Focus	Not active	Set Capillary	4500 V	Set Dry Heater	200 °C
Scan Begin	50 m/z	Set End Plate Offset	-500 V	Set Dry Gas	8.0 l/min
Scan End	3000 m/z	Set Collision Cell RF	150.0 Vpp	Set Divert Valve	Waste



Bruker Compass DataAnalysis 4.0

printed: 5/18/2017 4:03:02 PM

Page 1 of 1

Figure A.26 Mass spectroscopy of CM9

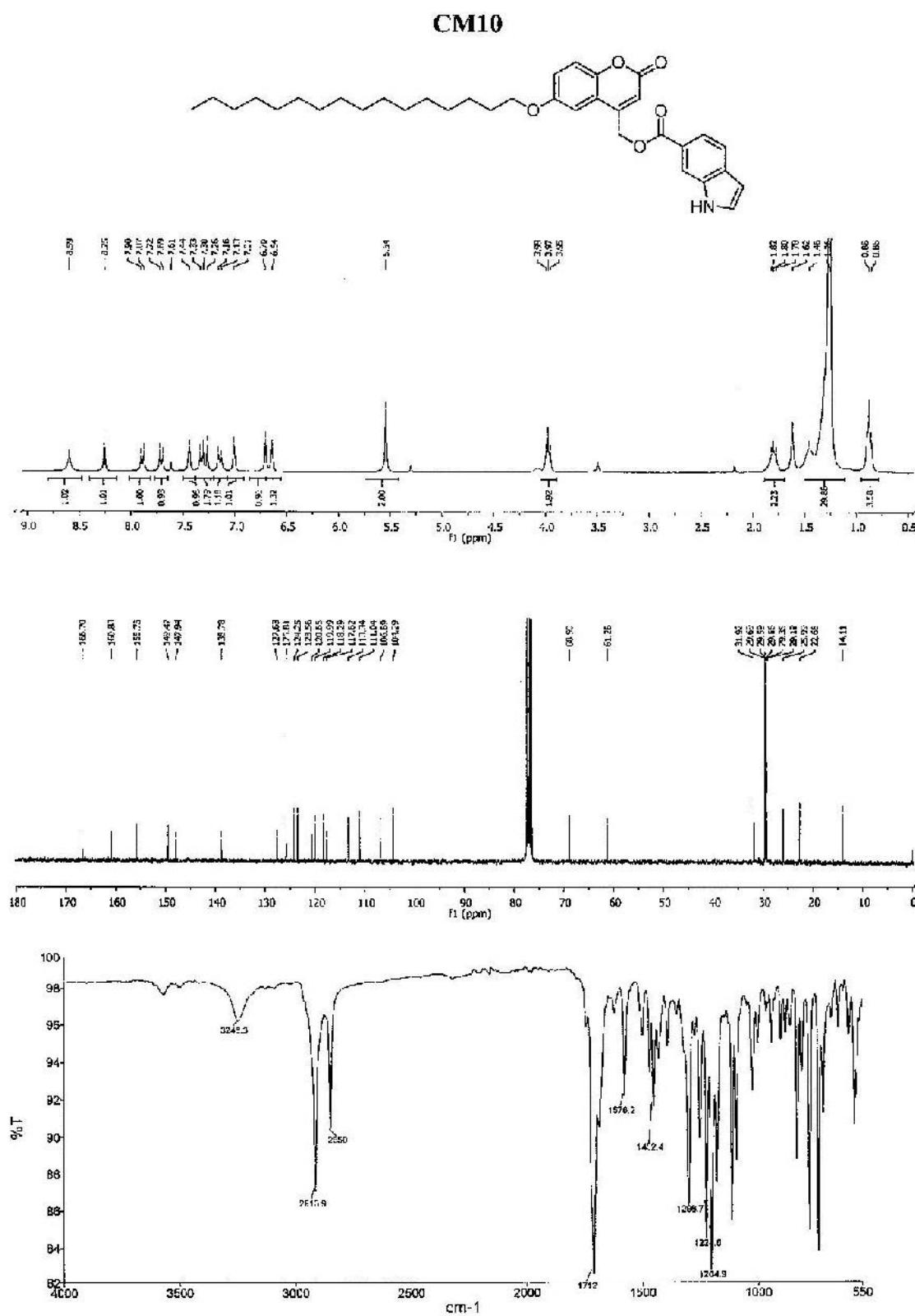


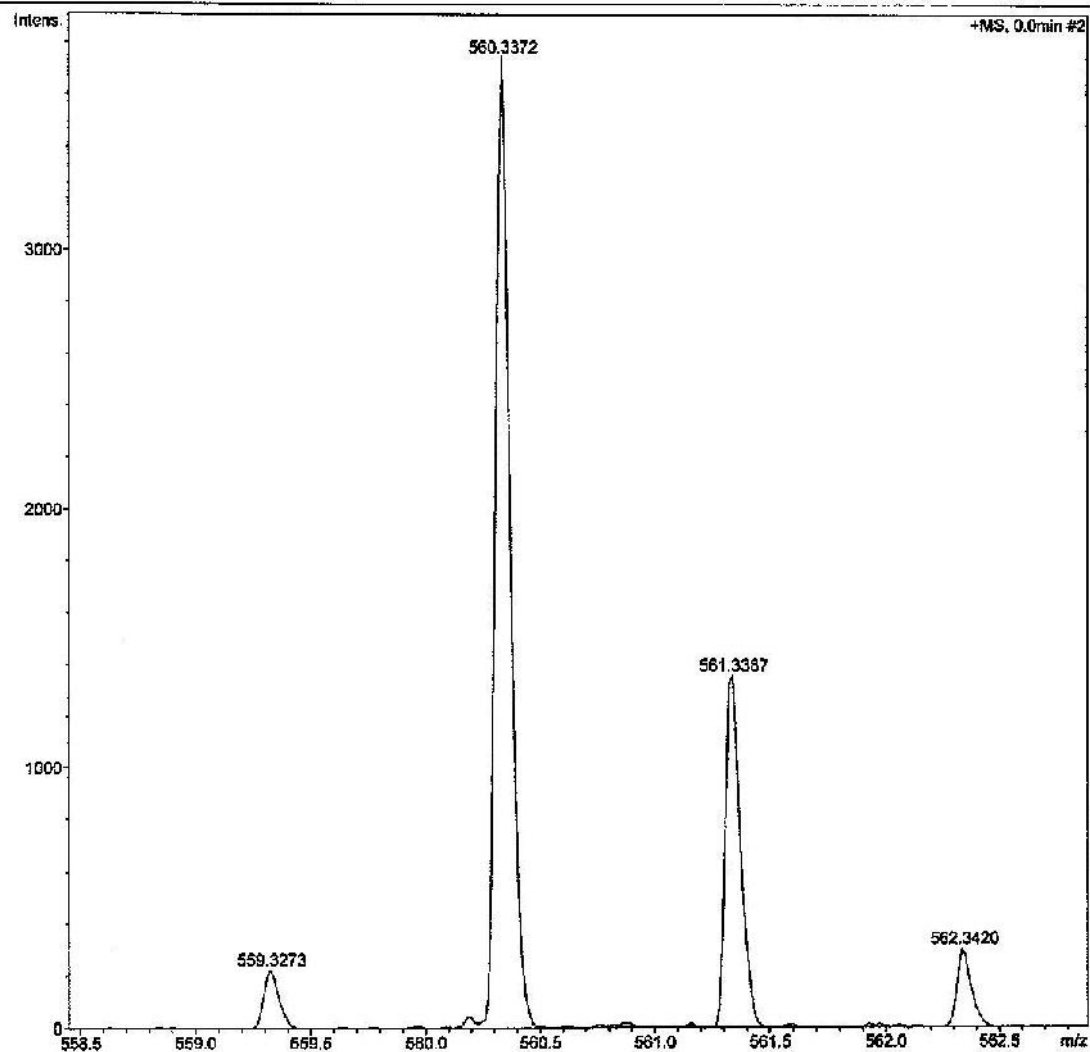
Figure A.27 ^1H , ^{13}C NMR in CDCl_3 and ATR-FTIR of CM10

Method tune_low_APCI_PEG.m
Sample Name
Comment

Operator CTB
Instrument microTOF-Q II 10414

Acquisition Parameter

Source Type	APCI	Ion Polarity	Positive	Set Nebulizer	1.6 Bar
Focus	Not active	Set Capillary	4500 V	Set Dry Heater	200 °C
Scan Begin	50 m/z	Set End Plate Offset	-500 V	Set Dry Gas	8.0 l/min
Scan End	3000 m/z	Set Collision Cell RF	150.0 Vpp	Set Divert Valve	Waste



Bruker Compass DataAnalysis 4.0

printed: 5/18/2017 4:04:50 PM

Page 1 of 1

Figure A.28 Mass spectroscopy of CM10

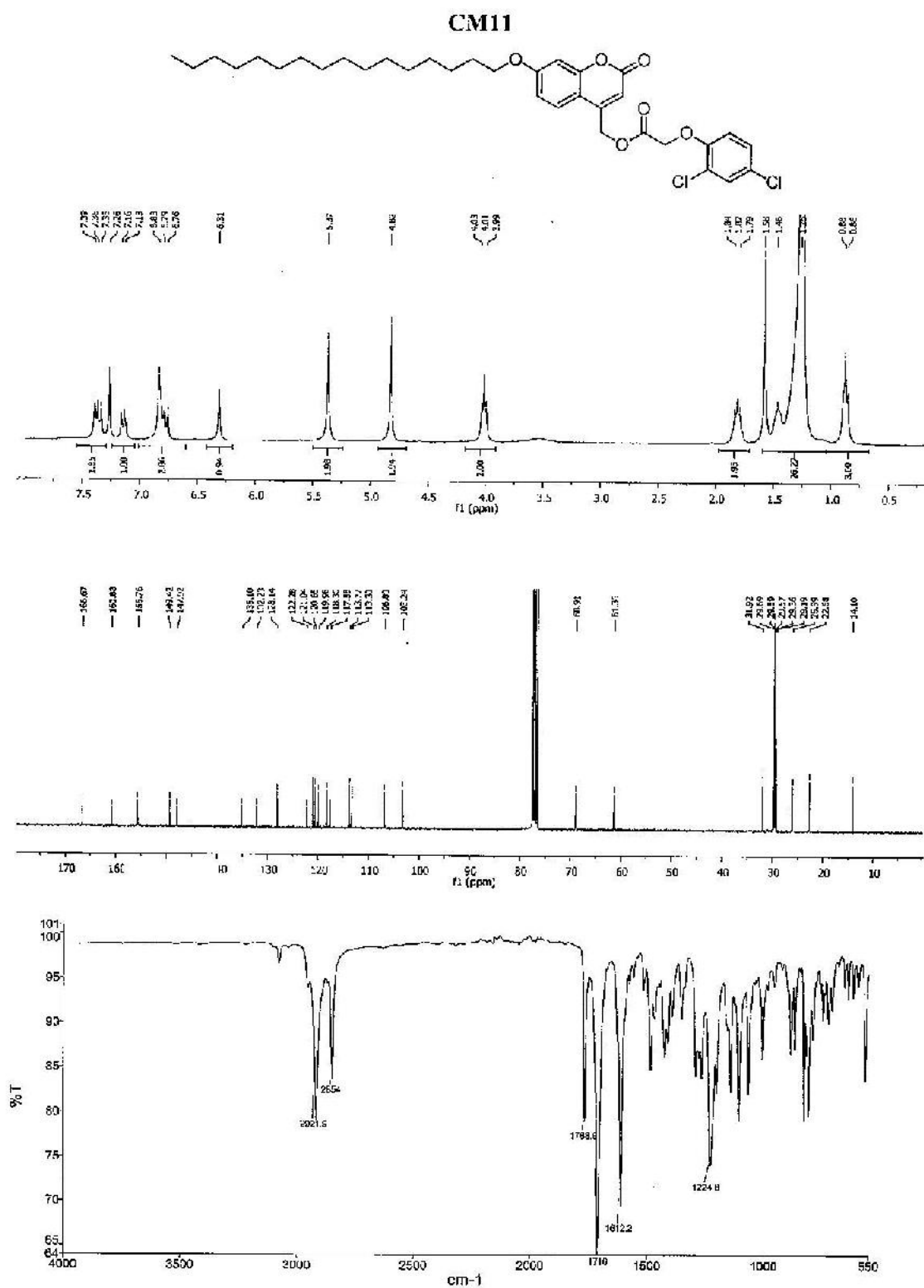


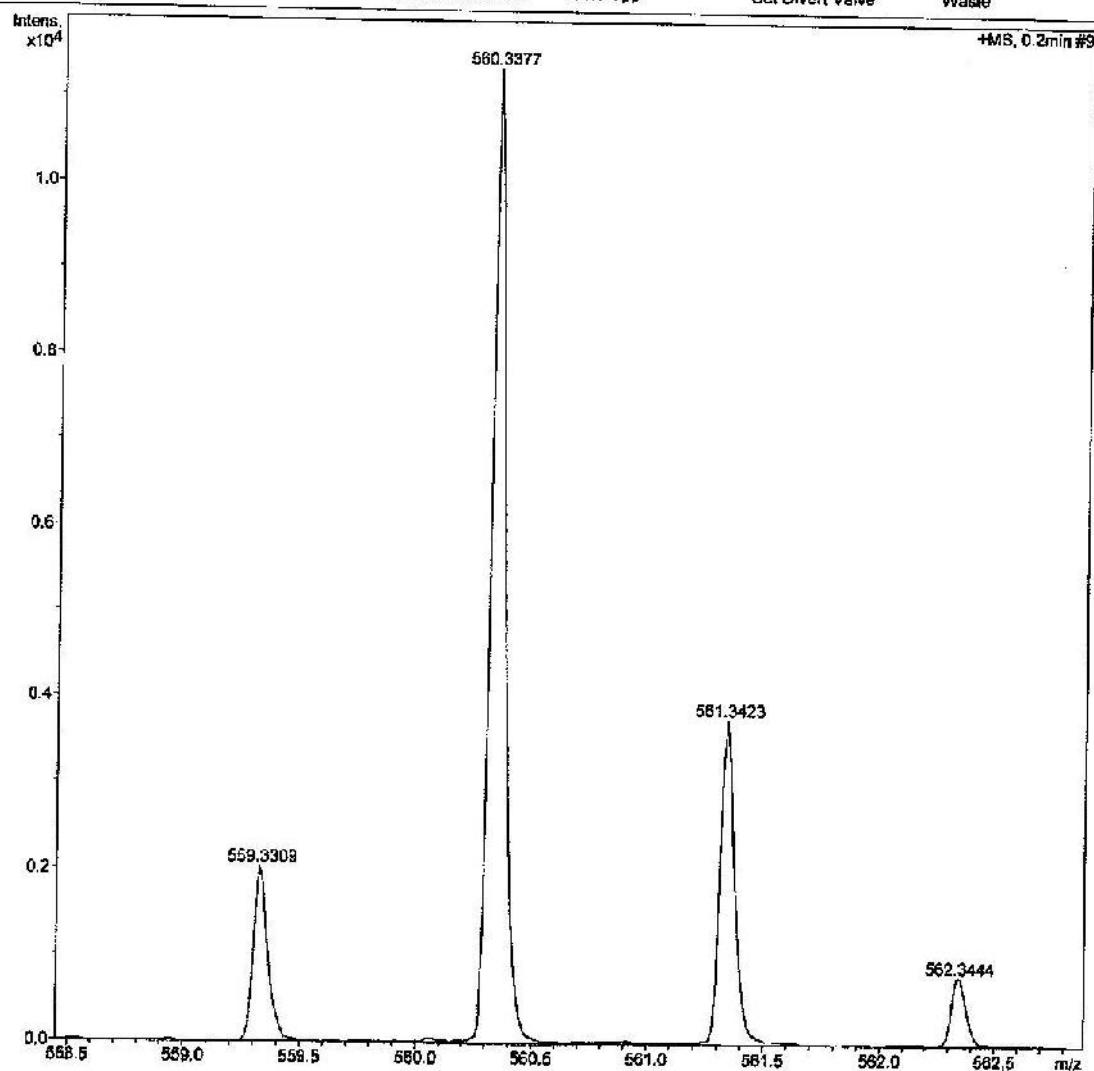
Figure A.29 ^1H , ^{13}C NMR in CDCl₃ and ATR-FTIR of CM11

Method tune_low_APCI_PEG.m
Sample Name
Comment

Operator CTB
Instrument microTOF-Q II 10414

Acquisition Parameter

Source Type	APCI	Ion Polarity	Positive	Set Nebulizer	1.6 Bar
Focus	Not active	Set Capillary	4500 V	Set Dry Heater	200 °C
Scan Begin	50 m/z	Set End Plate Offset	-500 V	Set Dry Gas	8.0 l/min
Scan End	3000 m/z	Set Collision Cell RF	150.0 Vpp	Set Divert Valve	Waste



Bruker Compass DataAnalysis 4.0

printed: 5/19/2017 4:05:38 PM

Page 1 of 1

Figure A.30 Mass spectroscopy of CM11

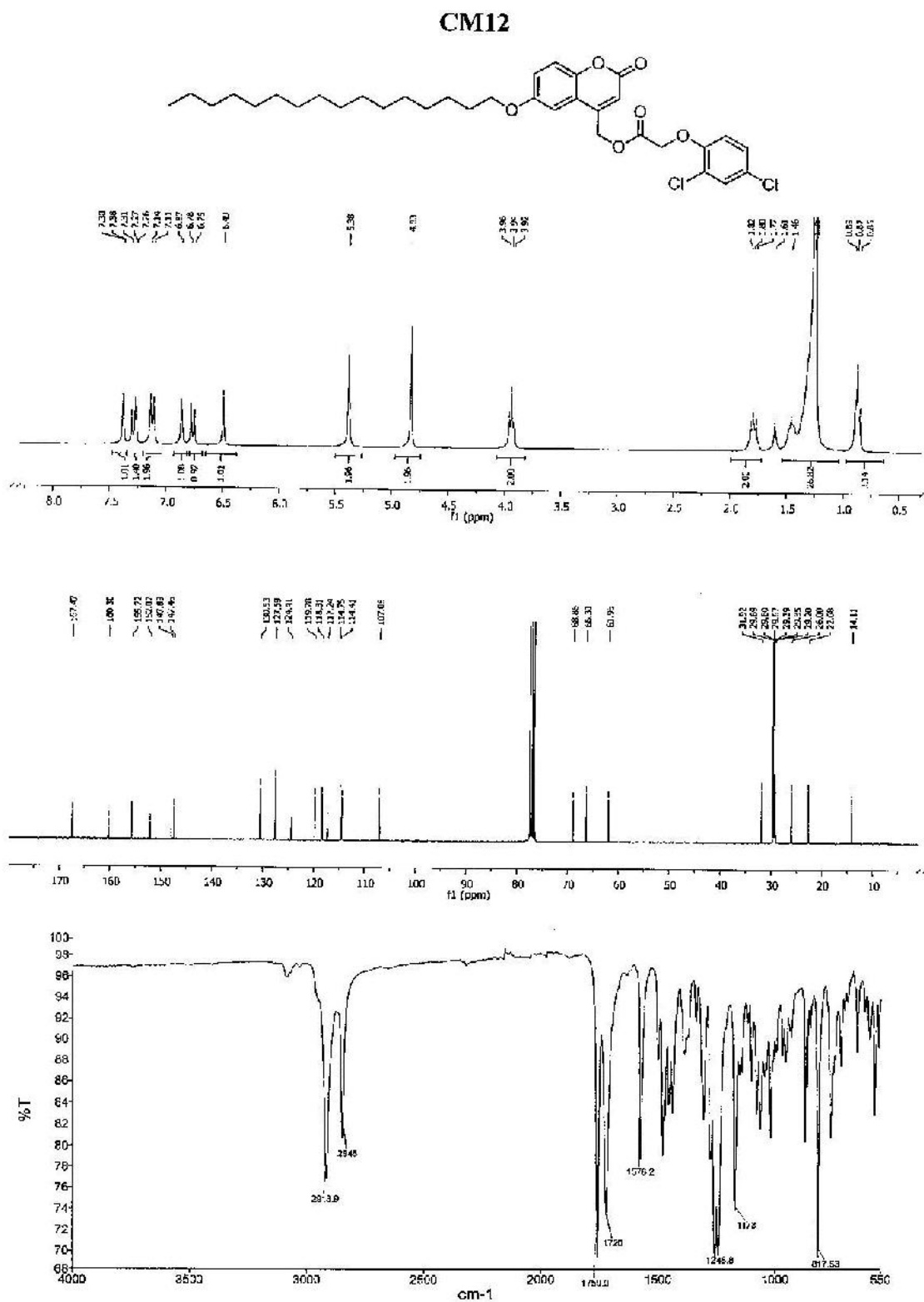


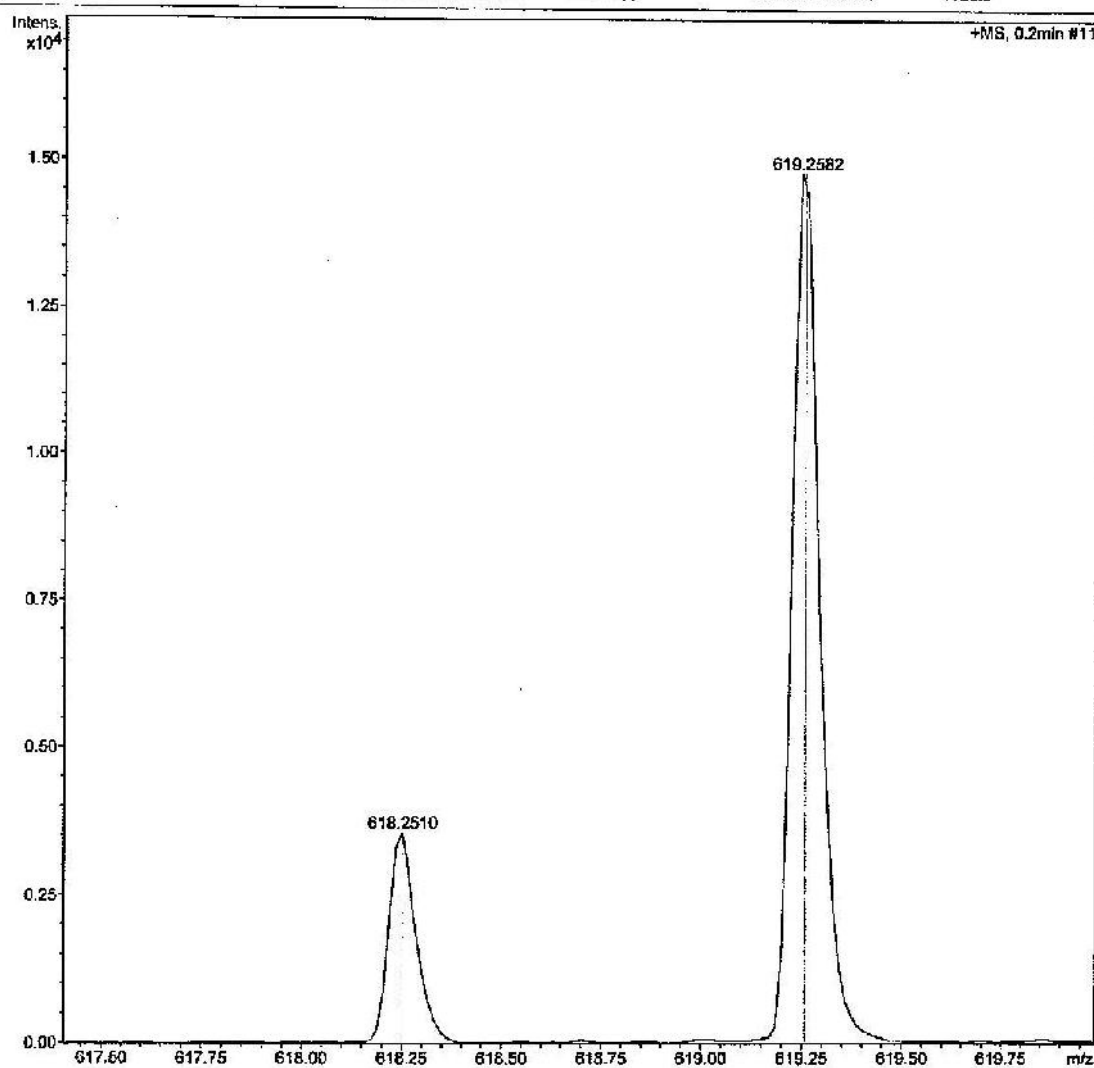
Figure A.31 ^1H , ^{13}C NMR in CDCl_3 and ATR-FTIR of CM12

Method tune_low_APCI_PEG.m
Sample Name
Comment

Operator CTB
Instrument microTOF-Q II 10414

Acquisition Parameter

Source Type	APCI	Ion Polarity	Positive	Set Nebulizer	1.6 Bar
Focus	Not active	Set Capillary	4500 V	Set Dry Heater	200 °C
Scan Begin	50 m/z	Set End Plate Offset	-500 V	Set Dry Gas	8.0 l/min
Scan End	3000 m/z	Set Collision Cell RF	150.0 Vpp	Set Divert Valve	Waste

**Figure A.32 Mass spectroscopy of CM12**

APPENDIX B

Photophysical properties and photolysis data

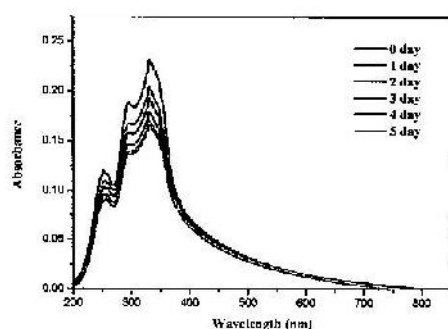
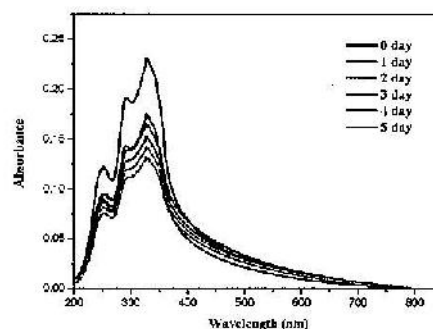
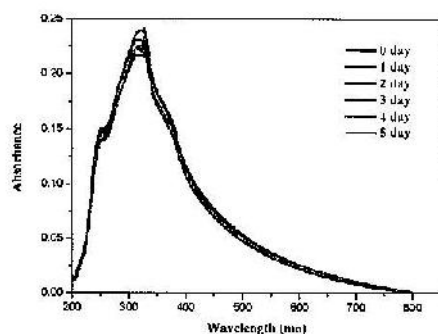
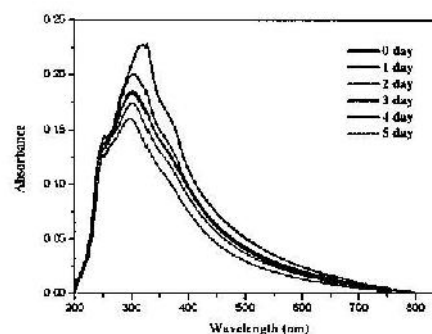
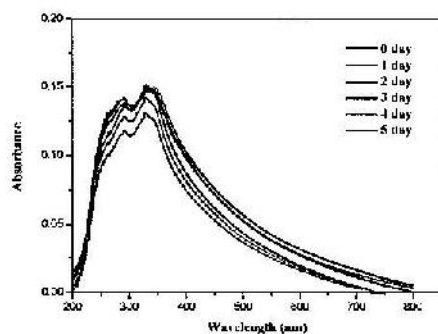
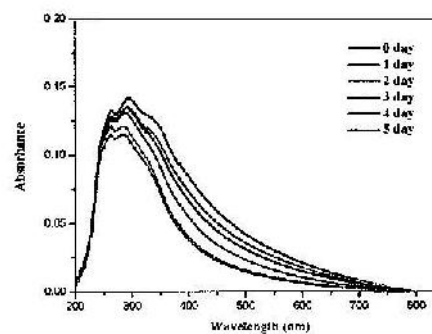
CM1 under UV light (365 nm)**CM1 under sunlight****CM2 under UV light (365 nm)****CM2 under sunlight****CM3 under UV light (365 nm)****CM3 under sunlight**

Figure B.1 Absorption spectra after 5 day irradiation by UV light (left) and sunlight (right)

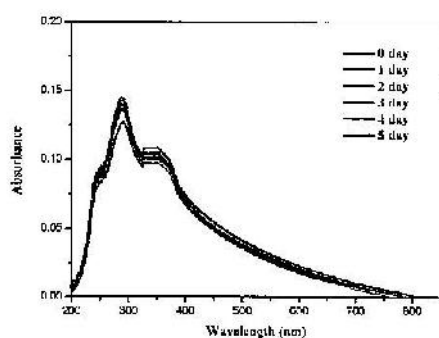
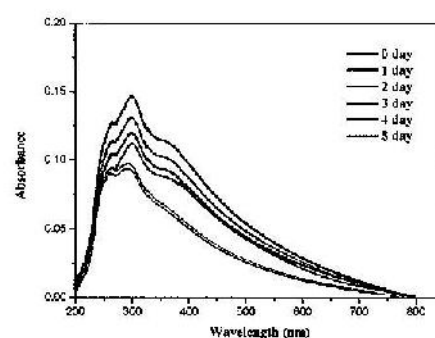
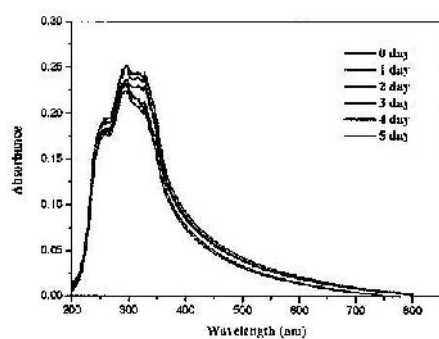
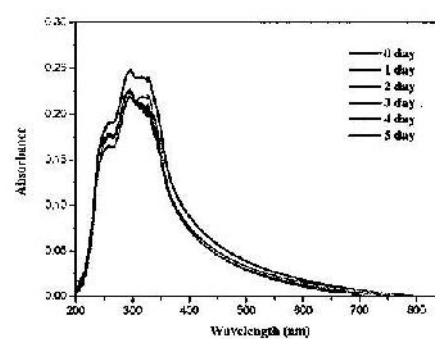
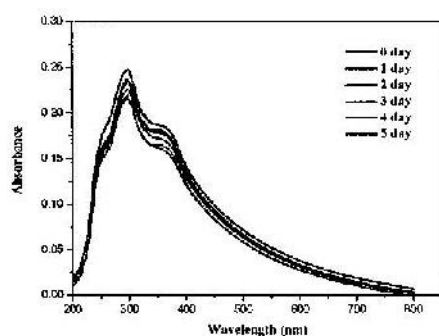
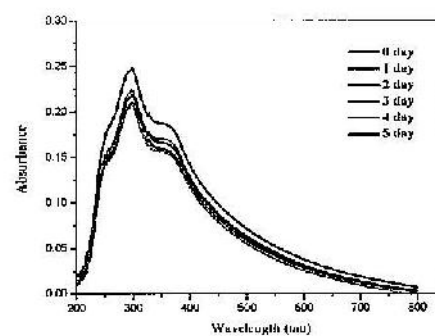
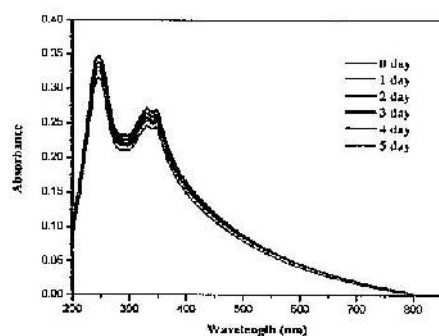
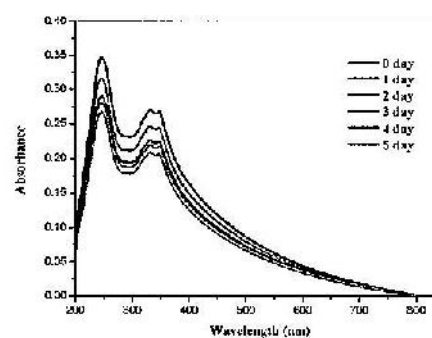
CM4 under UV light (365 nm)**CM4 under sunlight****CM5 under UV light (365 nm)****CM5 under sunlight****CM6 under UV light (365 nm)****CM6 under sunlight**

Figure B.1 Absorption spectra after 5 day irradiation by UV light (left) and sunlight (right) (continued)

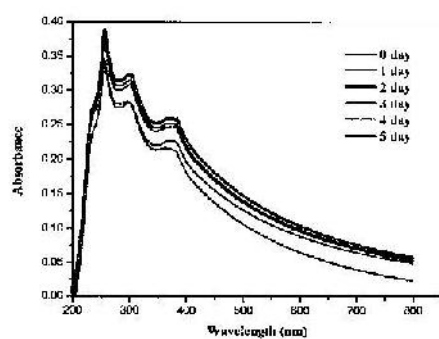
CM7 under UV light (365 nm)



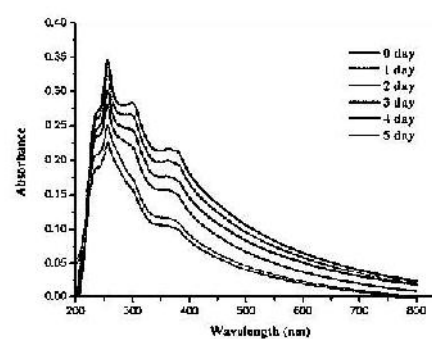
CM7 under sunlight



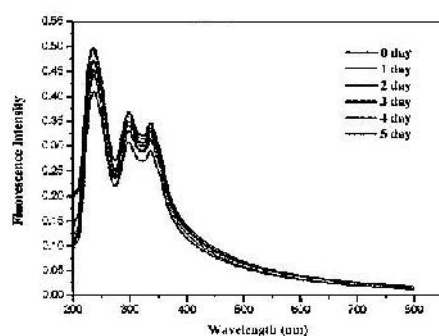
CM8 under UV light (365 nm)



CM8 under sunlight



CM9 under UV light (365 nm)



CM9 under sunlight

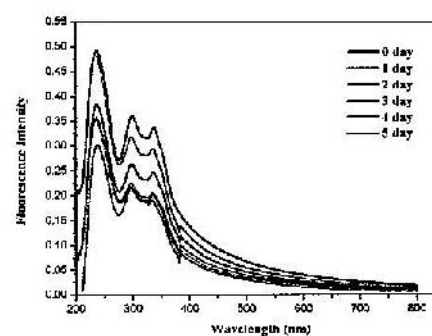
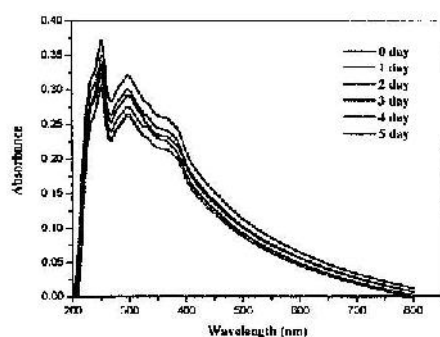
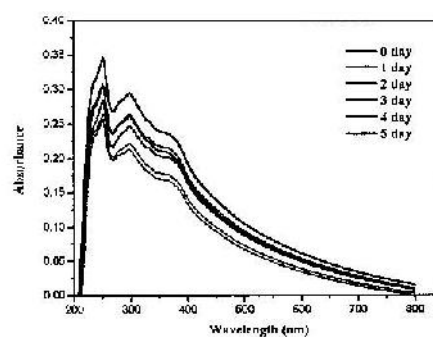


Figure B.1 Absorption spectra after 5 day irradiation by UV light (left) and sunlight (right) (continued)

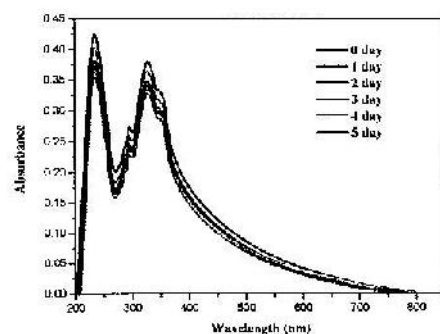
CM10 under UV light (365 nm)



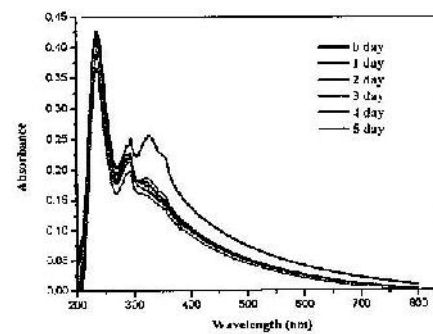
CM10 under sunlight



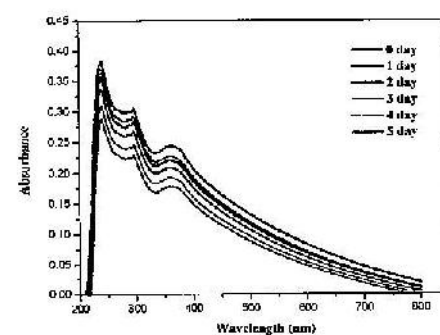
CM11 under UV light (365 nm)



CM11 under sunlight



CM12 under UV light (365 nm)



CM12 under sunlight

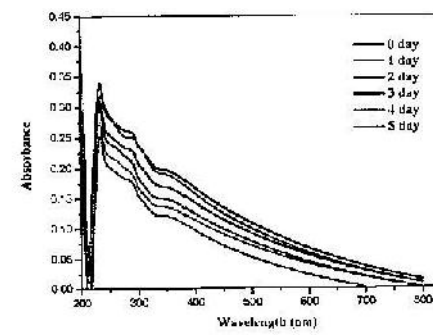


Figure B.1 Absorption spectra after 5 day irradiation by UV light (left) and sunlight (right) (continued)

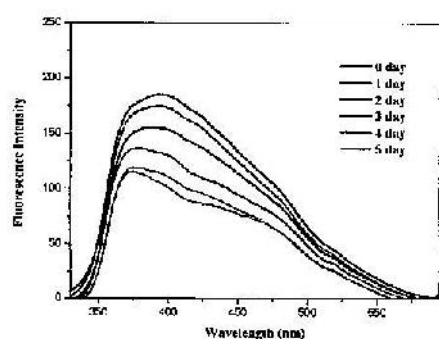
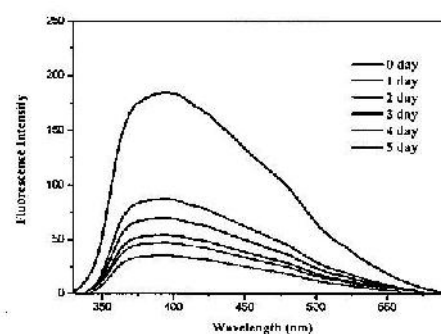
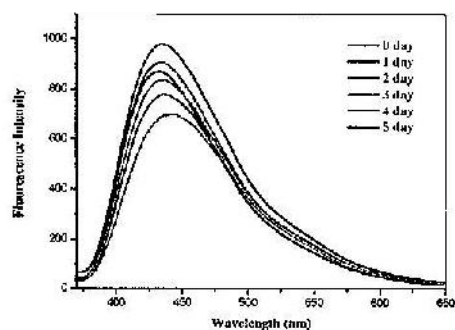
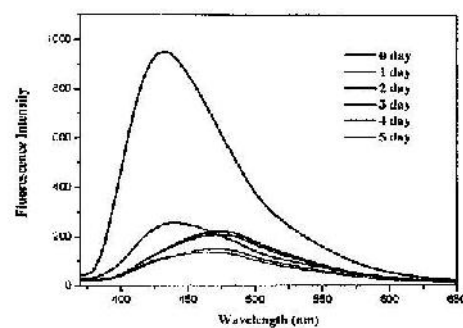
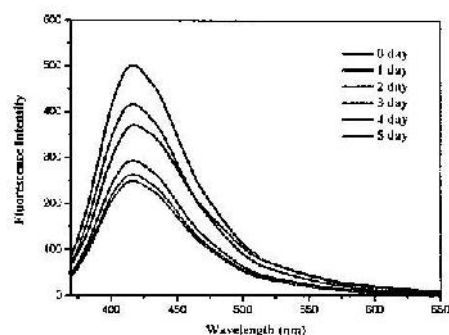
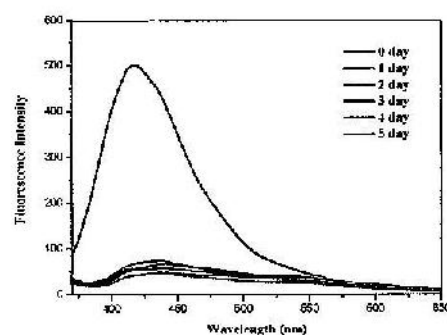
CM1 under UV light (365 nm)**CM1 under sunlight****CM2 under UV light (365 nm)****CM2 under sunlight****CM3 under UV light (365 nm)****CM3 under sunlight**

Figure B.2 Fluorescence spectra after 5 day irradiation by UV light (left) and sunlight (right)

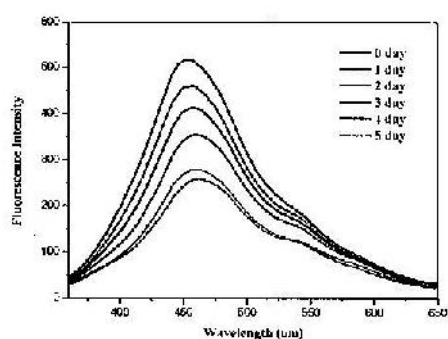
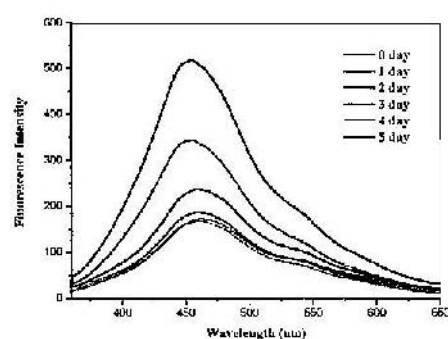
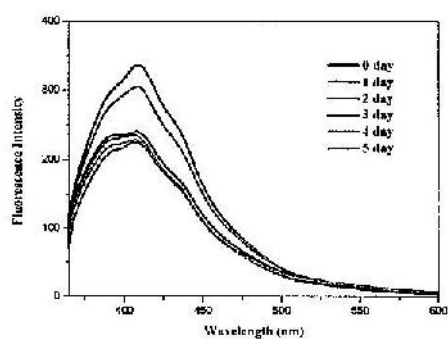
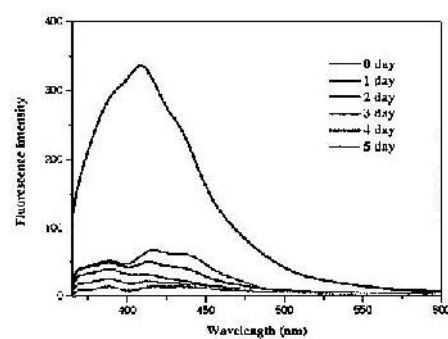
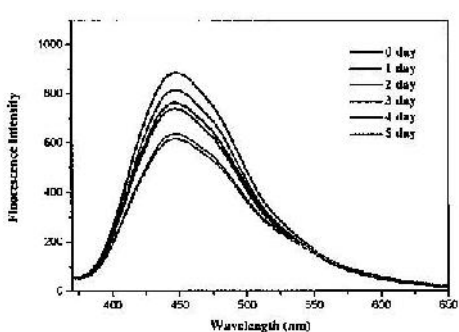
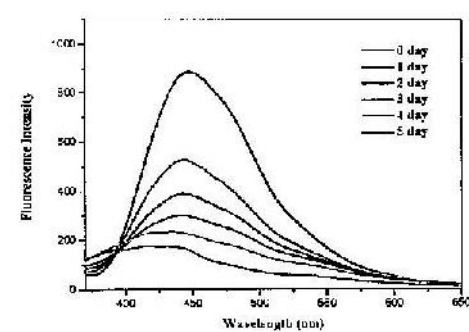
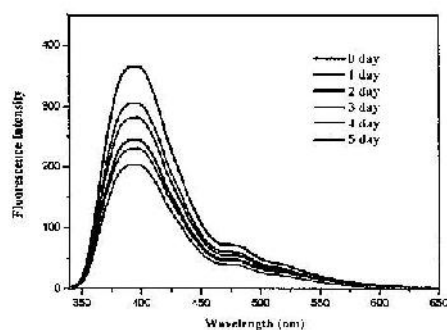
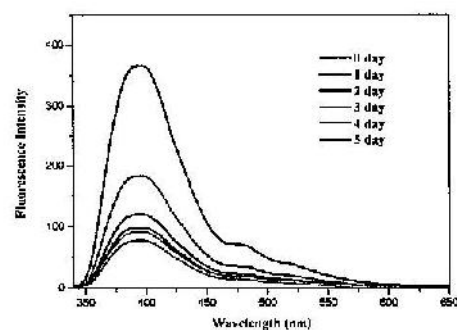
CM4 under UV light (365 nm)**CM4 under sunlight****CM5 under UV light (365 nm)****CM5 under sunlight****CM6 under UV light (365 nm)****CM6 under sunlight**

Figure B.2 Fluorescence spectra after 5 day irradiation by UV light (left) and sunlight (right) (continued)

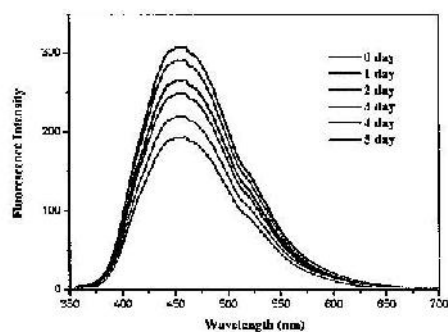
CM7 under UV light (365 nm)



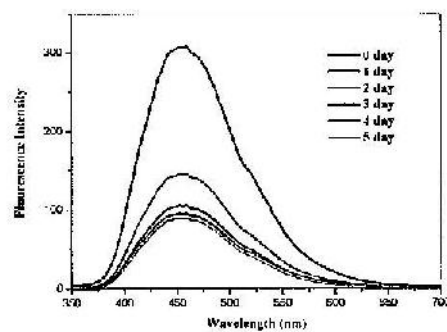
CM7 under sunlight



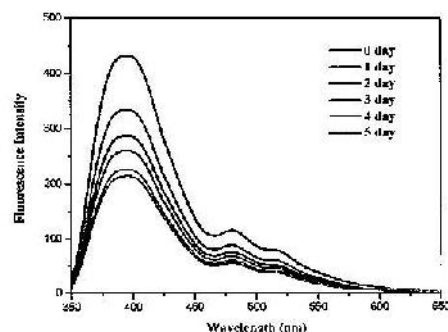
CM8 under UV light (365 nm)



CM8 under sunlight



CM9 under UV light (365 nm)



CM9 under sunlight

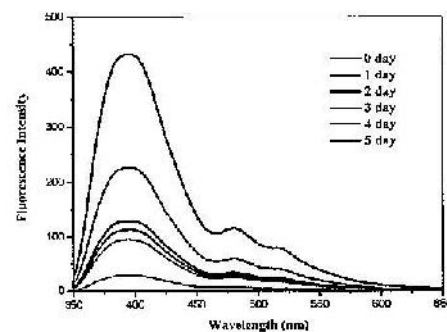
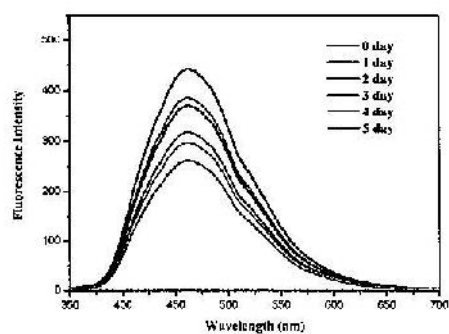
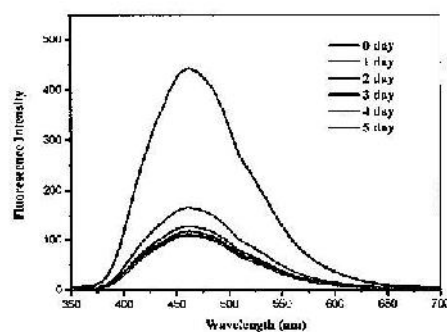


Figure B.2 Fluorescence spectra after 5 day irradiation by UV light (left) and sunlight (right) (continued)

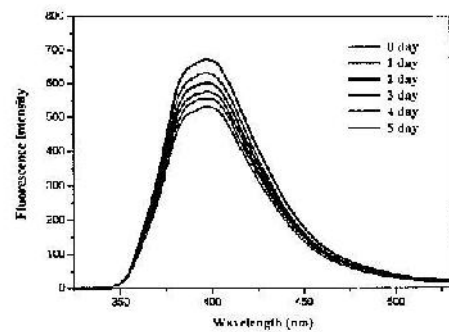
CM10 under UV light (365 nm)



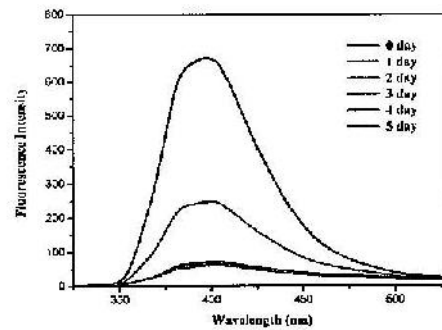
CM10 under sunlight



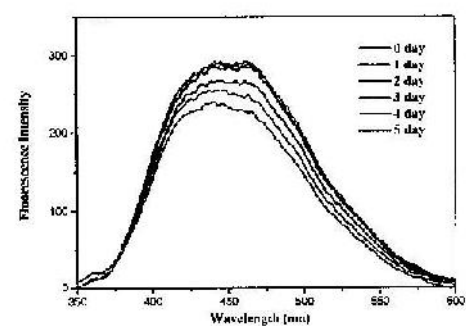
CM11 under UV light (365 nm)



CM11 under sunlight



CM12 under UV light (365 nm)



CM12 under sunlight

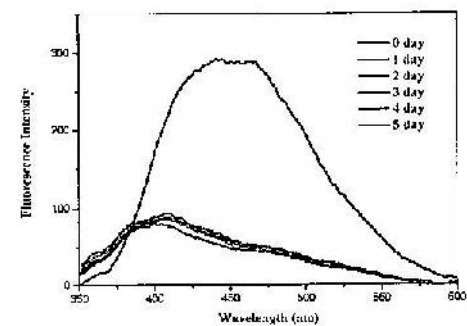


Figure B.2 Fluorescence spectra after 5 day irradiation by UV light (left) and sunlight (right) (continued)

APPENDIX C

Publication

Publication Papers

Defect and Diffusion Forum
ISSN: 1662-9507, Vol. 381, pp 26-30
doi:10.4028/www.scientific.net/DDF.381.26
© 2017 Trans Tech Publications, Switzerland

Submitted: 2017-05-25
Accepted: 2017-06-23
Online: 2017-11-30

Photoresponsive Nano-Coumarin with Indole Auxin Hormone

Witsanu Sombat¹, Kittiya Wongkhan¹, Suwatchai Jarussophon²
and Rukkiat Jitchati^{1*}

¹Organometallic and Catalytic Center (OCC), Department of Chemistry, Faculty of Science,
Ubon Ratchathani University, Warinchumrap, Ubon Ratchathani Province, 34190, Thailand

²National Nanotechnology Center, National Science and Technology Development Agency, 130
Thailand Science Park, Paholyothin Road, Klong Luang, Pathumthani, 12120 Bangkok, Thailand

*rukkiat_j@hotmail.com

Keywords: Photoresponsive, Coumarin, Indole, Auxin

Abstract. In this work, we designed and synthesized two photoresponsive materials with 3-indoleacetic acid (IAA) plant hormone which can be monitored from the photoreposive properties of coumarin. The varied position of the long alkoxy side chain ($-OC_{16}H_{33}$) was purposely introduced to adhesive on the plant leaves. Two coumarin-caged nanomaterials showed average particle diameter about 400 nm and gave the maximum emission wavelength at 425 and 450 nm. The formulated nanoemulsion showed good wettability ($\theta=48^\circ$) with *Cassia fistula* leave surface. Interestingly, CM2 gave the short photoreponse of photolysis within one day.

Introduction

In 2015, a statistics showed that the imported chemicals to Thailand were more than 150,000 tons, valued at 19,000 million baht [1]. Using pesticides and plant hormones are often limited by adhesion resulting in huge losses of such active compounds, especially by doing several repeated foliate applications. In fact, more than 90% of sprayed insecticides and hormones lost to other destinations which affected to environmental. Recently, nano-encapsulated products, especially for pesticides/plant hormones were claimed to meet the demands in that they enable smaller quantities to be used effectively without much damage to the environment [2-4]. Coumarin is found naturally in many plants such as cinnamon, tonka bean, vanilla grass which has been used as a precursor in the pharmaceutical and cosmetic industry. Moreover, the coumarin chromophore has also been extensively studied as a photolabile-protective group for carboxylates [5-7] which could make a significant improvement on the agrochemical applications [8-11]. In 2012, S. Atta et al. studied a photoreposive coumarin with IAA and naphthoxyacetic acid (NOAA). The result showed that the bioactivity of photoreposive coumarin showed better enhancement in the root and shoot length growth of *Cicer arietinum* after 10 days of sunlight exposure. Here in, we synthesized two photoresponsive materials (see Scheme 1) and studied the varied the position of alkoxy long chain coumarin (C16) in indole auxin hormone. The photo-responsive mechanism was proposed in Fig. 1.

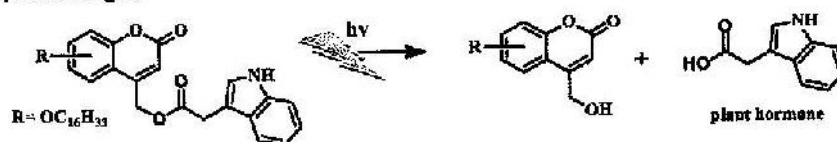
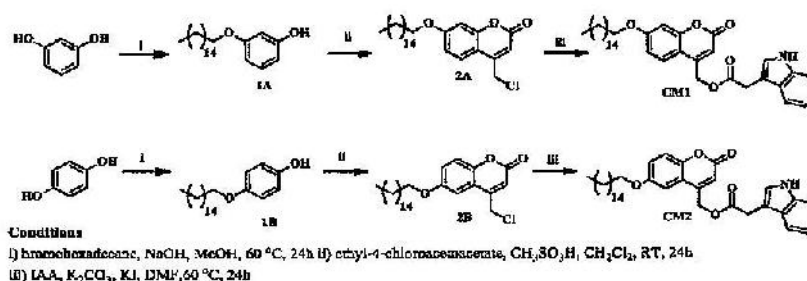


Fig. 1. Proposed photo-responsive coumarin compounds controlled release system



Scheme 1. Synthetic route of CM1 and CM2

Experimental

Materials and methods

All reactant and solvents were purchased from commercial sources and used without further purification. ¹H and ¹³C NMR spectra were recorded on a Bruker ARX300 NMR spectrometer. Mass spectra were obtained using a HRMS mass spectrometer on a Bruker MicroTOF-Q II. UV-Vis absorption and fluorescence emission spectra were studied with Perkin Elmer UV-visible spectrophotometer. Fluorescence emission spectra were acquired with a Perkin Elmer fluorescence spectrophotometer (model LS50). FT-IR spectra were recorded on a Perkin-Elmer RXI spectrometer.

3-(hexadecyloxy)phenol (1A); resorcinol (0.5 g) was dissolved in methanolic sodium hydroxide (20 mL). Then 1-bromohexadecane (1 eq) was added to the reaction mixture and refluxed overnight. Completing reaction was followed by TLC and extracted with DCM. The combined organic extraction were concentrated on rotary evaporator and the residue was purified by column chromatography using 40% DCM:hexane as eluent and solvent was removed by rotary evaporator to get white solid product (31% yield); ¹H NMR (300 MHz, CDCl₃) δ (ppm) 7.12 (t, *J* = 10.4, 1H), 6.48 (d, *J* = 8.1 Hz, 1H), 6.44–6.34 (m, 2H), 4.94–4.75 (m, 1H), 3.92 (t, *J* = 6.5 Hz, 2H), 1.87–1.67 (m, 2H), 1.41–1.26 (m, 26H), 0.88 (t, *J* = 6.4 Hz, 3H); ¹³C NMR (75 MHz, CDCl₃) δ 160.5, 156.6, 130.0, 107.5, 107.1, 102.0, 68.0, 31.9, 29.7–29.2(11C), 26.0, 22.6, 14.1; FTIR ν_{max}(cm⁻¹) 3447, 2915, 2848, 1595, 1180; HRMS cal. for C₂₂H₃₉O₂ [M-H]⁺, 334.2950; found, 335.2952.

4-(hexadecyloxy)phenol (1B) was synthesized using a similar route to that of 1A except that of the resorcinol was replaced by hydroquinone to get white solid product (25% yield); ¹H NMR (300 MHz, CDCl₃) δ (ppm) 6.76 (m, 4H), 4.60 (s, 1H), 3.88 (t, *J* = 6.2 Hz, 2H), 1.87–1.68 (m, 2H), 1.42–1.26 (m, 26H), 0.87 (t, *J* = 6.1 Hz, 3H); ¹³C NMR (75 MHz, CDCl₃) δ 153.3, 149.2, 115.9(2C), 115.6(2C), 68.7, 31.9, 29.6–29.3(x11C), 26.0, 22.6, 14.1; FTIR ν_{max}(cm⁻¹) 3434, 2916, 2849, 1513, 1231; HRMS cal. for C₂₂H₃₉O₂ [M-H]⁺, 334.2950; found, 335.2950.

4-(chloromethyl)-7-(hexadecyloxy)-2H-chromen-2-one (2A); a mixture of 1A (0.2 g) in chloroform (2 mL) was slowly added by ethyl 4-chloroacetoacetate (1.5 eq) and methanesulfonic acid (1 mL, dropwise) at room temperature. The mixture was stirred at room temperature overnight. Completing reaction was followed by TLC and extracted with dichloromethane. The combined organic extraction were concentrated on rotary evaporator and the residue was purified by column chromatography using 40% DCM:hexane as eluent. The solvent was removed by rotary evaporator to give the coumarins product (60% yield); ¹H NMR (300 MHz, CDCl₃) δ (ppm) 7.55 (d, *J* = 8.8 Hz, 1H), 6.88 (d, *J* = 8.8 Hz, 1H), 6.84 (s, 1H), 6.39 (s, 1H), 4.62 (s, 2H), 4.02 (t, *J* = 6.5 Hz, 2H), 1.80 (m, 2H), 1.46–1.26 (s, 26H), 0.88 (t, *J* = 6.4 Hz, 3H); ¹³C NMR (75 MHz, CDCl₃) δ 162.6, 160.8, 155.7, 149.6, 125.0, 113.0, 112.4, 110.5, 101.7, 68.7, 41.3, 31.9, 29.6–28.9(11C), 25.9, 22.6, 14.1; FTIR ν_{max}(cm⁻¹) 2918, 2850, 1702, 1282, 769; HRMS cal. for C₂₆H₄₀ClO₃ [M+H]⁺, 435.2666; found, 435.2666.

4-(chloromethyl)-6-(hexadecyloxy)-2H-chromen-2-one (2B) was synthesized using a similar route to that of **2A** except compound **1A** was replaced by **1B** to give the coumarins product (60% yield); ^1H NMR (300 MHz, CDCl_3) δ (ppm) 7.30 (d, $J = 9.0$ Hz, 1H), 7.14 (d, $J = 9.0$ Hz, 1H), 7.08 (s, 1H), 6.58 (s, 1H), 4.65 (s, 2H), 4.00 (t, $J = 6.2$ Hz, 2H), 1.77 (m, 2H), 1.66–1.10 (m, 26H), 0.87 (t, $J = 6.3$ Hz, 3H); ^{13}C NMR (75 MHz, CDCl_3) δ 160.4, 155.6, 149.1, 148.1, 119.8, 118.3, 117.7, 116.2, 107.8, 68.8, 41.3, 31.9, 29.6–29.1 (11C), 26.0, 22.6, 14.1; FTIR ν_{max} (cm^{-1}) 2913, 2849, 1782, 1248, 734 HRMS cal. for $\text{C}_{26}\text{H}_{40}\text{ClO}_3$ $[\text{M}+\text{H}]^+$: 435.2666, found: 435.2666.

(7-(hexadecyloxy)-2-oxo-2H-chromen-4-yl)methyl 2-(3a,7a-dihydro-1H-indol-3-yl)acetate (CM1); 7-hexadecylcoumarin coupling with 3-indoleacetic acid (IAA) was performed in DMF. Completing reaction was followed by TLC and extracted by DCM. The combined organic extraction were concentrated on rotary evaporator and the residue was purified by column chromatography using 50–100% DCM:hexane as eluent. The solvent was removed by rotary evaporator to get white solid coumarin-cage plant hormones **CM1**. (40% yield); ^1H NMR (300 MHz, CDCl_3) δ (ppm) 8.17 (s, 1H), 7.62 (d, $J = 7.8$ Hz, 1H), 7.39 (d, $J = 8.0$ Hz, 1H), 7.34–7.06 (m, 4H), 6.80 (s, 1H), 6.75 (d, $J = 8.9$ Hz, 1H), 6.24 (s, 1H), 5.26 (s, 2H), 3.99 (t, $J = 6.4$ Hz, 2H), 3.92 (s, 2H), 1.87–1.68 (m, 2H), 1.65–1.08 (m, 26H), 0.87 (t, $J = 6.3$ Hz, 3H); ^{13}C NMR (75 MHz, CDCl_3) δ 171.1, 162.4, 161.0, 155.4, 149.2, 136.1, 127.0, 124.4, 123.2, 122.4, 119.8, 118.6, 112.9, 111.3, 110.3, 109.8, 107.6, 101.6, 68.6, 61.5, 31.9, 31.2, 29.6–28.9 (11C), 25.9, 22.6, 14.1; FTIR ν_{max} (cm^{-1}) 3396, 2916, 2852, 1723, 1242; HRMS cal. for $\text{C}_{36}\text{H}_{48}\text{NO}_5$ $[\text{M}+\text{H}]^+$, 573.3532; found, 573.3535.

(6-(hexadecyloxy)-2-oxo-2H-chromen-4-yl)methyl 2-(3a,7a-dihydro-1H-indol-3-yl)acetate (CM2) was synthesized using a similar route to that of **CM1** except compound **2A** was replaced by **2B** to give coumarin-cage plant hormones **CM2** (23% yield). ^1H NMR (300 MHz, CDCl_3) δ (ppm) 7.98 (d, $J = 8.0$ Hz, 1H), 7.85 (dd, $J = 18.4, 5.9$ Hz, 2H), 7.65–7.49 (m, 4H), 7.46 (d, $J = 4.3$ Hz, 1H), 7.21 (d, $J = 8.8$ Hz, 2H), 6.78 (s, 1H), 6.71 (d, $J = 8.3$ Hz, 1H), 6.17 (s, 1H), 5.23 (s, 2H), 4.21 (s, 2H), 3.99 (t, $J = 6.3$ Hz, 2H), 1.91–1.65 (m, 2H), 1.59–1.16 (m, 26H), 0.87 (d, $J = 6.8$ Hz, 3H); ^{13}C NMR (75 MHz, CDCl_3) δ 171.1, 160.6, 155.6, 148.7, 147.8, 136.1, 127.0, 123.2, 122.4, 119.9, 119.8, 118.6, 118.2, 117.4, 113.4, 111.3, 107.6, 106.8, 68.8, 61.3, 31.9, 31.2, 29.6–29.1 (11C), 25.9, 22.6, 14.1; FTIR ν_{max} (cm^{-1}) 3360, 2921, 2851, 1723, 1249; HRMS cal. for $\text{C}_{36}\text{H}_{48}\text{NO}_5$ $[\text{M}+\text{H}]^+$, 573.3532; found: 573.3533.

Results and Discussion

Synthesis of photoresponsive coumarin

Two coumarin-cage plant hormones (**CM1** and **CM2**) were prepared as shown in Scheme 1. The O-alkylation of resorcinol and hydroquinone with bromohexadecane in the presence of NaOH as a base to give **1A** and **1B**. Coumarin intermediates (**2A** and **2B**) were synthesized by condensation of **1A** or **1B** with ethyl-4-chloroacetoacetate in the presence of methanesulphonic acid. Then, **2A** and **2B** were coupling with 3-indoleacetic acid (IAA) in DMF to give coumarin-caged plant hormones (**CM1** and **CM2**) in 40–50% yield. The structures of **CM1** and **CM2** were characterized by ^1H , ^{13}C NMR, IR and mass techniques which showed good agreement with their structures.

Preparation of nanoemulsion

The aqueous nanoemulsions of **CM1** and **CM2** were formulated by using a mixture of poly(vinyl)alcohol (PVA) and sodium dodecyl sulfate (SDS) as the stabilizer and surfactants, respectively. The process was exemplified using a model water-insoluble compound to obtain the optimized ratio = 75:25 (0.2% **CM1** or **CM2**: 1 wt% SDS solution in 3 wt% PVA). Analysis of the nanodispersions by dynamic light scattering (DLS) are shown in Fig. 2. Both nanoemulsions give average particle diameters about 400 nm.

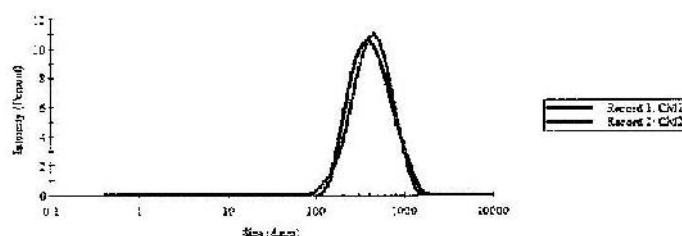


Fig. 2. Dynamic light scattering analysis of the nanoemulsion of formulated CM1 and CM2

Wettability properties of photoresponsive coumarin on the plant leaf surface

The optimized CM1 and CM2 nanoemulsion on the *Cassia fistula* leave were investigated. The wettability of CM1 and CM2 indicates a strong hydrophobicity with contact angle of 48° , as show in Fig. 3, compared with water (contact angle 91°) and stabilizers (contact angle 73°).

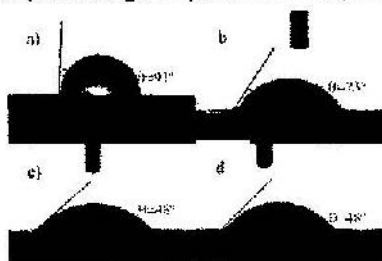


Fig. 3. Contact angle of samples drop on plant leave (*Cassia fistula*); a) water, b) PVA/SDS, c) CM1, and d) CM2

Photolysis of photoresponsive coumarin

A suspension of 200 ppm of CM1 and CM2 were irradiated under sun light for 7 hour daily for 5 days. The fluorescence decay of photoresponsive coumarin CM1 and CM2 using fluorescence spectroscopy were monitored. Both CM1 and CM2 exhibited good fluorescence with maximum emission wavelength at 450 and 425 nm for CM1 and CM2, respectively (Fig. 4). The exemplary change of CM1 and CM2 emission spectra after irradiation one day intervals are shown in Fig. 4(a) and (b). The fluorescence intensity of CM2 dramatically reduced within only 1 day compare to that CM1. This result suggested that the position of 6-alkoxy chain coumarin could be a responsible from reactive coumarin core.

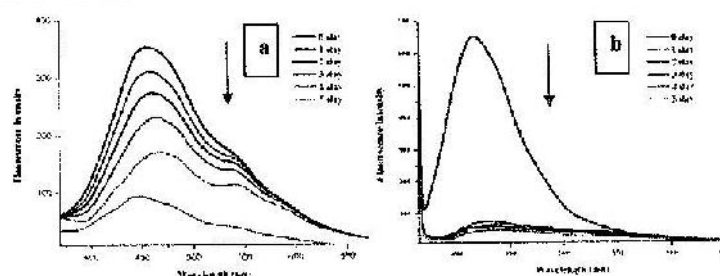


Fig. 4. Fluorescence spectra of coumarin photolysis; a) CM1 and b) CM2

Conclusion

We developed two long alkoxy side chain (C16) photoresponsive with plant growth regulators by varied the position in a coumarin core. Both coumarin-caged showed good fluorescence and their nanodispersions average size was about 400 nm with good hydrophilic properties. CM2 showed a good photolysis characteristic within one day. This study could be a guideline for a design photoresponsive material in agriculture in the future.

Acknowledgments

We thank Science Achievement Scholarship of Thailand (SAST) and the Office of the Higher Education Commission (OHEC) under research grant 185724 for financial support.

References

- [1] Information on <http://www.doa.go.th/ard>
- [2] A. Jana, B. Saha, D.R. Banerjee, S.K. Ghosh, K.T. Nguyen, X. Ma, Q. Qu, Y. Zhao, N.P. Singh, Photocontrolled Nuclear-Targeted Drug Delivery by Single Component Photoresponsive Fluorescent Organic Nanoparticles of Acridin-9-Methanol, *Bioconjugate Chem.* 24 (2013) 1828-1839.
- [3] A. Jana, K.S.P. Devi, T.K. Maiti, N.P. Singh, Perylene-3-ylmethanol: Fluorescent Organic Nanoparticles as a Single-Component Photoresponsive Nanocarrier with Real Time Monitoring of Anticancer Drug Release, *J. Am. Chem. Soc.* 134 (2012) 7656-7659.
- [4] S. Karthik, N. Puvvada, B.P. Kumar, S. Rajput, A. Pathak, M. Mandal, N.P. Singh, Photoresponsive Coumarin-Tethered Multifunctional Magnetic Nanoparticles for Release of Anticancer Drug, *ACS Appl. Mater. Interfaces* 5 (2013) 5232-5238.
- [5] R. Subramaniam, Y. Xiao, Y. Li, S.Y. Qian, W. Sun, S. Mallik, Light-mediated and H-bond facilitated liposomal release: the role of lipid head groups in release efficiency, *Tetrahedron Lett.* 51 (2010) 529-532.
- [6] S. Atta, M. Ikbal, A. Kumar, N.P. Singh, Application of photoremovable protecting group for controlled release of plant growth regulators by sunlight, *J. Photochem. Photobiol. B, Biol.* 111 (2012) 39-49.
- [7] P. Bourbon, Q. Peng, G. Ferraudi, C. Stauffacher, O. Wiest, P. Helquist, Synthesis and photochemical behavior of coumarin-caged Cholesterol, *Bioorg. Med. Chem. Lett.* 23 (2013) 2162-2165.
- [8] M. Kah, S. Beulke, K. Tiede, T. Hofmann, Nanopesticides: State of Knowledge, Environmental Fate, and Exposure Modeling, *Crit Rev Environ Sci Technol.* 43 (2013) 1823-1867.
- [9] Q. Lin, C. Bao, G. Fan, S. Cheng, H. Liu, Z. Liu, L. Zhu, 7-Amino coumarin based fluorescent phototriggers coupled with nano/bio-conjugated bonds: Synthesis, labeling and photorelease, *J. Mater. Chem.* 22 (2012) 6680-6688.
- [10] S. Atta, A. Jana, R. Ananthakrishnan, and P. S. N. Dhuleep, Fluorescent Caged Compounds of 2,4-Dichlorophenoxyacetic Acid (2,4-D): Photorelease Technology for Controlled Release of 2,4-D, *J. Agric. Food. Chem.* 58 (2010) 11844-11851.
- [11] S. Atta, A. Paul, R. Banerjee, M. Bera, M. Ikbal, D. Dhara, N.P. Singh, Photoresponsive polymers based on a coumarin moiety for the controlled release of pesticide 2, 4-D, *RSC Advances* 5 (2015) 99968-99975.

Oral presentation

1. 2017 6th International Conference on Engineering and Innovative Materials (ICEIM 2017) in the title of "A Novel Charged Iridium Polymer for Light Emitting Diode" 3-5 September 2017, Tokyo, Japan



Poster presentation

1. 2017 International Conference on Nanomaterials, Functional and Composite Materials (ICNFCM2017) in the title of "Photoresponsive Nano-Coumarin with Indole Auxin Hormone". 22-23 July 2017, Hong Kong, China
2. Pure and Applied Chemistry International Conference (PACCON 2017) in the title of "Design and synthesis of photoresponsive coumarin for plant hormone" 2-3 February 2017, Bangkok, Thailand
3. International Conference on Material Science (ICMS-2017) in the title of "A novel photoresponsive coumarin with plant hormone". 16 - 18 February 2017, Tripura, India
4. 2015 20th Microoptics Conference (MOC) in the title of "CHARGED IRIDIUM COMPLEXES FOR ORGANIC AMINE SENSOR APPLICATION". 25 - 28 October 2015, Fukuoka International Congress Center 2-1 Sekijo-machi, Hakata-ku Fukuoka, Japan

DESIGN AND SYNTHESIS OF PHOTORESPONSIVE COUMARIN FOR PLANT HORMONE

IPACCON
2017



Witsanu Sombat, Kittiya Wongkhan and Rukkai Jitthachai*

Organometallic and Catalytic Center (OCC), Department of Chemistry, Faculty of Science, Ubon Ratchathani University, Ubon Ratchathani Province, 34190, Thailand
*E-mail: rukkai_j@hotmail.com

INTRODUCTION

Coumarin is found naturally in many plants such as cinnamon, tonka bean, vanilla grass which has been used as a precursor in the pharmaceutical and cosmetic industry. Moreover, the coumarin chromophore has also been extensively studied as a photolabile-protective group for carboxylates^[1] and it might be a useful tool in photo-controlled release system which could make a significant improvement on the agrochemical applications (Fig.1).^{[2][3]} Certain plant leaves are known to be hydrophobic part in nature. The use of pesticides/plant regulated hormones is often limited by its adhesion resulting in huge losing. In fact, more than 90% of sprayed insecticides and herbicides reach a destination, including air, water and soil. Recently, nano-encapsulated products especially for pesticides/plant hormones are claimed to meet the demands in that they enable smaller quantities to be used effectively without much damage to the environment.

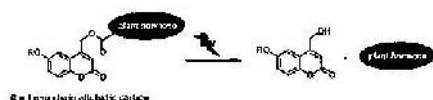
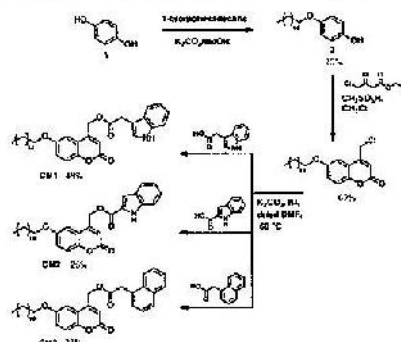


Fig. 1 Proposed photo-responsive coumarin compound for light controlled release system

EXPERIMENTAL

The photoresponsive coumarins with plant hormone (CM1, CM2 and CM3) were prepared as shown in Scheme 1 by conversion of the hydroquinone (1) to 2 via O-alkylation with 1-bromohexadecane in the presence of K_2CO_3 as the base.



Scheme 1 Synthesis of photoresponsive coumarin with plant hormone

Coumarin intermediates were synthesized by condensation 2 and ethyl-4-chloroacetate in the presence of methan sulphonic acid as catalyst to yield 6-hexadecylcoumarin. The esterification with 3-indoleacetic acid (IAA), 2-indoleacetic acid (NAA) and 1-naphthaleneacetic acid (NAA) was performed in *ortho* DMF to give coumarin-cage plant hormones (CM1, CM2 and CM3) respectively in 30-50% yields. The structures of these compounds were characterized by 1H NMR, ^{13}C NMR, IR and mass techniques which showed good agreement with their structures.

RESULTS AND DISCUSSION

All target coumarins showed similar pattern of 1H NMR. The example spectra of CM1 was showed in the Fig. 2. The result showed that the aromatic protons (10H) were observed around 8.20 – 8.25 ppm. Two singlet signals at 5.25 ppm(2H) and 3.92 ppm(2H) were assigned as benzyl and methylene positions, respectively. The long alkoxy side chain protons ($-OC_{16}H_{33}$) was found at 4.00 ppm(2H), 1.81 ppm(2H), 1.45-1.26 ppm(26H) and 0.85 ppm(3H).

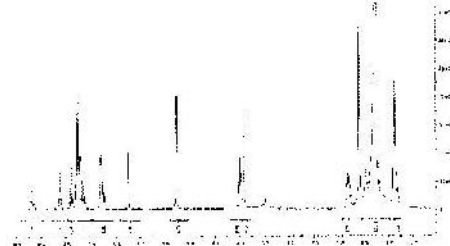


Fig. 2 1H NMR spectra of CM1 in $CDCl_3$

The photophysical properties of CM1, CM2 and CM3 were investigated. UV/vis absorption spectra clearly showed that have two strong intense absorption bands with maximum wavelength 350 nm and 280 nm (Fig. 3A). The long wavelength absorption band corresponds to coumarin chromophore^[4] and short wavelength was assigned as aromatic part of plant hormone. Furthermore, the target coumarins exhibited good fluorescence with maximum emission wavelength at 450 nm (Fig. 3B).

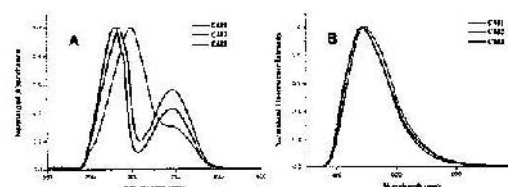



Fig. 3 (A) Absorption spectra and (B) Emission spectra of CM1, CM2 and CM3 in chloroform at room temperature

CONCLUSIONS AND ACKNOWLEDGEMENTS


We synthesized the novel photoresponsive material based on photo deluted natural coumarin core and cleavable ester bond with plant hormone. The molecules were attached with the long alkoxy side chain (C_{16}) which allows to adhesive on the surface of plant leaves. The target products are CM1, CM2 and CM3 which were characterized by 1H NMR, ^{13}C NMR, IR and mass techniques. The compounds absorbed in the UV region with maximum wavelength 350 nm and 280 nm and emitted strong fluorescence with maximum emission wavelength 450 nm. These molecules will be studied the photolysis and wettability in the future. Witsanu Sombat would like to acknowledge the financial support from Science Achievement Scholarship of Thailand (SAST). The partial finance support from Office of the Higher Education Commission (OHEC) under research grant 155724

[1] R. Subramanian, Y. Xiao, Y. Li, S. Y. Ghah, W. Sun and S. Mallik, *Tetrahedron Lett.* Vol. 51 (2010), p. 829-832. [2] M. Rah, B. Zeuke, K. Tiede and T. Holmann, *Ordnal Reviews in Environmental Science and Technology* (2012). [3] D. Lin, G. Rao, G. Fan, S. Cheng, H. Liu, Z. Lu and L. Zhu, *J. Mater. Chem.* Vol. 22 (2012), p. 6680. [4] S. Ato, A. Jono, R. Anandakrishnan, and P. S. N. Unilever, *J. Agric. Food Chem.* Vol. 58 (2010), p. 11844-11851.



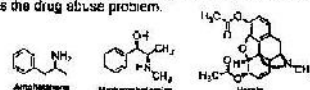
CHARGED IRIIDIUM COMPLEXES FOR ORGANIC AMINE SENSOR APPLICATION

Organometallic and Catalytic Center (OCC), Department of Chemistry, Faculty of Science,
Ubon Ratchathani University, Wanchanurap, Ubon Ratchathani Province, 34190, Thailand
E-mail: rukkiat.j@hotmail.com



INTRODUCTION

The organic amine based such as ecstasy, methamphetamine and heroin have been known as the drug abuse problem.



The convenient, simple and cheap method for detection these amine drugs is chemical color reaction (CCR). However, this method is limited with less accuracy compared to other methods. The charged Iridium(III) complexes have been extensively studied and well known with the strong photophysical properties. The emission color of Iridium(III) complexes are dependent on their structures by changing the ancillary ligands [1]. With this information in hand, NU-02, SY-11 and WS-02 (Fig. 1) were designed and synthesized which were used as organic amine chemical sensor.

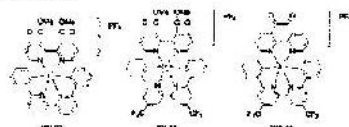
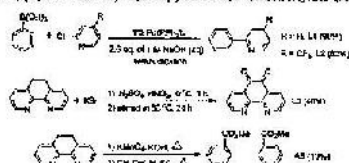


Fig. 1 The structures of our charged Iridium(III) complexes

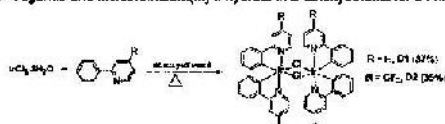
SYNTHETIC METHODOLOGY

The synthetic method for the charged Iridium complex is classified as 3 steps.

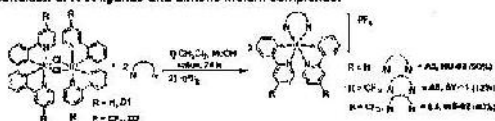
1. **Ligand synthesis:** The reactions were reported elsewhere to obtain 2-phenylpyridine (L1) [2], 2-phenyl-4-trifluoromethyl pyridine (L2), 1,10-phenanthroline-5,6-dione (L3) [3] and dimethyl-2,2'-bipyridine-3,3'-dicarboxylate (AB) [4].



2. **Dimeric Iridium(III) synthesis:** The complexes can be synthesized by refluxing of C-N ligands and trichloroiodine(III) trihydrate in 2-ethoxyethanol for 24 hrs.



3. **Charged Iridium(III) synthesis:** The reaction proceed very well in the refluxing condition of N-N ligands and dimeric Iridium complexes.



All synthetic ligands and Iridium(III) complexes were fully characterized by ^1H , ^{13}C NMR and mass spectroscopy.

RESULTS AND DISCUSSION

The photo properties of chemical sensor using NU-02, SY-11 and WS-02 were studied by UV-Vis absorption, shown in Fig. 2-5.

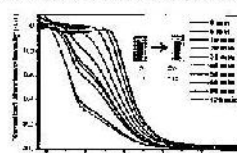


Fig. 2 UV-Vis absorption spectra of 2.5×10^{-5} M NU-02 with the addition of n-BuNH₂ in CH₃CN solution (various 100 nM HCl)

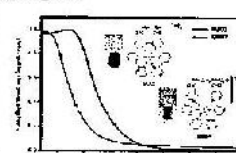


Fig. 3 UV-Vis absorption spectra of NU-02 and KM-07 of 2.5×10^{-5} M in CH₃CN at various temperature

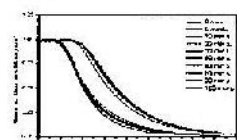


Fig. 4 UV-Vis absorption spectra of 2.5×10^{-5} M SY-11 with the addition of n-BuNH₂ in CH₃CN solution (under 1.0 eq HCl (left) and the reaction color (right)).

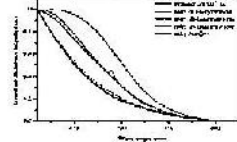


Fig. 5 UV-Vis absorption spectra of 2.5×10^{-5} M WS-02 with the addition of n-BuNH₂, BuNH, Bu₃N, NaOH in dichloromethane solution (left) and the reaction color (right).

The chemical sensor was tested with n-BuNH₂ and HCl in CH₃CN solutions. We found that the reaction using SY-11 proceed faster than NU-02. The solution color changed from orange to yellow within 30 minutes suggested a formation of new chromophore. This is due to the formation of ester functional groups from an amide after the addition of n-BuNH₂. To prove that, we synthesized and studied the amide complex (KM-07). The result confirmed that KM-07 shows significantly blue shifted compared with NU-02 (Fig. 3). In addition, the chemical sensor was modified to WS-02 which is more reactive than NU-02. The study show that WS-02 can be a sensor with three kinds of organic amine (n-BuNH₂, BuNH and Bu₃N) and NaOH in dichloromethane with immediately color changed (30 sec), see Fig. 5.

CONCLUSIONS AND ACKNOWLEDGEMENTS

The chemical sensor of n-butylamine with the reactive Iridium(III) complexes can be synthesized. The reaction color was monitored with UV-Vis absorption and naked eye. The reaction suggested a formation of new chromophore. In addition, the reactive WS-02 was developed which was used as a sensing material with three organic amines and NaOH. This study could be a benefit system to detect various types of narcotic drugs in the future. The authors would like to acknowledge the financial support from the National Research Council of Thailand (NRCT) under research grant NRCT-2558A11702191 and Science Achievement Scholarship of Thailand (SAST).

CURRICULUM VITAE

NAME	Mr. Witsanu Sombat
BIRTH DATE	8 October 1992
BIRTH PLACE	Ubon Ratchathani Province, Thailand
EDUCATION	B. Sc. (Chemistry), Department of Chemistry, Faculty of Science, Ubon Ratchathani University, Ubon Ratchathani, Thailand, 2011-2014. M. Sc. (Chemistry), Department of Chemistry, Faculty of Science, Ubon Ratchathani University, Ubon Ratchathani, Thailand, 2015-2017.
SCHOLARSHIPS	Science Achievement Scholarship of Thailand, SAST
RESEARCH GROUP	Organometallic and Catalytic Center (OCC)

